



#418

ATS-6

ENERGETIC PARTICLE SPECTROMETER DATA

74-039A-07A

ATS 6

ENERGETIC PARTICLE SPECTROMETER

74-0394-C7A

THIS DATA SET HAS BEEN RESTORED. ORIGINALLY
THERE WERE 4 9-TRACK, 1600 BPI TAPES WRITTEN IN BINARY.
THERE IS ONE RESTORED TAPE. THE DR TAPE IS A 3480
CARTRIDGE AND THE DS TAPE IS 9-TRACK, 6250 BPI.
THE TAPES WERE CREATED ON A CDC 7600 COMPUTER. THE
DR AND DS NUMBERS ALONG WITH THE CORRESPONDING D
NUMBERS AND THE TIME SPANS ARE AS FOLLOWS:

DR#	DS#	D#	FILES	TIME SPAN
DR03618	DS03618	D30956	1	06/14/74 - 12/31/74
		D35157	2	01/01/75 - 12/31/75
		D35158	3	01/01/76 - 12/31/76
		D35159	4	01/01/77 - 12/31/77

REQ. AGENT
VJP

RAND NO.
RC9048
RD3216

ACQ. AGENT
LLD
BCD

ATS-6

ENERGETIC PARTICLE SPECTROMETER DATA

74-039A-07A

This data set catalog consists of 4 ATS-6 data tapes. Tape D30956 and C19778 are both 1600 BPI, D35157-59 are 6250 BPI, and there C tapes are 1600 BPI. All of the tapes are 9 track, Binary with 1 file of data. The tapes were created on a CDC 7600 computer.

Time span are as follows:

<u>D#</u>	<u>C#</u>	<u>TIME SPAN</u>
D-30956	C-19778	6/14/74 - 12/31/74
D-35157	C-20768	1/01/75 - 12/31/75
D-35158	C-20769	1/01/76 - 12/31/76
D-35159	C-20770	1/01/77 - 12/31/77

User's Guide to Data Obtained by The Aerospace Corporation Energetic Particle Spectrometer on ATS-6

Prepared by G. A. PAULIKAS and H. H. HILTON
Space Sciences Laboratory

3 October 1977

Prepared for
NASA GODDARD SPACE FLIGHT CENTER
Greenbelt, Maryland 20771

Contract No. NAS5-23788

The Ivan A. Getting Laboratories
THE AEROSPACE CORPORATION



THE IVAN A. GETTING LABORATORIES

The Laboratory Operations of The Aerospace Corporation is conducting experimental and theoretical investigations necessary for the evaluation and application of scientific advances to new military concepts and systems. Versatility and flexibility have been developed to a high degree by the laboratory personnel in dealing with the many problems encountered in the nation's rapidly developing space and missile systems. Expertise in the latest scientific developments is vital to the accomplishment of tasks related to these problems. The laboratories that contribute to this research are:

Aerophysics Laboratory: Launch and reentry aerodynamics, heat transfer, reentry physics, chemical kinetics, structural mechanics, flight dynamics, atmospheric pollution, and high-power gas lasers.

Chemistry and Physics Laboratory: Atmospheric reactions and atmospheric optics, chemical reactions in polluted atmospheres, chemical reactions of excited species in rocket plumes, chemical thermodynamics, plasma and laser-induced reactions, laser chemistry, propulsion chemistry, space vacuum and radiation effects on materials, lubrication and surface phenomena, photo-sensitive materials and sensors, high precision laser ranging, and the application of physics and chemistry to problems of law enforcement and biomedicine.

Electronics Research Laboratory: Electromagnetic theory, devices, and propagation phenomena, including plasma electromagnetics; quantum electronics, lasers, and electro-optics; communication sciences, applied electronics, semi-conducting, superconducting, and crystal device physics, optical and acoustical imaging; atmospheric pollution; millimeter wave and far-infrared technology.

Materials Sciences Laboratory: Development of new materials; metal matrix composites and new forms of carbon; test and evaluation of graphite and ceramics in reentry; spacecraft materials and electronic components in nuclear weapons environment; application of fracture mechanics to stress corrosion and fatigue-induced fractures in structural metals.

Space Sciences Laboratory: Atmospheric and ionospheric physics, radiation from the atmosphere, density and composition of the atmosphere, aurorae and airglow; magnetospheric physics, cosmic rays, generation and propagation of plasma waves in the magnetosphere; solar physics, studies of solar magnetic fields; space astronomy, x-ray astronomy; the effects of nuclear explosions, magnetic storms, and solar activity on the earth's atmosphere, ionosphere, and magnetosphere; the effects of optical, electromagnetic, and particulate radiations in space on space systems.

THE AEROSPACE CORPORATION
El Segundo, California

USER'S GUIDE TO DATA OBTAINED BY
THE AEROSPACE CORPORATION ENERGETIC
PARTICLE SPECTROMETER ON ATS-6

Prepared by
G. A. Paulikas and H. H. Hilton
Space Sciences Laboratory

3 October 1977

The Ivan A. Getting Laboratories
THE AEROSPACE CORPORATION
El Segundo, California 90245

Contract No. NAS5-23788

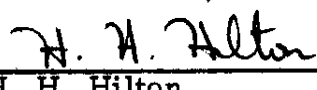
Prepared for
NASA GODDARD SPACE FLIGHT CENTER
Greenbelt, Maryland 20771

USER'S GUIDE TO DATA OBTAINED BY
THE AEROSPACE CORPORATION ENERGETIC
PARTICLE SPECTROMETER ON ATS-6

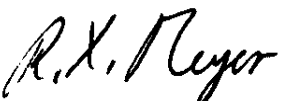
Prepared


G. A. Paulikas, Director

Space Sciences Laboratory


H. H. Hilton
Senior Staff Scientist

Approved


R. X. Reyer
for G. W. King
Vice President and General
Manager
The Ivan A. Getting Laboratories

ABSTRACT

This report is the user's guide to the data obtained by the ATS-6 Aerospace Corporation energetic particle detector and deposited at the National Space Science Data Center. Contained are descriptions of the instrument, calibration data, information on instrumental and operational anomalies and a description of the procedures used to reduce the data. A description of the format of the data is also presented.

CONTENTS

ABSTRACT	v
I. EXPERIMENT DESCRIPTION	1
II. OPERATIONAL, INSTRUMENTAL AND DATA ANOMALIES	9
A. Instrumental Anomalies	9
B. Operational Anomalies	9
C. Data Anomalies	10
III. DESCRIPTION OF DATA	13
A. Aerospace Corporation Experimental Tapes	13
B. Data Reduction and Processing	13
C. The Data Tape Formats	15
IV. DATA CATALOG	37
V. REPRINTS	65

1. EXPERIMENT DESCRIPTION

ATS-6

Energetic Particle Radiation Measurement at Synchronous Altitude

G. A. PAULIKAS
J.B. BLAKE
S. S. IMAMOTO
Space Physics Laboratory
The Aerospace Corporation
El Segundo, Calif. 90245

Abstract

The Aerospace Corporation energetic electron-proton spectrometer operating on Applications Technology Satellite-6 (ATS-6) detects energetic electrons in four channels between 140 keV and greater than 3.9 MeV, and measures energetic protons in five energy channels between 2.3 and 80 MeV and energetic alpha particles in three channels between 9.4 and 94 MeV. After more than a year of operation in orbit, the experiment continues to return excellent data on the behavior of energetic magnetospheric electrons as well as information regarding the fluxes of solar protons and alpha particles.

I. Introduction

The region of space near the synchronous altitude is a fascinating part of space where various domains of the magnetosphere meet and interact. Fig. 1, taken from Frank [1], graphically illustrates the confluence of the plasma-pause, the extraterrestrial ring current, the boundary of the zone of energetic particles, and the Earthward terminus of the plasma sheet in the immediate vicinity of $6.6 R_e$. The study of the interaction of the various plasmas with vastly different densities and temperatures and the energization and dynamics of these plasmas are the goals of the Environmental Measurements Experiments (EME) on Applications Technology Satellite-6 (ATS-6).

The aerospace experiment described in this paper contributes to these goals through measurements of the high energy tail of the electron distribution function. The experiment covers the energy range for electrons from 140 keV to greater than 3.9 MeV, and the experiment is expected to yield important results regarding the acceleration and dynamics of the energetic electrons. While previous measurements (see the compilations [8] and [9]) have contributed a great deal of information regarding the behavior of energetic electrons at the synchronous altitude, comprehensive measurements such as those being made on ATS-6 of the entire distribution function for a given particle species have never been made.

Not shown in Fig. 1, but also present in this region of space during solar particle events, are energetic protons and alpha particles (and possibly electrons) of solar origin. These solar particles may penetrate to altitudes as low as $4 R_e$ (depending on particle rigidity and magnetic activity) but, in general, the gradient of solar protons is located somewhere in the vicinity of $6.6 R_e$. The experiment measures the fluxes and spectra of solar particles reaching the synchronous orbit. (The proton thresholds of this experiment are too high to permit the detection of the proton component of the trapped radiation.)

II. Description of the Experiment

A. Physical and Electronic Configuration

The instrument consists of four separate sensors, one two-detector element telescope and three omnidirectional single-detector units. An overall view of the instrument is presented in Fig. 2, and a functional schematic of the electronics is presented in Fig. 3.

The counter telescope uses silicon surface-barrier detectors of ORTEC manufacture behind a disk-loaded collimator. The first detector is 50 mm^2 in area and $230 \mu\text{m}$ deep and the second detector is 200 mm^2 in area and $100 \mu\text{m}$ deep. Both are totally depleted. Five electronic discriminator levels are used with the first detector. The two upper levels are set above the maximum energy a proton can deposit in the detector and thus are sensitive to alphas only (actually $Z \geq 2$). The next two levels are sensitive to protons (actually all ions) but not electrons, and the lowest

Manuscript received August 1, 1975. Copyright 1975 by IEEE Trans. Aerospace and Electronic Systems, vol. AES-11, no. 6, November 1975.

This work was supported in part by the U. S. Air Force Space and Missile Systems Organization, under Contract F04701-74-C-0075, and in part by the National Aeronautics and Space Administration, under Contract NASW-2762.

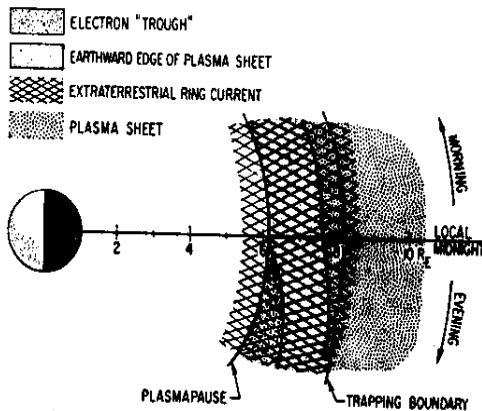


Fig. 1. Spatial relationships near the synchronous orbit at local midnight between the ring current, the plasmapause, the energetic particle trapping boundary, and the Earthward terminus of the plasma sheet. This figure is qualitative and representative of magnetic quiet (from Frank [1]).

level is sensitive to all particles in the appropriate energy range. The sole function of the second detector is to inhibit from analysis any penetrating particles. Section II B provides details about the energy channels.

The three omnidirectional sensors use small cubical lithium-drifted silicon detectors centered under a hemispherical shell and heavily shielded (relative to the hemispherical shield) over the rear 2π solid angle. Protons are separated unambiguously from electrons by setting the second discriminator level well above the maximum energy an electron can deposit in the small semiconductor detector. The fact that dE/dx (energy loss per unit path length) is much greater for protons than for electrons (in the energy range of geophysical interest) is utilized. The absence of electron contamination in the proton channels was verified by electron irradiation of the sensors. The proton threshold of each of the three sensors was determined primarily by the thickness of the hemispherical shield, with the energy threshold of the two most lightly shielded units somewhat affected by the electronic thresholds as well. The most lightly shielded omnidirectional sensor has a third electronic level set above the maximum proton energy deposit to provide an alpha particle channel. The two heavier hemispherical shields were made of beryllium to minimize Bremsstrahlung and maximize the threshold sharpness. The most lightly shielded shield is aluminum since an aluminum shield is much cheaper and the performance difference negligible for such a thin shield.

The electronic subsystem of the experiment is shown schematically in Fig. 3. The input stage of the preamps utilize an n-channel field-effect transistor. In order to maintain a low system noise, the input stage is enclosed in a shielded compartment. The characteristic long-tail pulse from the preamplifier is shaped by a pole-zero shaping network into a pulse with a $1-\mu s$ time constant. The high level discriminators (greater than 8 MeV) are driven directly from the output of the shaping circuit. Output from the shaping network is also coupled to an operational amplifier which provides the additional gain required to trigger the

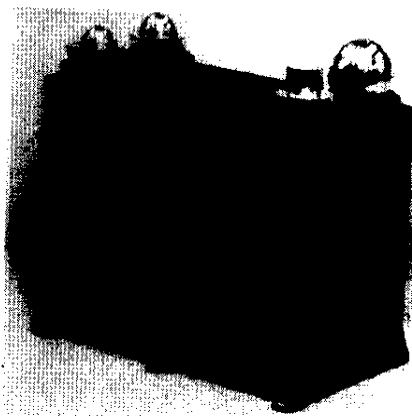


Fig. 2. Overall view of the energetic particle spectrometer on ATS-6. Directional detectors are housed inside the cylindrical collimator structure in the foreground.

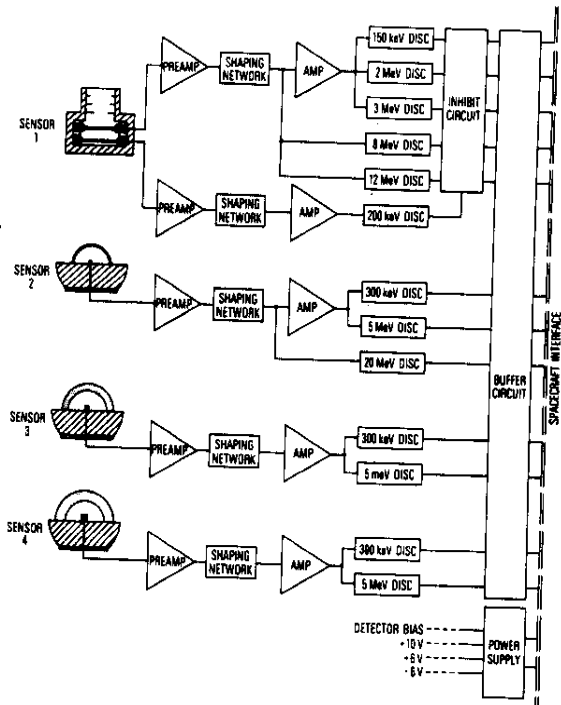


Fig. 3. Schematic block diagram of detector/electronic system.

low energy thresholds. Preamplifier gain is set by an adjustable feedback capacitor. Gain of the operation amplifier is set by a feedback resistor.

The discriminator is essentially a comparator driving a tunnel diode. The threshold voltage is set by a lab-set resistor. Output from the discriminator is a 0-5-V pulse with an approximate duration of a microsecond. A COS/MOS buffer circuit accepts the 0-5-V discriminator pulse and provides a 0-10-V pulse to interface with the spacecraft encoder.

Sensor 1 uses two sets of circuits identical to those used for sensors 2, 3, and 4. The front detector of the two-detector array has five discriminators which drive an inhibit circuit; particles penetrating through the first detector are

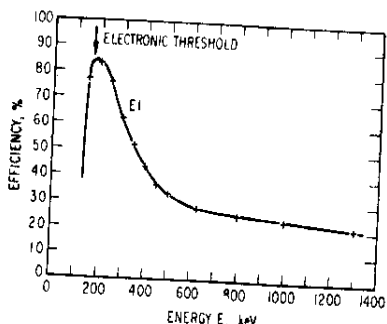


Fig. 4. Efficiency of detection of electrons in the E_1 channel. This channel has a nominal energy sensitivity of 140-600 keV. Sensitivity of this channel below the nominal electronic threshold is associated with the finite noise of the detector.

Table I

Channel	Passband or Threshold (MeV)	ϵG
E_1	0.140 - 0.600	$.115 \text{ cm}^2 \cdot \text{sr}$
E_2	0.700	$.00349 \text{ cm}^2$
E_3	1.55	$.0176 \text{ cm}^2$
E_4	3.90	$.0688 \text{ cm}^2$

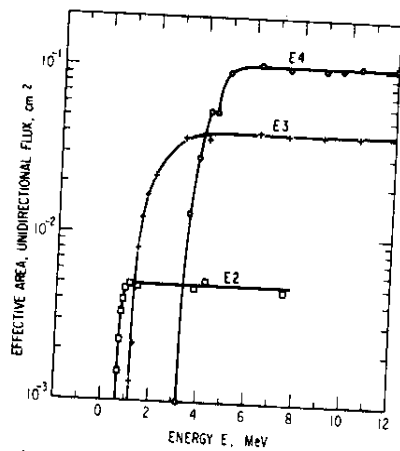


Fig. 5. Effective area of the E_2 , E_3 , and E_4 electron channels as a function of electron energy. This effective area, when integrated over the angular response of the detector, yields the omnidirectional geometric factor.

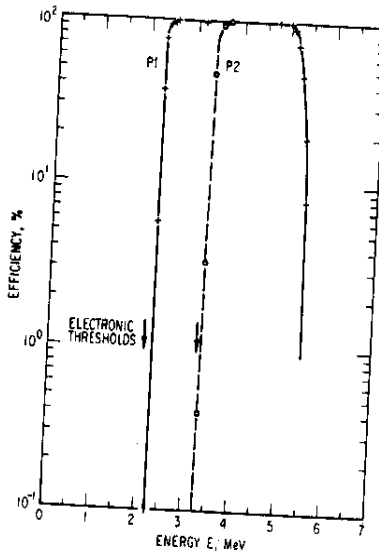


Fig. 6. Efficiency for detection of protons in the P_1 and P_2 channels of the counter telescope.

thus rejected. COS/MOS logic is used to perform the trailing edge logic in the inhibit circuit. Trailing edge logic is used to compensate for "walk" in the discriminators. Outputs from the inhibit circuit are also buffered to interface with the encoder.

A DC-DC converter provides the required instrument bias voltages. Power from the spacecraft is coupled to a series pass stage to limit the experiment turn on transient and to protect spacecraft relays. The converter section is completely enclosed in an electrostatic shield to minimize undesirable pickup by the counting circuits. Total power consumption is 475-540 mW, depending on the count rate at which the instrument is operating.

Terminal boards with discrete components and point-to-point wiring are used in the construction of the amplifiers, discriminators, and power supply. Printed circuit and integrated circuits are used for the inhibit and buffer circuits. Total experiment weight is 1.2 kg.

B. Detector Calibration Data

1) *Electron Channels:* Figs. 4 and 5 display the electron calibration data in graphical form. The E_1 channel employs a directional geometry of $1.6 \times 10^{-1} \text{ cm}^2 \cdot \text{sr}$, the E_2 , E_3 , and E_4 channels used on omnidirectional geometry and thus the calibration data, obtained with a plane parallel beam, must be integrated over the angular acceptance of these detectors in order to arrive at the omnidirectional efficiency as a function of energy. However, it is convenient to define thresholds and geometric factors for obtaining rapid estimates of fluxes. These thresholds and geometric factors are calculated by numerically integrating the response function over various spectral shapes and finding the threshold which minimizes the variation of the calculated geometric with spectral shape. The results are given in Table I.

The proton and alpha particle channels have negligible sensitivity to electrons.

2) *Proton Channels:* The proton calibration data for channels P_1 and P_2 are shown in Fig. 6. The thresholds of these two channels are sharp enough [$\Delta E/E_{threshold} \ll 1$, where $\Delta E \sim E$ ($\epsilon = 90$ percent) — E ($\epsilon = 10$ percent)] to eliminate the need for numerically integrating over the response function. The geometric factors of the other proton channels (the omnidirectional sensors) were computed and spot checked at several energies where accelera-

tor protons were available. Table II gives the results. Unfortunately, ATS-6 weight constraints prevented the use of sufficient back shielding to render back penetration negligible for all proton spectra. Two different thicknesses of shielding covered the rear hemisphere and thus each channel has three passbands and geometric factors. These "rear passbands" are also given in Table II.

In all cases the electron channels are sensitive to protons. However, as a general rule, at the synchronous orbit the electron fluxes far exceed those of the trapped protons. Under unusual conditions, i.e., during solar proton events apparent electron counts can be due to protons. The efficiencies of the electron channels for protons are given in Table III.

The proton channels can be triggered by alphas (or higher Z particles); the relative abundance of alphas to protons renders this contamination negligible.

III. Operational History

The experiment on ATS-6 was first powered in orbit on June 14, 1974, and has been operating almost continuously since that time; such brief shutdowns of the experiment as have occurred have been associated with tests of other experiments on ATS-6. Several minor anomalies in the performance of the experiment have been observed during the first year of operation. None of these affect the quality of utility of the data in any significant way and all goals of the experiment are being met.

IV. Preliminary Results

This brief summary of the preliminary results already obtained from the ATS-6 experiment is an indication of some of the unique contributions ATS-6 data will make to our understanding of the behavior of the magnetosphere and the entry and motion of solar particles in the magnetosphere.

A. Energetic Electrons

The first data on energetic electrons obtained by ATS-6 showed that the electron fluxes were much more dynamic than earlier observations [5]-[7] on ATS-1 had indicated. ATS-6 data indicated the virtual disappearance of energetic electrons during portions of the orbit in the nighttime quadrant. Such "dropouts" were observed only rarely on ATS-1. In order to make a quantitative check on this impression, data were obtained from the experiment from ATS-1 for the same time period for a direct comparison of ATS-6 and ATS-1 energetic electron observations. These comparisons are shown in Figs. 7 and 8. Fig. 7 illustrates observations made during a magnetically quiet period (day 201) which was preceded by three days of magnetic quiet. In general, ATS-6 and ATS-1 energetic electron count rates

Table II

Channel	Energy (MeV)	G	Particle
P1	2.3-5.3	.160 cm ² - sr	p
P2	3.4-5.3	.160 cm ² - sr	p
P3	9.4-21.2	.160 cm ² - sr	α
P8	13.4-21.2	.160 cm ² - sr	α
P4	12-26	.0045 cm ²	p
P5	46-100	.0048 cm ²	α
P6	20-52	.0188 cm ²	p
P7	40-90	.0412 cm ²	p
<u>Rear Passbands</u>			
P4a	58-68	.0023 cm ²	p
P4b	85-96	.0017 cm ²	p
P5a	.232-265	.0033 cm ²	α
P5b	344-370	.0031 cm ²	α
P6a	58-86	.0135 cm ²	p
P6b	86-109	.0128 cm ²	p
P7a	58-108	.0368 cm ²	p
P7b	86-132	.0318 cm ²	p

Table III

Channel	Energy (MeV)	G	Particle
E1	See footnote	.16 cm ² - sr	p
E2	12-190	.0074 cm ²	p
E3	21-290	.0287 cm ²	p
E4	40-520	.0617 cm ²	p
<u>Rear Passbands</u>			
E2a	58-310	.0061 cm ²	p
E2b	86-330	.0057 cm ²	p
E3a	58-470	.0260 cm ²	p
E3b	86-490	.0244 cm ²	p
E4a	58-550	.0595 cm ²	p
E4b	86-650	.0565 cm ²	p

*The E1 electron channel is sensitive to protons with energies greater than 710 keV. The upper limit of sensitivity is of the order 190 MeV without the veto trigger, about 5.3 MeV when the particle enters in such a way as to hit the veto detector.

show similar behavior. The sharp decreases in flux near 0430 UT and 0630 UT visible in the ATS-6 data are the results of substorms. Note that the effects of substorms on the energetic electrons are much attenuated at ATS-1 as compared with ATS-6.

During geomagnetically active periods, there is a substantial difference in the count rates observed by the two spacecraft. Fig. 8 illustrates a comparison of observations made at ATS-6 and ATS-1 during a disturbed period. Note the total disappearance of flux at ATS-6 while ATS-1 always observes finite fluxes.

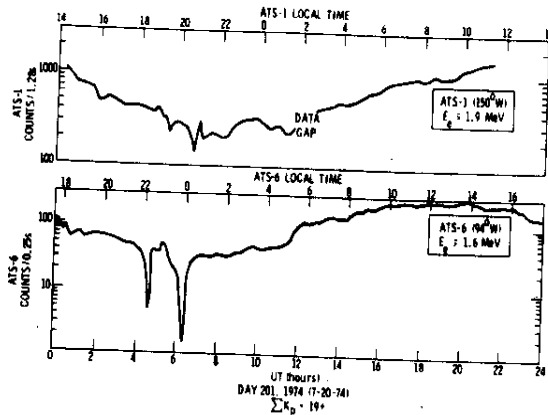


Fig. 7. Comparison of energetic electron count rates observed by ATS-6 and ATS-1 during a magnetically quiet day (day 201). The three days preceding day 201 were also quiet.

The differences in phenomenology appear to be due to the different magnetic latitudes of the spacecraft. ATS-6 is located at about 10° magnetic latitude at its location of 94° W longitude, while ATS-1 is almost exactly on the magnetic equator at 150° W. The approximately 10° difference in magnetic latitude appears to be sufficient to place ATS-6, at times, into regions of space devoid of energetic electrons. Substorms, for example, as illustrated in Fig. 7, have a greater effect on the energetic particle population off the magnetic equator. We can postulate that, during the later stages of a substorm, the geomagnetic field relaxes to more dipole-like configuration and the boundary of energetic particle trapping moves inward and equatorward past the ATS-6 spacecraft.

The comparisons of with ATS-1 ATS-6, data while still preliminary, indicate a surprisingly steep gradient in the energetic electron population as one moves away from the equator, in other words, a disk-like region of trapping of energetic electrons near $6.6 R_e$.

B. The Solar Proton Event of July 4, 5, 6, 1974

Several solar proton events have been observed by the ATS-6 detectors during the first year of operation. Although the present time is a relatively quiescent part of the cycle of solar activity, modest outburst of protons (and heavy nuclei) were emitted by the sun during July and September 1974 and detected by this experiment and other experiments aboard ATS-6.

Solar protons of even relatively low energy are able to reach the synchronous altitude quite readily, without very much decrease in the flux as these particles transverse the outer regions of the geomagnetic field. This surprising result was first noted by experiments on ATS-1 [2], [4]. The ATS-6 experiments will provide very much better insight regarding the trajectories by which solar particles penetrate deeply into the magnetosphere, the gradients of solar particle fluxes near the synchronous orbits, and the effects of electromagnetic waves on the motion and lifetime of solar particles inside the geomagnetic cavity.

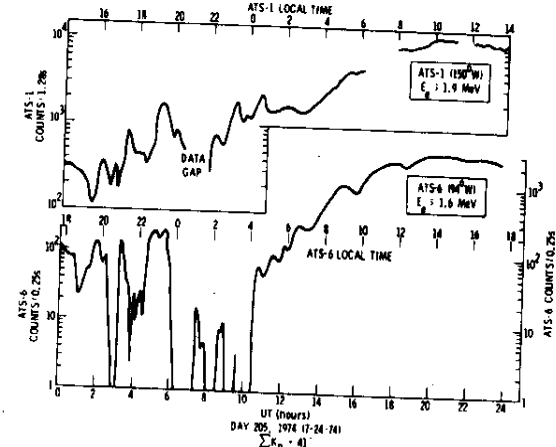


Fig. 8. Comparison of energetic electron count rates observed by ATS-6 and ATS-1 during a magnetically disturbed day (day 205).

An overall view of July 1974 solar proton event, as observed by the experiment on ATS-6, is presented in Fig. 9. The entire event is quite complex. The complexity arises partly because several emissions of particles by the Sun, somewhat separated in time, are superimposed and partly because disturbances in the geomagnetic field were also affecting the fluxes of solar particles.

The effect of one such disturbance, a compression of the geomagnetic field (presumably by an interplanetary shock) on solar protons moving within the geomagnetic field, is shown in Fig. 10. The effect of such a compression is to increase the observed flux within a given energy channel because particles are accelerated. The acceleration process is identical to that which operates in betatrons. Furthermore, the changes in the configuration of the geomagnetic field cause the particle flux gradient to move past the detector. Study of the time development of flux changes, such as shown in Fig. 10, can give information regarding the way particles interact with the spectrum at electromagnetic waves created during geomagnetic activity [3].

V. Summary

After more than a year of operation in orbit, the experiment continues to provide excellent data. All design goals of the experiment have been met. While data analysis is still in the preliminary stages, it is clear that the experiment on ATS-6 will provide new and unique data regarding the behavior of energetic electrons at the synchronous altitude. In particular, correlation of ATS-6 data with data from other synchronous orbit spacecraft now operating (ATS-1, ATS-5) or planned for the future launches will give a much more complete view of the magnetospheric processes operating at high altitudes.

Acknowledgment

This experiment was the product of a large number of people whose efforts spanned many years, not because the

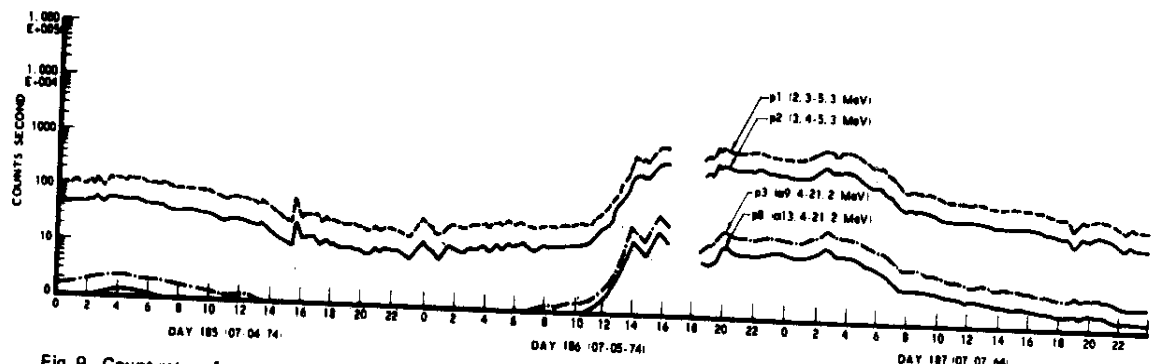


Fig. 9. Count rates of proton and alpha channels during the solar proton event of July 1974. Data for two proton channels and two alpha channels for 4, 5, and 6 July 1974 are presented here.

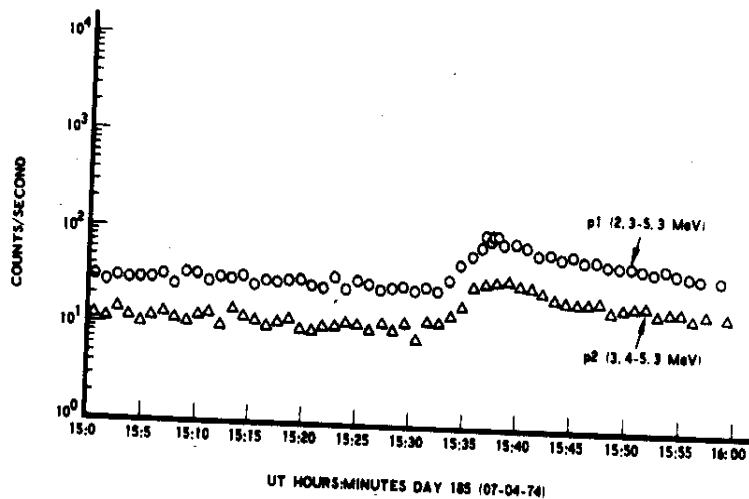


Fig. 10. Increase in solar proton flux associated with a sudden commencement (a compression of the geomagnetic field) near 15:35 on July 4, 1974.

experiment was particularly complex but because the launch of ATS-6 receded several times. We are particularly grateful to Mrs. G. Roberts for the mechanical design of the experiment, to the Westinghouse group, particularly F. McNally, J. Ramsey, and W. King, for their excellent support in the many test and checkout activities, and to R. Wales of NASA Goddard Space Flight Center (GSFC) and his associates who saw the experiment through from beginning to end. P. McKowan of GSFC is providing excellent support in the data acquisition phase of this work. Mrs. T. Becker wrote the data analysis program which we have used to date.

References

- [1] L.A. Frank, "Relationships of the plasma sheet, ring current, trapping boundary and plasmapause near the magnetic equator and local midnight," *J. Geophys. Res.*, vol. 76, p. 2265, 1971.
- [2] L. Lanzerotti, "Penetration of solar protons and alphas to the geomagnetic equator," *Phys. Rev. Lett.*, vol. 21, p. 929, 1968.
- [3] G.A. Paulikas and J.B. Blake, "Effects of sudden commencements on solar protons at the synchronous altitude," *J. Geophys. Res.*, vol. 75, p. 734, 1970.
- [4] —, "Penetration of solar protons to synchronous altitude," *J. Geophys. Res.*, vol. 74, p. 2161, 1969.
- [5] —, "The particle environment at the synchronous altitude, models of the trapped radiation environment, vol. 7: Long term variations," NASA, Washington, D.C., SP-3024, 1971.
- [6] G.A. Paulikas, J.B. Blake, S.C. Freden, and S.S. Imamoto, "Observations of energetic electrons at synchronous altitude, I: General features and diurnal variations," *J. Geophys. Res.*, vol. 73, p. 4915, 1968.
- [7] G.A. Paulikas, J.B. Blake, and J.A. Palmer, "Energetic electrons at the synchronous altitude: A compilation of data," Aerospace Corp., El Segundo, Calif., Rept. TR-0066 (5260-20)-4, November 1969.
- [8] G.W. Singley and J.I. Vette, "A model environment for outer zone electrons," NSSDC 72-13, December 1972.
- [9] J.I. Vette and A.B. Lucero, "Models of the trapped radiation environment, vol. 3: Electrons at synchronous altitudes," NASA, Washington, D.C., SP-3024, 1967.

George A. Paulikas received the B.S. degree in engineering physics and the M.S. degree in physics from the University of Illinois, Urbana, in 1957 and 1958, respectively, and the Ph.D. degree in physics from the University of California, Berkeley, in 1961.

While at the University of California he was associated with the Lawrence Radiation Laboratory, doing research in plasma physics and atomic physics. In 1961 he joined the Space Physics Laboratory, The Aerospace Corporation, El Segundo, Calif., as a Member of the Technical Staff. In this capacity he conducted experimental space physics research, specializing in studies of trapped and quasitrapped radiation. He is now the Director of the Space Physics Laboratory. His fields of specialization include studies of the trapped radiation in the inner Van Allen Belt, measurements of the access of solar particles to the polar caps and to the synchronous orbit, construction of models of trapped radiation, and measurement of trapped alpha particles.

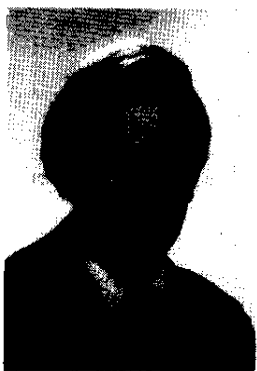
Dr. Paulikas is a member of the American Geophysical Union, the American Astronomical Society, the American Institute of Aeronautics and Astronautics, and Sigma Xi and is a Fellow of the American Physical Society. During 1957-1958 he was awarded a University of Illinois Fellowship, and from 1958-1961 he held a National Science Foundation Fellowship.



J. Bernard Blake received the B.S. degree in engineering physics in 1957, the M.S. degree in physics in 1958, and the Ph.D. degree in physics in 1962 from the University of Illinois, Urbana.

He was a Research Associate at the University of Illinois during 1962 when he joined the Space Physics Laboratory, The Aerospace Corporation, El Segundo, Calif., as a Member of the Technical Staff. He is presently Head of the Space Particles and Fields Department. His professional activity has included work in nuclear beta decay and parity nonconservation, the Mossbauer effect, studies of the geomagnetically trapped particles and auroral phenomena, cosmic ray sources, propagation and entry into the magnetosphere, and nuclear astrophysics. In applied work he has been concerned with nuclear weapons effects on ground and space systems, test monitoring, the interaction of the natural space environment with satellite systems, radiation damage effects, and the analysis of various satellite subsystems.

Dr. Blake is a member of the American Astronomical Society, the American Geophysical Union, the American Association for the Advancement of Science, Sigma Xi, and the American Physical Society. While he was at the University of Illinois he held industrial fellowships from Raytheon and Texas Instruments.



Sam S. Imamoto received an Engineering Associate of Arts degree from El Camino College El Camino College, Calif., in 1964.

He joined the Space Physics Laboratory, The Aerospace Corporation, El Segundo, Calif., in 1962. He is presently a Research Associate in the Space Particles and Fields Department. He has contributed to the design of space instrumentation orbited on more than 20 spacecraft. He was responsible for the design of the Aerospace Corp. experiment on ATS-1 as well as for the design of the Aerospace Corp. experiment on ATS-6. His responsibilities have included all phases of engineering effort from inception to spacecraft integration.



II. OPERATIONAL, INSTRUMENTAL AND DATA ANOMALIES

The various anomalies observed during the 1974-1977 interval in our data are described below. The anomalies have been grouped into several categories and have each been given a distinctive (if sometimes irreverent) name.

A. Instrumental Anomalies

This category describes malfunctions which are directly traceable to our experiment.

1. The E2 Anomaly

We found, early in the operations of ATS-6, that the E2 channel totally ceased counting for a few hours at a time on a given day. This anomaly was found to be associated with the temperature of our instrument: when our instrument was very cold, apparently an intermittent open-can develop in the E2 data stream. This anomaly was observed only early after experiment turn-on (< 170, 1974). The practical consequence is that there are some zero hourly averages for E2 during mid-1974, which have been detected.

2. The E4 Anomaly

The E4 channel exhibited noisy behavior for some local times between Day 140, 1975 and Day 130, 1976. We suspect that the temperature of the E4 detector was sufficiently high so that the detector became noisy. Because of the UNH anomaly (see Section B1, below), we were not able to determine the temperature at which this (the E4) anomaly occurred. The practical consequences of the E4 anomaly is that we have ignored all E4 data between 140, 1975 and 130, 1976 in our work and have deleted these data from our input to NSSDC.

B. Operational Anomalies

The class of anomalies includes all malfunctions which affected our data, but whose sources were elsewhere in the ATS-6 spacecraft.

1. The UNH Anomaly

Turn-on of the University of New Hampshire (UNH) experiment on Day 169, 1974 caused a malfunction in the EME encoder. Specifically, word 189, which contained the health data from our experiment, was affected so that no valid measurements of the temperatures in our experiment were obtained after that date. The encoder apparently partially recovered around Day 139, 1977, however, the decision to operate the UNH experiment starting on Day 171, 1977, again destroyed Word 189. The practical consequences are that no temperature data from our experiment are available to aid in the analysis of other anomalies we have observed.

2. The HAC Anomaly

The operation of the Hughes Aircraft Company solar cell experiment on the ATS-6 EME caused a peculiar (and not understood) interaction, with the spacecraft data encoder which had the effect of dropping a "one" in the most significant bit of the E1 channel (only) at high counting rates. This occurred between 0030 and 0330 UT (during the early ATS-6 operation period) and was apparently associated with a mode change ("lockout") of the HAC experiment. Although only the E1 channel was affected, this anomaly apparently introduced a sufficient number of warning flags into the data tapes we received from Goddard, that our data processing program did not process the first three (UT) hours of data for days shortly after experiment turn-on. As a result, the first three (UT) hourly averages may be missing from the data for some fraction of 1974.

C. Data Anomalies

The anomalies described below are associated with malfunctions in the data processing systems on the ground as well as with introduction of noise into the data stream by telemetry noise or link dropouts.

1. Proton Data

The proton channels of our experiments, as expected, registered only very low countrates except during solar proton events (rare in 1974-1977) and except during some classes of magnetospheric disturbances (also relatively rare). Consequently, noisy data, if uncorrected, has a very

significant effect on long-term averages of the countrates. There has not been any systematic effort to remove noisy data points from the proton data, although we have edited out suspect hourly averages. Users of the proton data are hereby cautioned: proceed carefully, the counts you see may be but noise.

2. Mis-Labeled Data

Despite the best efforts of all concerned, tapes are occasionally mislabeled, not labeled in a consistent manner (date/day number), etc. We have tried to eliminate all such "malfunctions" using such tests as we considered appropriate, but there may well be some pathological cases (i.e., mis-identified days of data) that we did not detect. Users are encouraged to communicate their suspicions to us so that we may improve the data set.

3. Missing Days of Data, Partial Days

The data quality from ATS-6, although truly outstanding, was nevertheless not perfect. The users will find that the present data set contains some partial days of data and some days are entirely missing. The missing days are typically those which have defied processing for various reasons. After several attempts, we have simply called a halt and have asked NASA for replacement tapes. When these tapes arrive, they will be processed and the gaps will be filled. The problem should be put into perspective: at the time of writing (August 1977), for example, only 5 days of 1974 data have resisted processing and 4 days of 1975 data have not been processed. No doubt some interesting geophysical event will have occurred on one of those missing days, following the well-known perversity of nature.

4. Magnetometer Data

The magnetometer data incorporated into our data set was graciously provided by Dr. R. L. McPherron of UCLA. The field information was derived from the telemetry data as described in Section III.

Magnetometer data may not be associated with all days of our data because we have processed some quick-look tapes which did not include the magnetometer data (or, for that matter, any ephemeris or aspect information). There was also a malfunction in the UCLA magnetometer which we did not detect in a timely fashion. As a result, some of the magnetometer data appears strange because our processing routine did not compensate for the malfunction (failure of one axis). Upon notification of the malfunction, we changed the magnetometer data displays from the V, D, H system to one which presented the data in coordinates of the magnetometer axes (plus to total field). We suggest that users interested in the magnetometer data go directly to the UCLA magnetometer data held by NSSDC, rather than attempting to use our version of the UCLA data.

III. DESCRIPTION
OF DATA

III. DESCRIPTION OF DATA REDUCTION AND DATA FORMATS

A. Aerospace Corporation Experimental Tapes

Each data tape received from GSFC contains one day of data, including data from the Aerospace Corporation Omnidirectional Spectrometer and the UCLA Magnetometer, housekeeping data, and ephemeris data. The tapes contain several files, each file headed by a 132 8-bit word (18 CDC 60-bit words) coded title record, followed by many 64 second frames of data, 32x64 9-bit T/M words and 22 36-bit coded ephemeris words (321 CDC 60-bit words).

B. Data Reduction and Processing

Each record of T/M data contains one frame, 64 seconds, of data. From the original T/M Aerospace receives 32 measurements/second, including the following:

<u>Word</u>	<u>Description</u>
27, 28, 29	UT in milliseconds
1, 25	Counter, 0-63
23	Flag, 0 if no error
12	(E1, E2, E3, E4) x 16
15	(P1, P2, P3, P4, P5, P6, P7, P8) x 8
22	Temps, at seconds 53, 54, 55, 56
3, 4, 5	B _x , B _y , B _z , fine
6, 7, 8	B _x , B _y , B _z , medium

The data is checked to insure that the counters (words 1 and 25) are correct, the flag (word 23) is correct, and that the time (words 27, 28, 29) are increasing. If all this checks are passed that data is processed, otherwise not.

The processing includes conversion of the T/M data to fluxes for the omnidirectional spectrometer, gammas for the magnetometer, and degrees for the thermistors. In addition to the second by second values, frame averages, 5 minute averages, and one hour averages are calculated. These are used in detailed plots, and for our two data tape formats, the Detailed Data Tape Format and Master Data Tape Format described in section C.

1. The Ephemeris Data

The ephemeris data consists of 47 values for each 64 second frame, in the ORB/ATT format, detailed in Appendix A. In particular the radius, latitude and longitude are obtained from words 18, 19 and 20.

For the calculation of local time the day and year are taken from the title record, and the time in milliseconds from word 2 of the ephemeris data. Then the position of the sun in ECI coordinates is calculated, and compared with the satellite position in ECI coordinates, words 3, 5, and 7, to calculate the local time.

The attitude transformation matrix, to transform a vector from local vertical to spacecraft body axes, is read from words 36 to 44.

Finally, the matrix to transform from local vertical to dipole coordinates is calculated. This coordinate system has the z-axis parallel to the earth's dipole axis (north positive) and the x-axis chosen so that the satellite is in the x-z plane.

2. The Particle Measurements

The particle measurements are transmitted in the T/M as 9-bit floating point numbers. These T/M values are converted to counts, and then to fluxes, using the values below. Four electron measurements are made each second, and eight "proton" measurements are made each second. The energies and geometric factors for the 12 measurements are listed below. (Note that the electron multiplication factors differ from that given in Section I because they include a factor of 4 to convert from counts/.25 sec to counts/sec).

<u>Channel</u>	<u>Particle</u>	<u>Passband/ Threshold (MeV)</u>	<u>Factor</u>
E1	e	.140-.600	$\text{cm}^2/\text{sec-sr}$
E2	e	>.700	cm^2/sec
E3	e	>1.55	cm^2/sec
E4	e	>3.90	cm^2/sec
P1	P	2.3-5.3	$\text{cm}^2/\text{sec-sr}$
P2	P	3.4-5.3	$\text{cm}^2/\text{sec-sr}$
P3	α	9.4-21.2	$\text{cm}^2/\text{sec-sr}$
P4	P	12-26	cm^2/sec
P5	α	46-100	cm^2/sec
P6	P	20-52	cm^2/sec
P7	P	40-90	cm^2/sec
P8	α	13.4-21.2	$\text{cm}^2/\text{sec-sr}$

3. The Magnetometer Measurements

The UCLA Magnetometer gives medium and fine readings for three axes once/second, or 64 samples/frame. The T/M values are converted to gammas in spacecraft coordinates. Then if the local vertical-spacecraft body axis transformation is available, the three components are rotated to local vertical, and then to "dipole" coordinates. If the local vertical-spacecraft body axis is not available, the magnitude of the field is calculated, and the three components set to -1.

The calibration coefficients used were obtained using a least-squares fit to processed magnetometer data supplied by R. McPherron. The toggling of the fine and medium readings was handled improperly, so an error as much as 16 gamma may occur on any reading, but the 5 minute and 1 hour averages should be unaffected.

C. The Data Tape Formats

1. The Detailed Data Tape

The Detailed Data Tape Format is shown in Appendix B. It contains the processed data on a frame by frame basis, followed by

5 minute and 1 hour averages. Generally there are 10 days of data per tape.

The electron and proton measurements are decommutated each frame, in order to keep the times correct. Only every fourth magnetometer measurement is copied. Time is monotonic increasing, and data is filled with -1's in cases of overlap.

After the frame data, there is one record of 0's to indicate the beginning of the 5 minute and 1 hour averages.

2. The Master Data Tape

The Master Data Tape Format is shown in Appendix C. It contains the hourly averages from the electron, proton and magnetometer data, one day per record. All the days for which there is data are in order chronologically on one tape. It is anticipated that this will be the more useful data for continuing studies.

These data have been examined in detail and all suspect data for the electron and proton measurements have been set to -1.

APPENDIX A

ATS-F EPHEMERIS DATA ORB/ATT TAPE FORMAT

WORD		
1	(1) DAY COUNT	(2) MILLISECONDS OF DAY
2	(3) X COORDINATE	(4) X COORDINATE
3	(5) Y COORDINATE	(6) Y COORDINATE
4	(7) Z COORDINATE	(8) Z COORDINATE
5	(9) YAW	(10) YAW RATE
6	(11) ROLL	(12) ROLL RATE
7	(13) PITCH	(14) PITCH RATE
8	(15) Z _B - AXIS INTERCEPT LATITUDE	(16) Z _B - AXIS INTERCEPT LONGITUDE
9	(17) ROTATION OF BODY Y _B -AXIS FROM NORTH	(18) HEIGHT ABOVE EARTH (SUBSATELLITE POINT)
10	(19) SUBSATELLITE LATITUDE	(20) SUBSATELLITE LONGITUDE
11	(21) RANGE FROM SPACECRAFT TO Z _B - AXIS INTERCEPT	(22) CROSS POLARIZATION ANGLE
12	(23) θ (Theta)	(24) ϕ (Phi)
13	(25) NF x-COORDINATE	(26) NF y-COORDINATE
14	(28) EF x-COORDINATE	(29) EF y-COORDINATE
15	(31) YAW UNCERTAINTY	(32) ROLL UNCERTAINTY
16	(34) α (Alpha)	(35) ATTITUDE SENSOR I.D.
17	(36) α_{11}	(37) α_{12}
18	(38) α_{13}	(39) α_{21}
19	(40) α_{22}	(41) α_{23}
20	(42) α_{31}	(43) α_{32}
21	(44) α_{33}	(45) PROGRAM STATUS
22	(46) CALIBRATION I.D.	(47) MISALIGNMENT I.D.

OUTPUT PARAMETER NO. 1

Name - Day Count of Year

Analytic Definition - This identifies the day on which the processed telemetry frame was transmitted by the spacecraft. The starting point for the count is 0000 hours of the first day of the calendar year (1 January).

Units - Days

Format - This is a nine-bit binary word with the most significant bit (MSB) leading. No sign bit exists.

OUTPUT PARAMETER NO. 2

Name - Milliseconds of Day

Analytic Definition - This identifies the time of day on which the processed telemetry frame was transmitted by the spacecraft. The starting point for this parameter is 0000 hours of the day specified in Output Parameter No. 1 (Day Count of Year).

Units - Milliseconds (Seconds $\times 10^{+3}$)

Format - This is a 27-bit binary word with the MSB leading. No sign bit exists.

OUTPUT PARAMETER NO. 3

Name - X-Coordinate

Analytic Definition - The X-component of the position vector of the ATS-F spacecraft expressed in an earth centered inertial (ECI) coordinate system defined below.

X-axis points to the first point of Aries true-of-date and lies in the equatorial plane of the earth

Z-axis points along the Polaris spin axis of the earth; the positive direction is north

Y-axis is chosen to complete a right-handed orthogonal set

Units - Tents of kilometers (kilometers $\times 10^{+1}$)

Format - This is a 20-bit binary word. The first bit is used for the sign and the following nineteen bits for magnitude with the MSB leading.

OUTPUT PARAMETER NO. 4

Name - X-Coordinate

Analytic Definition - The X-component of the velocity vector of the ATS-F spacecraft expressed in the ECI coordinate system described in the Analytic Definition of Output Parameter No. 3

Units - Meters per second

Format - This is a 16-bit binary word. The first bit is used for the sign and the following 15 bits for magnitude with the MSB leading.

OUTPUT PARAMETER NO. 5

Name - Y-Coordinate

Analytic Definition - The Y-component of the position vector of the ATS-F spacecraft expressed in the ECI coordinate system described in the Analytic Definition of Output Parameter No. 3

Units - Tents of kilometers (kilometers $\times 10^{+1}$)

Format - This is a 20-bit binary word. The first bit is used for the sign and the following 19 bits for magnitude with the MSB leading.

OUTPUT PARAMETER NO. 6

Name - Y-Coordinate

Analytic Definition - The Y-component of the velocity vector of the ATS-F spacecraft expressed in the ECI coordinate system defined in the Analytic Definition of Output Parameter No. 3

Units - Meters per second

Format - This is a 16-bit binary word. The first bit is used for the sign and the following 15 bits for magnitude with the MSB leading.

OUTPUT PARAMETER NO. 7

Name - Z-Coordinate

Analytic Definition - The Z-component of the position vector of the ATS-F spacecraft expressed in the ECI coordinate system described in the Analytic Definition of Output Parameter No. 3

Units - Tents of kilometers (kilometers $\times 10^{+1}$)

Format - This is a 20-bit binary word. The first bit is used for the sign and the following 19 bits for magnitude with the MSB leading.

OUTPUT PARAMETER NO. 8

Name - Z-Coordinate

Analytic Definition - The Z-component of the velocity vector of the ATS-F spacecraft expressed in the ECI coordinate system defined in the Analytic Definition of Output Parameter No. 3

Units - Meters per second

Format - This is a 16-bit binary word. The first bit is used for the sign and the following 15 bits for magnitude with MSB leading.

OUTPUT PARAMETER NO. 9

Name - Yaw

Analytic Definition - The first of three rotations about ATS-F body axes that are used to define ATS-F attitude relative to the Local Vertical (LV) coordinate system defined below.

Z_C points along the local vertical toward the center of mass of the earth

X_C points east parallel to the earth's equatorial plane

Y_C is chosen to complete a right-handed orthogonal set (nominally points south)

The Euler rotations, in the sequence of their application, are as follows:

Yaw - rotation about the spacecraft body Z-axis (Z_B)

Roll - rotation about the spacecraft body X-axis (X_B)

Pitch - rotation about the spacecraft body Y-axis (Y_B)

Units - Thousandths of a degree (degrees $\times 10^{+3}$). Yaw is always taken to be positive ranging from 0 to 360 degrees.

Format - This is a 20-bit binary word with MSB leading. No sign bit exists.

OUTPUT PARAMETER NO. 10

Name - Yaw Rate

Analytic Definition - The time rate of change of the yaw Euler angle defined in the Analytic Definition of Output Parameter No. 9

Units - Thousandths of a degree per minute (degrees per minute $\times 10^{+3}$)

Format - This is a 16-bit binary word. The first bit is used for the sign and the following 15 bits for magnitude with MSB leading.

OUTPUT PARAMETER NO. 11

Name - Roll

Analytic Definition - The second rotation in the Euler sequence used to define ATS-F attitude. This rotation is about the spacecraft body X-axis (X_B). The attitude is relative to the LV coordinate system defined in the Analytic Definition of Output Parameter No. 9

Units - Thousandths of a degree (degrees $\times 10^{+3}$)

Format - This is a 20-bit binary word. The first bit is used for the sign and the following 19 bits for magnitude with MSB leading.

OUTPUT PARAMETER NO. 12

Name - Roll Rate

Analytic Definition - The time rate of change of the roll Euler angle defined in the Analytic Definition of Output Parameter No. 11

Units - Thousandths of a degree per minute (degrees per minute $\times 10^{+3}$).

Format - This is a 16-bit binary word. The first bit is used for the sign and the following 15 bits for magnitude with the MSB leading.

OUTPUT PARAMETER NO. 13

Name - Pitch

Analytic Description - The third rotation in the Euler sequence used to define ATS-F attitude. This rotation is about the spacecraft body Y-axis. The attitude is relative to the LV coordinate system defined in the Analytic Definition of Output Parameter No. 9

Units - Thousandths of a degree (degrees $\times 10^{+3}$).

Format - This is a 20-bit binary word. The first bit is used for the sign and the following 19 bits for magnitude with the MSB leading.

OUTPUT PARAMETER NO. 14

Name - Pitch Rate

Analytic Definition - The time rate of change of the pitch Euler angle defined in the Analytic Definition of Output Parameter No. 13

Units - Thousandths of a degree per minute (degrees per minute $\times 10^{+3}$).

Format - This is a 16-bit binary word. The first bit is used for the sign and the following 15 bits for magnitude with the MSB leading.

OUTPUT PARAMETER NO. 15

Name - Z_B -Axis Intercept Latitude

Analytic Definition - The latitude of the intercept point of a line coincident with the spacecraft body Z-axis (Z_B) and the surface of the earth. An ellipsoidal model of the earth is used.

Units - Hundredths of a degree (degrees $\times 10^{+2}$).

Format - This is an 18-bit binary word. The first bit is used for the sign and the following 17 bits for magnitude with MSB leading.

OUTPUT PARAMETER NO. 16

Name - Z_B -Axis Intercept Longitude

Analytic Description - The longitude of the intercept point of a line coincident with the spacecraft body Z-axis (Z_B) and the surface of the earth. An ellipsoidal model of the earth is used.

Units - Hundredths of a degree (degrees $\times 10^{+2}$). Longitude is always positive measured East from Greenwich and lies in the range 0 to 360 degrees.

Format - This is an 18-bit binary word with the MSB leading. No sign bit exists.

OUTPUT PARAMETER NO. 17

Name - Rotation of Y_B -Axis from North

Analytic Definition - The angle between the following planes.

Plane 1: Plane formed by the spacecraft Z-axis (Z_B) and the local north vector (i.e., $-Y_C$, see Analytic Definition of Output Parameter No. 9).

Plane 2: Plane formed by the spacecraft Z-axis (Z_B) and Y-axis (Y_B).

Units - Hundredths of a degree (degrees $\times 10^{+2}$).

Format - This is an 18-bit binary word with MSB leading. No sign bit exists.

OUTPUT PARAMETER NO. 18

Name - Height Above Subsatellite Point

Analytic Definition - The height of the ATS-F spacecraft above the surface of the earth measured along the line between the spacecraft and the center of mass of the earth. An ellipsoidal model of the earth is used.

Units - Kilometers

Format - This is an 18-bit binary word. No sign bit exists.

OUTPUT PARAMETER NO. 19

Name - Subsatellite Latitude

Analytic Definition - The geodetic latitude of the intercept point on the surface of the earth of a line between the spacecraft and the center of mass of the earth. An ellipsoidal model of the earth is used.

Units - Hundredths of a degree (degrees $\times 10^{+2}$).

Format - This is an 18-bit binary word. The first bit is used for the sign and the following 17 bits for magnitude with the MSB leading.

OUTPUT PARAMETER NO. 20

Name - Subsatellite Longitude

Analytic Definition - The longitude of the intercept point on the surface of the earth of a line between the spacecraft and the center of mass of the earth. An ellipsoidal model of the earth is used.

Units - Hundredths of a degree (degrees $\times 10^{+2}$). Longitude is always positive measured east from Greenwich and lies between 0 and 360 degrees.

Format - This is an 18-bit binary word with the MSB leading. No sign bit exists.

OUTPUT PARAMETER NO. 21

Name - Range from Spacecraft to Z_B -Axis Intercept

Analytic Description - The distance between the spacecraft and the point defined by the intersection of the Z-axis (Z_B) with the earth's surface given in the Analytic Descriptions of Output Parameters Nos. 15 and 16.

Units - Tents of a kilometer (kilometers $\times 10^{+1}$).

Format - This is a 20-bit binary word with MSB leading. No sign bit exists.

OUTPUT PARAMETER NO. 22

Name - Cross-Polarization Angle

Analytic Description - The angle between the ATS-F receiver and a vertically polarized antenna located at the Z-axis (Z_B) intercept point. It is the acute angle between the following two planes:

Plane 1: Defined by (a) center of mass of the earth and (b)
the spacecraft body Z-axis (Z_B)

Plane 2: Defined by (a) the location of an antenna element in
the spacecraft body X-Y plane (X_B-Y_B), and (b) the
spacecraft body Z-axis (Z_B).

Units - Hundredths of a degree (degrees $\times 10^{+2}$), in the range 0 to 360 degrees.

Format - This is a 16-bit binary word with the MSB leading. No sign bit exists.

OUTPUT PARAMETER NO. 23

Name - Antenna Pattern Angle θ

Analytic Description - The angle between the spacecraft Z-axis (Z_B) and the vector to a preselected ground station.
The ground station coordinates will be user specified and available upon request.

Units - Hundredths of a degree (degrees $\times 10^{+2}$).

Format - This is an 18-bit binary word with the MSB leading. No sign bit exists.

OUTPUT PARAMETER NO. 24

Name - Antenna Pattern Angle ϕ

Analytic Description - The angle between the following two planes.

Plane 1: Plane defined by the spacecraft body X and Z axes (X_B , Z_B)

Plane 2: Plane defined by the vector to a preselected ground station and the spacecraft body Z-axis (Z_B)

The ground station coordinates will be user specified and available upon request.

Format - This is an 18-bit binary word with the MSB leading. No sign bit exists.

OUTPUT PARAMETER NO. 25

Name - NFX

Analytic Description - The X-component (i_{NF} direction) of the unit vector to the sun expressed in the Quartz experiment's coordinate system for the sensor assembly on the north face of the Earth Viewing Module (EVM).

Units - Thousandths of a unit (unit $\times 10^{+3}$).

Format - This is a 12-bit binary word. The first bit is used for the sign and the following 11 bits for magnitude with the MSB leading.

OUTPUT PARAMETER NO. 26

Name - NFY

Analytic Description - The Y-component (j_{NF} direction) of the unit vector to the sun expressed in the Quartz experiment's coordinate system for the sensor assembly on the north face of the EVM.

Units - Thousandths of a unit (unit $\times 10^{+3}$).

Format - This is a 12-bit binary word. The first bit is used for the sign and the following 11 bits for magnitude with the MSB leading.

OUTPUT PARAMETER NO. 27

Name - NFZ

Analytic Description - The Z-component (k_{NF} direction) of the unit vector to the sun expressed in the Quartz experiment's coordinate system for the sensor assembly on the north face of the EVM.

Units - Thousandths of a unit (unit $\times 10^{+3}$).

Format - This is a 12-bit binary word. The first bit is used for the sign and the following 11 bits for magnitude with the MSB leading.

OUTPUT PARAMETER NO. 28

Name - EFX

Analytic Description - The X-component (i direction) of the unit vector to the sun expressed in the ATF Experiment's coordinate system for the sensor assembly on the east face of the EVM.

Units - Thousandths of a unit (unit $\times 10^{+3}$).

Format - This is a 12-bit binary word. The first bit is used for the sign and the following 11 bits for magnitude with the MSB leading.

OUTPUT PARAMETER NO. 29

Name - EFY

Analytic Description - The Y-component (j direction) of the unit vector to the sun expressed in the ATF Experiment's coordinate system for the sensor assembly on the east face of the EVM.

Units - Thousandths of a unit (unit $\times 10^{+3}$).

Format - This is a 12-bit binary word. The first bit is used for the sign and the following 11 bits for magnitude with the MSB leading.

OUTPUT PARAMETER NO. 30

Name - EFZ

Analytic Description - The Z-component (k direction) of the unit vector to the sun expressed in the ATF Experiment's coordinate system for the sensor assembly on the east face of the EVM.

Units - Thousandths of a unit (unit $\times 10^{+3}$).

Format - This is a 12-bit binary word. The first bit is used for the sign and the following bits for magnitude with the MSB leading.

OUTPUT PARAMETER NO. 31

Name - Yaw Uncertainty

Analytic Description - The statistical uncertainty in the estimate of the yaw angle. It is the square root of the diagonal element of the state covariance matrix corresponding to the yaw state.

Units - Thousandths of a degree (degrees $\times 10^{+3}$).

Format - This is a 12-bit binary word with the MSB leading. No sign bit exists.

OUTPUT PARAMETER NO. 32

Name - Roll Uncertainty

Analytic Description - The statistical uncertainty in the estimate of the roll angle. It is the square root of the diagonal element of the state covariance matrix corresponding to the roll state.

Units - Thousandths of a degree (degrees $\times 10^{+3}$).

Format - This is a 12-bit binary word with the MSB leading. No sign bit exists.

OUTPUT PARAMETER NO. 33

Name - Pitch Uncertainty

Analytic Description - The statistical uncertainty in the estimate of the pitch angle. It is the square root of the diagonal element of the state covariance matrix corresponding to the pitch state.

Units - Thousandths of a degree (degrees $\times 10^{+3}$).

Format - This is a 12-bit binary word with the MSB leading. No sign bit exists.

OUTPUT PARAMETER NO. 34

Name - Offset Pointing Angle, α

Analytic Description - The angle between the line of sight to the subsatellite point (output parameters 19 and 20) and the spacecraft Z-axis (Z_B).

Units - Hundredths of a degree (degrees $\times 10^{+2}$).

Format - This is a 14-bit binary word with the MSB leading. No sign bit exists.

OUTPUT PARAMETER NO. 35

Name - Attitude Sensor ID

Analytic Description - This identifies the attitude sensors whose data is being utilized in the attitude estimation process.

Units - None (binary flags)

Format - This is a string of 22 bits. Each bit corresponds to a specific sensor on ATS-F and indicates whether that sensor's output is used in the attitude estimation process. The state "1" indicates it is used. The bits refer to the following sensors in the indicated order.

<u>Bit No.</u>	<u>Sensor</u>
1	Earth Sensor
2	Polaris Sensor No. 1
3	Polaris Sensor No. 2
4	Digital Sun Sensor No. 1
5	Digital Sun Sensor No. 2
6	Digital Sun Sensor No. 3
7	Digital Sun Sensor No. 4
8	Digital Sun Sensor No. 5
9	Interferometer No. 1
10	Interferometer No. 2
11	Monopulse VHF
12	Monopulse S-Band
13	Monopulse C-Band
14	Coarse Sun Sensor No. 1
15	Coarse Sun Sensor No. 2
16	Coarse Sun Sensor No. 3
17	Coarse Sun Sensor No. 4
18	Fine Sun Sensor No. 1
19	Fine Sun Sensor No. 2
20	Rate Gyro Assembly No. 1
21	Rate Gyro Assembly No. 2
22	Spare

OUTPUT PARAMETERS NOS. 36 THROUGH 44

Name - Elements of the Attitude Transformation Matrix (a_{ij})

Analytic Description - Elements of the transformation matrix from the local vertical (L-V) coordinate frame to the spacecraft body coordinate frame. The matrix is of the form:

$$[A] = \begin{vmatrix} a_{11} & a_{12} & a_{13} \\ a_{21} & a_{22} & a_{23} \\ a_{31} & a_{32} & a_{33} \end{vmatrix}$$

The matrix transforms a vector in the local vertical coordinate frame (\bar{V}_{L-V}) to a vector in the spacecraft body frame (\bar{V}_B) according to the following relationship:

$$\bar{V}_B = [A] \bar{V}_{L-V}$$

Units - Hundred thousandths of a unit (unit $\times 10^{+5}$)

Format - Each element is an 18-bit binary word. The first bit is used for the sign and the following 17 bits for magnitude with the MSB leading.

Output Parameter No.	a_{ij}
36	a_{11}
37	a_{12}
38	a_{13}
39	a_{21}
40	a_{22}
41	a_{23}
42	a_{31}
43	a_{32}
44	a_{33}

OUTPUT PARAMETER NO. 45

Name - Program Status

Analytic Description - Code words for internal use by attitude generation personnel to identify program modifications

Units - None. Code words.

Format - To be determined.

OUTPUT PARAMETER NO. 46

Name - Calibration Identifier

Analytic Description - Code words for internal use by attitude generation personnel to identify telemetry calibration curves used in generating attitude

Units - None. Code words.

Format - To be determined

OUTPUT PARAMETER NO. 47

Name - Misalignment Identifier

Analytic Description - Code words for internal use by attitude generation personnel to identify attitude sensor misalignment sets used in generating attitudes

Units - None. Code words.

Format - To Be determined

APPENDIX B.

DETAILED DATA TAPE FORMAT

Each day is one file of many 288 CDC 60-bit records.

Record 1:

<u>Word</u>	<u>Type</u>	<u>Description</u>
1- 18	Bits	The original title record (132 8-bit characters) plus 24 "0" bits.
19	Hollerith	Date of data
20	"	Date Processed by Aerospace Corporation
21	"	Tape Number Assigned by Aerospace Corporation
22-288		Fill, "0"s.

Records 2 - Number of Frames, N, +1.

<u>Word</u>	<u>Type</u>	<u>Description</u>
1	Integer	Day of Year
2	"	Year } From Title Record
3	Real	UT, seconds, of ephemeris, or -1.
4	"	Radius, ER, or -1.
5	"	Latitude, Deg., or -1.
6	"	Longitude, Deg., or -1.
7	"	Local Time, Hrs., or -1.
8	"	0.
9- 72	"	UT, seconds, or -1.
73-136	"	(E1, E2, E3, E4) x 16, or -1.
137-200	"	(P1, P2, P3, P4, P5, P6, P7, P8) x 8, or -1.
201-216	"	B _x
217-232	"	B _y } From Frames 4, 64, 4, or -1.
233-248	"	B _z
249-264	"	B

<u>Word</u>	<u>Type</u>	<u>Description</u>
265-268	"	Temperatures
269-288	"	Fill, 0

Records N + 2 to N + 20, all words real.

<u>Record</u>	<u>Words</u>	<u>Description</u>
N+ 2	1-288	Fill, 0
N+ 3	"	E1, 288 5 minute averages, or -1.
N+ 4	"	E2,
N+ 5	"	E3,
N+ 6	"	E4,
N+ 7	"	P1,
N+ 8	"	P2,
N+ 9	"	P3,
N+10	"	P4,
N+11	"	P5,
N+12	"	P6,
N+13	"	P7,
N+14	"	P8,
N+15	"	B _x
N+16	"	B _y
N+17	"	B _z
N+18	"	B,
N+19	1- 24	E1, 24 1 hour averages, or -1.
"	25- 48	E2,
"	49- 72	E3,
"	73- 96	E4,
"	97-120	P1,
"	121-144	P2,
"	145-168	P3,
"	169-192	P4,
"	193-216	P5,
"	217-240	P6,
"	241-264	P7,
"	265-288	P8,

<u>Record</u>	<u>Words</u>	<u>Description</u>
N+20	1- 24	B _x
"	25- 48	B _y
"	49- 72	B _z
"	73- 95	B,
"	96-288	Fill, 0

APPENDIX C.

MASTER DATA TAPE FORMAT

Each day is a 496 CDC 60-bit word record.

<u>Word</u>	<u>Type</u>	<u>Description</u>
1	Hollerith	Tape Number Assigned by Aerospace Corporation
2	"	Date Processed by Aerospace Corporation
3	Integer	Day of Year
4	"	Month
5	"	Day of Month
6	"	Year
7	Real	Radius, ER, or -1.
8	"	Latitude, Deg., or -1.
9	"	Longitude, Deg., or -1.
10- 16	"	Fill, -1.
17- 40	"	E1, Hourly averages, or -1.
41- 64	"	E2 "
65- 88	"	E3 "
89-112	"	E4 "
113-136	"	P1 "
137-160	"	P2 "
161-184	"	P3 "
185-208	"	P4 "
209-232	"	P5 "
233-256	"	P6 "
257-280	"	P7 "
281-304	"	P8 "
305-328	"	B _x "
329-352	"	B _y "
353-376	"	B _z "
377-400	"	B
401-496	"	Fill, -1.

IV. DATA CATALOG

IV. DATA CATALOG

FEC	AC TAPE	P#OC	CY	MN	DM	YEAR	F	LAT	LONG	E1	P1	BX
52	045680	HD	07/15/77	216	8	4	1974	-6° 62'	-0° 00'	266° 27'	172548° 16'	-11° -108° 38'
53	079104	HD	08/22/75	217	8	5	1974	-6° 00'	-0° 00'	-0° 00'	375871° 95'	-31° -0° 00'
54	079111	HD	08/23/75	218	8	6	1974	-6° 00'	-0° 00'	-0° 00'	265396° 49'	-31° -0° 00'
	INCONSISTENT DAYS											
55	79051	01/05/76	219	7	8	6	1974	-7° 00'	-0° 00'	-0° 00'	374645° 62'	-15° -0° 00'
56	79071	01/16/76	220	7	8	7	1974	-7° 00'	-0° 00'	-0° 00'	371686° 03'	-12° -0° 00'
57	79061	01/06/76	221	7	8	8	1974	-7° 00'	-0° 00'	-0° 00'	3229097° 35'	-3° -0° 00'
	INCONSISTENT DAYS											
58	79072	01/07/76	1112	7	9	6	1974	-7° 00'	-0° 00'	-0° 00'	444539° 67'	-67° -0° 00'
59	044506	HD	07/03/76	223	7	10	1974	-6° 62'	-0° 00'	-0° 00'	3545187° 02'	-1° -0° 00'
60	044514	HD	07/13/76	224	7	11	1974	-6° 62'	-0° 01'	-0° 01'	446408° 02'	-1° -0° 00'
61	79013	HD	08/27/75	225	7	12	1974	-6° 62'	-0° 00'	-0° 00'	2664744° 24'	-1° -0° 00'
62	79016	HD	08/29/75	226	7	13	1974	-6° 62'	-0° 00'	-0° 00'	2664744° 24'	-1° -0° 00'
63	79018	HD	08/29/75	227	7	14	1974	-6° 62'	-0° 00'	-0° 00'	2664744° 24'	-1° -0° 00'
64	79015	HD	08/23/75	228	7	15	1974	-6° 62'	-0° 00'	-0° 00'	2664744° 24'	-1° -0° 00'
65	79006	HD	07/13/76	229	7	16	1974	-6° 62'	-0° 00'	-0° 00'	2664744° 24'	-1° -0° 00'
66	79034	HD	01/16/76	230	7	17	1974	-6° 62'	-0° 00'	-0° 00'	2664744° 24'	-1° -0° 00'
67	79009	HD	09/02/75	231	7	18	1974	-6° 62'	-0° 00'	-0° 00'	2664744° 24'	-1° -0° 00'
68	79029	HD	01/16/76	232	7	19	1974	-6° 62'	-0° 00'	-0° 00'	2664744° 24'	-1° -0° 00'
69	79029	HD	01/16/76	233	7	20	1974	-6° 62'	-0° 00'	-0° 00'	2664744° 24'	-1° -0° 00'
70	79029	HD	01/16/76	234	7	21	1974	-6° 62'	-0° 00'	-0° 00'	2664744° 24'	-1° -0° 00'
71	79029	HD	01/16/76	235	7	22	1974	-6° 62'	-0° 00'	-0° 00'	2664744° 24'	-1° -0° 00'
	1 DAYS MISSING											
72	044468	HD	07/13/76	237	8	1	1974	-6° 62'	-0° 00'	-0° 00'	478375° 66'	-23° -0° 00'
73	79105	HD	09/03/75	238	8	2	1974	-6° 62'	-0° 00'	-0° 00'	395616° 93'	-23° -0° 00'
74	79033	HD	09/03/75	239	8	3	1974	-6° 62'	-0° 00'	-0° 00'	270603° 26'	-23° -0° 00'
	1 DAYS MISSING											
75	79073	09/05/75	1974	9	1	1	1974	-6° 62'	-0° 00'	-0° 00'	312096° 70'	-32° -0° 00'
76	79031	09/05/75	1974	9	2	2	1974	-6° 62'	-0° 00'	-0° 00'	304061° 71'	-32° -0° 00'
77	79073	09/05/75	1974	9	3	3	1974	-6° 62'	-0° 00'	-0° 00'	236330° 70'	-32° -0° 00'
78	79014	HD	07/13/76	1974	9	4	1974	-6° 62'	-0° 01'	-0° 01'	40327° 71'	-32° -0° 00'
79	044502	HD	07/13/76	1974	9	5	1974	-6° 62'	-0° 00'	-0° 00'	2664744° 78'	-32° -0° 00'
80	044503	HD	07/13/76	1974	9	6	1974	-6° 62'	-0° 00'	-0° 00'	22655° 77'	-32° -0° 00'
81	044504	HD	07/13/76	1974	9	7	1974	-6° 62'	-0° 00'	-0° 00'	22655° 77'	-32° -0° 00'
82	044505	HD	07/13/76	1974	9	8	1974	-6° 62'	-0° 00'	-0° 00'	22655° 77'	-32° -0° 00'
83	044506	HD	07/13/76	1974	9	9	1974	-6° 62'	-0° 00'	-0° 00'	22655° 77'	-32° -0° 00'
84	044507	HD	07/13/76	1974	9	10	1974	-6° 62'	-0° 00'	-0° 00'	22655° 77'	-32° -0° 00'
85	044508	HD	07/13/76	1974	9	11	1974	-6° 62'	-0° 00'	-0° 00'	22655° 77'	-32° -0° 00'
86	044509	HD	07/13/76	1974	9	12	1974	-6° 62'	-0° 00'	-0° 00'	22655° 77'	-32° -0° 00'
87	044510	HD	07/13/76	1974	9	13	1974	-6° 62'	-0° 00'	-0° 00'	22655° 77'	-32° -0° 00'
88	044511	HD	07/13/76	1974	9	14	1974	-6° 62'	-0° 00'	-0° 00'	22655° 77'	-32° -0° 00'
89	044512	HD	07/13/76	1974	9	15	1974	-6° 62'	-0° 00'	-0° 00'	22655° 77'	-32° -0° 00'
90	044513	HD	07/13/76	1974	9	16	1974	-6° 62'	-0° 00'	-0° 00'	22655° 77'	-32° -0° 00'
91	044514	HD	07/13/76	1974	9	17	1974	-6° 62'	-0° 00'	-0° 00'	22655° 77'	-32° -0° 00'
92	044515	HD	07/13/76	1974	9	18	1974	-6° 62'	-0° 00'	-0° 00'	22655° 77'	-32° -0° 00'
93	044516	HD	07/13/76	1974	9	19	1974	-6° 62'	-0° 00'	-0° 00'	22655° 77'	-32° -0° 00'
94	044517	HD	07/13/76	1974	9	20	1974	-6° 62'	-0° 00'	-0° 00'	22655° 77'	-32° -0° 00'
95	044518	HD	07/13/76	1974	9	21	1974	-6° 62'	-0° 00'	-0° 00'	22655° 77'	-32° -0° 00'
96	044519	HD	07/13/76	1974	9	22	1974	-6° 62'	-0° 00'	-0° 00'	22655° 77'	-32° -0° 00'
97	044520	HD	07/13/76	1974	9	23	1974	-6° 62'	-0° 00'	-0° 00'	22655° 77'	-32° -0° 00'
98	044521	HD	07/13/76	1974	9	24	1974	-6° 62'	-0° 00'	-0° 00'	22655° 77'	-32° -0° 00'
99	044522	HD	07/13/76	1974	9	25	1974	-6° 62'	-0° 00'	-0° 00'	22655° 77'	-32° -0° 00'
100	044523	HD	07/13/76	1974	9	26	1974	-6° 62'	-0° 00'	-0° 00'	22655° 77'	-32° -0° 00'
101	044524	HD	07/13/76	1974	9	27	1974	-6° 62'	-0° 00'	-0° 00'	22655° 77'	-32° -0° 00'
102	044525	HD	07/13/76	1974	9	28	1974	-6° 62'	-0° 00'	-0° 00'	22655° 77'	-32° -0° 00'
103	044526	HD	07/13/76	1974	9	29	1974	-6° 62'	-0° 00'	-0° 00'	22655° 77'	-32° -0° 00'
104	044527	HD	07/13/76	1974	9	30	1974	-6° 62'	-0° 00'	-0° 00'	22655° 77'	-32° -0° 00'
105	044528	HD	07/13/76	1974	9	31	1974	-6° 62'	-0° 00'	-0° 00'	22655° 77'	-32° -0° 00'
106	044529	HD	07/13/76	1974	9	32	1974	-6° 62'	-0° 00'	-0° 00'	22655° 77'	-32° -0° 00'
107	044530	HD	07/13/76	1974	9	33	1974	-6° 62'	-0° 00'	-0° 00'	22655° 77'	-32° -0° 00'
108	044531	HD	07/13/76	1974	9	34	1974	-6° 62'	-0° 00'	-0° 00'	22655° 77'	-32° -0° 00'
109	044532	HD	07/13/76	1974	9	35	1974	-6° 62'	-0° 00'	-0° 00'	22655° 77'	-32° -0° 00'
110	044533	HD	07/13/76	1974	9	36	1974	-6° 62'	-0° 00'	-0° 00'	22655° 77'	-32° -0° 00'
111	044534	HD	07/13/76	1974	9	37	1974	-6° 62'	-0° 00'	-0° 00'	22655° 77'	-32° -0° 00'
112	044535	HD	07/13/76	1974	9	38	1974	-6° 62'	-0° 00'	-0° 00'	22655° 77'	-32° -0° 00'
113	044536	HD	07/13/76	1974	9	39	1974	-6° 62'	-0° 00'	-0° 00'	22655° 77'	-32° -0° 00'
114	044537	HD	07/13/76	1974	9	40	1974	-6° 62'	-0° 00'	-0° 00'	22655° 77'	-32° -0° 00'
115	044538	HD	07/13/76	1974	9	41	1974	-6° 62'	-0° 00'	-0° 00'	22655° 77'	-32° -0° 00'
116	044539	HD	07/13/76	1974	9	42	1974	-6° 62'	-0° 00'	-0° 00'	22655° 77'	-32° -0° 00'
117	044540	HD	07/13/76	1974	9	43	1974	-6° 62'	-0° 00'	-0° 00'	22655° 77'	-32° -0° 00'
118	044541	HD	07/13/76	1974	9	44	1974	-6° 62'	-0° 00'	-0° 00'	22655° 77'	-32° -0° 00'
119	044542	HD	07/13/76	1974	9	45	1974	-6° 62'	-0° 00'	-0° 00'	22655° 77'	-32° -0° 00'
120	044543	HD	07/13/76	1974	9	46	1974	-6° 62'	-0° 00'	-0° 00'	22655° 77'	-32° -0° 00'
121	044544	HD	07/13/76	1974	9	47	1974	-6° 62'	-0° 00'	-0° 00'	22655° 77'	-32° -0° 00'
122	044545	HD	07/13/76	1974	9	48	1974	-6° 62'	-0° 00'	-0° 00'	22655° 77'	-32° -0° 00'
123	044546	HD	07/13/76	1974	9	49	1974	-6° 62'	-0° 00'	-0° 00'	22655° 77'	-32° -0° 00'
124	044547	HD	07/13/76	1974	9	50	1974	-6° 62'	-0° 00'	-0° 00'	22655° 77'	-32° -0° 00'
125	044548	HD	07/13/76	1974	9	51	1974	-6° 62'	-0° 00'	-0° 00'	22655° 77'	-32° -0° 00'
126	044549	HD	07/13/76	1974	9	52	1974	-6° 62'	-0° 00'	-0° 00'	22655° 77'	-32° -0° 00'
127	044550	HD	07/13/76	1974	9	53	1974	-6° 62'	-0° 00'	-0° 00'	22655° 77'	-32° -0° 00'
128	044551	HD	07/13/76	1974	9	54	1974	-6° 62'	-0° 00'	-0° 00'	22655° 77'	-32° -0° 00'
129	044552	HD	07/13/76	1974	9	55	1974	-6° 62'	-0° 00'	-0° 00'	22655° 77'	-32° -0° 00'
130	044553	HD	07/13/76	1974	9	56	1974	-6° 62'	-0° 00'	-0° 00'	22655° 77'	-32° -0° 00'
131	044554	HD	07/13/76	1974	9	57	1974	-6° 62'	-0° 00'	-0° 00'	22655° 77'	-32° -0° 00'
132	044555	HD	07/13/76	1974	9	58	1974	-6° 62'	-0° 00'	-0° 00'	22655° 77'	-32° -0° 00'
133	044556	HD	07/13/76	1974	9	59	1974	-6° 62'	-0° 00'	-0° 00'	22655° 77'	-32° -0° 00'
134	044557	HD	07/13/76	1974	9	60	1974	-6° 62'	-0° 00'	-0° 00'	22655° 77'	-32° -0° 00'
135	044558	HD	07/13/76	1974	9	61	1974	-6° 62'	-0° 00'	-0		

REC	AC TAPE	PROC	BY	MN	DM	YEAR	R	LAT	LON	E1	P1	BX
463	0 45746	HD	08/12/77				0	07/01/76	07/01/76	05	-6.55	-1.99
464	0 44530	HD	07/01/76				0	07/01/76	07/01/76	04	-1.92	-1.92
	I INCONSISTENT DAYS						0	07/01/76	07/01/76	03	-1.98	-1.98
465	0 44531	HD	08/12/77				0	07/01/76	07/01/76	02	-1.96	-1.96
466	0 44532	HD	08/12/77				0	07/01/76	07/01/76	01	-1.94	-1.94
	I INCONSISTENT DAYS						0	07/01/76	07/01/76	00	-1.92	-1.92
467	0 44533	HD	08/12/77				0	07/01/76	07/01/76	00	-1.90	-1.90
468	0 44534	HD	08/12/77				0	07/01/76	07/01/76	00	-1.88	-1.88
	I INCONSISTENT DAYS						0	07/01/76	07/01/76	00	-1.86	-1.86
469	0 44535	HD	08/12/77				0	07/01/76	07/01/76	00	-1.84	-1.84
470	0 44536	HD	08/12/77				0	07/01/76	07/01/76	00	-1.82	-1.82
	I INCONSISTENT DAYS						0	07/01/76	07/01/76	00	-1.80	-1.80
471	0 44537	HD	08/12/77				0	07/01/76	07/01/76	00	-1.78	-1.78
472	0 44538	HD	08/12/77				0	07/01/76	07/01/76	00	-1.76	-1.76
	I INCONSISTENT DAYS						0	07/01/76	07/01/76	00	-1.74	-1.74
473	0 44539	HD	08/12/77				0	07/01/76	07/01/76	00	-1.72	-1.72
474	0 44540	HD	08/12/77				0	07/01/76	07/01/76	00	-1.70	-1.70
	I INCONSISTENT DAYS						0	07/01/76	07/01/76	00	-1.68	-1.68
475	0 44541	HD	08/12/77				0	07/01/76	07/01/76	00	-1.66	-1.66
476	0 44542	HD	08/12/77				0	07/01/76	07/01/76	00	-1.64	-1.64
	I INCONSISTENT DAYS						0	07/01/76	07/01/76	00	-1.62	-1.62
477	0 44543	HD	08/12/77				0	07/01/76	07/01/76	00	-1.60	-1.60
478	0 44544	HD	08/12/77				0	07/01/76	07/01/76	00	-1.58	-1.58
	I INCONSISTENT DAYS						0	07/01/76	07/01/76	00	-1.56	-1.56
479	0 44545	HD	08/12/77				0	07/01/76	07/01/76	00	-1.54	-1.54
480	0 44546	HD	08/12/77				0	07/01/76	07/01/76	00	-1.52	-1.52
	I INCONSISTENT DAYS						0	07/01/76	07/01/76	00	-1.50	-1.50
481	0 44547	HD	08/12/77				0	07/01/76	07/01/76	00	-1.48	-1.48
482	0 44548	HD	08/12/77				0	07/01/76	07/01/76	00	-1.46	-1.46
	I INCONSISTENT DAYS						0	07/01/76	07/01/76	00	-1.44	-1.44
483	0 44549	HD	08/12/77				0	07/01/76	07/01/76	00	-1.42	-1.42
484	0 44550	HD	08/12/77				0	07/01/76	07/01/76	00	-1.40	-1.40
	I INCONSISTENT DAYS						0	07/01/76	07/01/76	00	-1.38	-1.38
485	0 44551	HD	08/12/77				0	07/01/76	07/01/76	00	-1.36	-1.36
486	0 44552	HD	08/12/77				0	07/01/76	07/01/76	00	-1.34	-1.34
	I INCONSISTENT DAYS						0	07/01/76	07/01/76	00	-1.32	-1.32
487	0 44553	HD	08/12/77				0	07/01/76	07/01/76	00	-1.30	-1.30
488	0 44554	HD	08/12/77				0	07/01/76	07/01/76	00	-1.28	-1.28
	I INCONSISTENT DAYS						0	07/01/76	07/01/76	00	-1.26	-1.26
489	0 44555	HD	08/12/77				0	07/01/76	07/01/76	00	-1.24	-1.24
490	0 44556	HD	08/12/77				0	07/01/76	07/01/76	00	-1.22	-1.22
	I INCONSISTENT DAYS						0	07/01/76	07/01/76	00	-1.20	-1.20
491	0 44557	HD	08/12/77				0	07/01/76	07/01/76	00	-1.18	-1.18
492	0 44558	HD	08/12/77				0	07/01/76	07/01/76	00	-1.16	-1.16
	I INCONSISTENT DAYS						0	07/01/76	07/01/76	00	-1.14	-1.14
493	0 44559	HD	08/12/77				0	07/01/76	07/01/76	00	-1.12	-1.12
494	0 44560	HD	08/12/77				0	07/01/76	07/01/76	00	-1.10	-1.10
	I INCONSISTENT DAYS						0	07/01/76	07/01/76	00	-1.08	-1.08
495	0 44561	HD	08/12/77				0	07/01/76	07/01/76	00	-1.06	-1.06
496	0 44562	HD	08/12/77				0	07/01/76	07/01/76	00	-1.04	-1.04
	I INCONSISTENT DAYS						0	07/01/76	07/01/76	00	-1.02	-1.02
497	0 44563	HD	08/12/77				0	07/01/76	07/01/76	00	-1.00	-1.00
498	0 44564	HD	08/12/77				0	07/01/76	07/01/76	00	-0.98	-0.98
	I INCONSISTENT DAYS						0	07/01/76	07/01/76	00	-0.96	-0.96
499	0 44565	HD	08/12/77				0	07/01/76	07/01/76	00	-0.94	-0.94
500	0 44566	HD	08/12/77				0	07/01/76	07/01/76	00	-0.92	-0.92
	I INCONSISTENT DAYS						0	07/01/76	07/01/76	00	-0.90	-0.90
501	0 44567	HD	08/12/77				0	07/01/76	07/01/76	00	-0.88	-0.88
502	0 44568	HD	08/12/77				0	07/01/76	07/01/76	00	-0.86	-0.86
	I INCONSISTENT DAYS						0	07/01/76	07/01/76	00	-0.84	-0.84
503	0 44569	HD	08/12/77				0	07/01/76	07/01/76	00	-0.82	-0.82
504	0 44570	HD	08/12/77				0	07/01/76	07/01/76	00	-0.80	-0.80
	I INCONSISTENT DAYS						0	07/01/76	07/01/76	00	-0.78	-0.78
505	0 44571	HD	08/12/77				0	07/01/76	07/01/76	00	-0.76	-0.76
506	0 44572	HD	08/12/77				0	07/01/76	07/01/76	00	-0.74	-0.74
	I INCONSISTENT DAYS						0	07/01/76	07/01/76	00	-0.72	-0.72
507	0 44573	HD	08/12/77				0	07/01/76	07/01/76	00	-0.70	-0.70
508	0 44574	HD	08/12/77				0	07/01/76	07/01/76	00	-0.68	-0.68
	I INCONSISTENT DAYS						0	07/01/76	07/01/76	00	-0.66	-0.66
509	0 44575	HD	08/12/77				0	07/01/76	07/01/76	00	-0.64	-0.64
510	0 44576	HD	08/12/77				0	07/01/76	07/01/76	00	-0.62	-0.62
	I INCONSISTENT DAYS						0	07/01/76	07/01/76	00	-0.60	-0.60
511	0 44577	HD	08/12/77				0	07/01/76	07/01/76	00	-0.58	-0.58
512	0 44578	HD	08/12/77				0	07/01/76	07/01/76	00	-0.56	-0.56
	I INCONSISTENT DAYS						0	07/01/76	07/01/76	00	-0.54	-0.54
513	0 44579	HD	08/12/77				0	07/01/76	07/01/76	00	-0.52	-0.52
514	0 44580	HD	08/12/77				0	07/01/76	07/01/76	00	-0.50	-0.50
	I INCONSISTENT DAYS						0	07/01/76	07/01/76	00	-0.48	-0.48
515	0 44581	HD	08/12/77				0	07/01/76	07/01/76	00	-0.46	-0.46
516	0 44582	HD	08/12/77				0	07/01/76	07/01/76	00	-0.44	-0.44
	I INCONSISTENT DAYS						0	07/01/76	07/01/76	00	-0.42	-0.42
517	0 44583	HD	08/12/77				0	07/01/76	07/01/76	00	-0.40	-0.40
518	0 44584	HD	08/12/77				0	07/01/76	07/01/76	00	-0.38	-0.38
	I INCONSISTENT DAYS						0	07/01/76	07/01/76	00	-0.36	-0.36
519	0 44585	HD	08/12/77				0	07/01/76	07/01/76	00	-0.34	-0.34
520	0 44586	HD	08/12/77				0	07/01/76	07/01/76	00	-0.32	-0.32
	I INCONSISTENT DAYS						0	07/01/76	07/01/76	00	-0.30	-0.30
521	0 44587	HD	08/12/77				0	07/01/76	07/01/76	00	-0.28	-0.28
522	0 44588	HD	08/12/77				0	07/01/76	07/01/76	00	-0.26	-0.26
	I INCONSISTENT DAYS						0	07/01/76	07/01/76	00	-0.24	-0.24
523	0 44589	HD	08/12/77				0	07/01/76	07/01/76	00	-0.22	-0.22
524	0 44590	HD	08/12/77				0	07/01/76	07/01/76	00	-0.20	-0.20
	I INCONSISTENT DAYS						0	07/01/76	07/01/76	00	-0.18	-0.18
525	0 44591	HD	08/12/77				0	07/01/76	07/01/76	00	-0.16	-0.16
526	0 44592	HD	08/12/77				0	07/01/76	07/01/76	00	-0.14	-0.14
	I INCONSISTENT DAYS						0	07/01/76	07/01/76	00	-0.12	-0.12
527	0 44593	HD	08/12/77				0	07/01/76	07/01/76	00	-0.10	-0.10
528	0 44594	HD	08/12/77				0	07/01/76	07/01/76	00	-0.08	-0.08
	I INCONSISTENT DAYS						0	07/01/76	07/01/76	00	-0.06	-0.06
529	0 44595	HD	08/12/77				0	07/01/76	07/01/76	00	-0.04	-0.04
530	0 44596	HD	08/12/77				0	07/01/76	07/01/76	00	-0.02	-0.02
	I INCONSISTENT DAYS						0	07/01/76	07/01/76	00	0.00	0.00
531	0 44597	HD	08/12/77				0	07/01/76	07/01/76	00	0.02	0.02
532	0 44598	HD	08/12/77				0	07/01/76	07/01/76	00	0.04	0.04
	I INCONSISTENT DAYS						0	07/01/76	07/01/76	00	0.06	0.06
533	0 44599	HD	08/12/77				0	07/01/76	07/01/76	00	0.08	0.08
534	0 44600	HD	08/12/77				0	07/01/76	07/01/76	00	0.10	0.10
	I INCONSISTENT DAYS						0	07/01/76	07/01/76	00	0.12	0.12
535	0 44601	HD	08/12/77				0	07/01/76	07/01/76	00	0.14	0.14
536	0 44602	HD	08/12/77				0	07/01/76	07/01/76	00	0.16	0.16
	I INCONSISTENT DAYS						0	07/01/76	07/01/76	00	0.18	0.18
537	0 44603	HD	08/12/77				0	07/01/76	07/01/76	00	0.20	0.20
538	0 44604	HD	08/12/77				0	07/01/76				

FEC	AC TAPE	PROC	LY	MN	DM	YEAR	K	LAT	LON	E1	P1	BX
734	045327	HD	03/26/77	164	7	2	1976	6° 62'	• 00	522691° 14'	• 32	-26° 41'
735	045295	HD	03/26/77	165	7	4	1976	6° 62'	- 00	52408229° 33	• 42	-20° 09'
736	045297	HD	03/26/77	186	7	4				52408229° 33	• 42	-20° 09'
1 DAYS MISSING												
737	045309	HD	03/26/77	168	7	6	1976	6° 62'	- 03	36502° 05	247	-24° 36'
738	045319	HD	03/26/77	169	7	6	1976	6° 62'	- 03	36502° 05	247	-24° 36'
739	045308	HD	03/26/77	191	7	9	1976	6° 62'	- 03	36502° 05	247	-24° 36'
740	045290	HD	03/26/77	192	7	10	1976	6° 62'	- 03	36502° 05	247	-24° 36'
741	045296	HD	03/26/77	193	7	11	1976	6° 62'	- 03	36502° 05	247	-24° 36'
1 DAYS MISSING												
742	045309	HD	03/26/77	169	7	7	1976	6° 62'	- 03	36502° 05	247	-24° 36'
743	044704	HD	03/26/77	195	7	13	1976	6° 62'	- 03	181374° 56	247	-24° 36'
744	044700	HD	03/26/77	196	7	14	1976	6° 62'	- 03	1203669° 09	247	-24° 36'
745	0445320	HD	04/04/77	197	7	14	1976	6° 62'	- 03	1203669° 09	247	-24° 36'
746	0445329	HD	04/04/77	198	7	14	1976	6° 62'	- 03	1203669° 09	247	-24° 36'
747	0445328	HD	04/04/77	199	7	14	1976	6° 62'	- 03	1203669° 09	247	-24° 36'
748	0445329	HD	04/04/77	200	7	14	1976	6° 62'	- 03	1203669° 09	247	-24° 36'
749	0445329	HD	04/04/77	201	7	14	1976	6° 62'	- 03	1203669° 09	247	-24° 36'
750	0445329	HD	04/04/77	202	7	14	1976	6° 62'	- 03	1203669° 09	247	-24° 36'
751	0445329	HD	04/04/77	203	7	14	1976	6° 62'	- 03	1203669° 09	247	-24° 36'
752	0445329	HD	04/04/77	204	7	14	1976	6° 62'	- 03	1203669° 09	247	-24° 36'
753	0445329	HD	04/04/77	205	7	14	1976	6° 62'	- 03	1203669° 09	247	-24° 36'
1 DAYS MISSING												
754	045306	HD	03/26/77	207	7	25	1976	6° 62'	- 00	155197° 30	• 18	-19° 21'
1 DAYS MISSING												
755	044705	HD	04/04/77	209	7	27	1976	6° 62'	- 02	165637° 97	247	-24° 36'
756	0445322	HD	04/15/77	210	7	27	1976	6° 62'	- 02	142184° 84	247	-24° 36'
757	0445328	HD	04/15/77	211	7	27	1976	6° 62'	- 02	1385462° 30	247	-24° 36'
758	0445328	HD	04/15/77	212	7	27	1976	6° 62'	- 02	1385462° 30	247	-24° 36'
759	0445316	HD	04/15/77	213	7	27	1976	6° 62'	- 02	1385462° 30	247	-24° 36'
760	0445316	HD	04/15/77	214	7	27	1976	6° 62'	- 02	1385462° 30	247	-24° 36'
761	0445326	HD	04/15/77	215	7	27	1976	6° 62'	- 02	1385462° 30	247	-24° 36'
762	0445326	HD	04/15/77	216	7	27	1976	6° 62'	- 02	1385462° 30	247	-24° 36'
763	0445313	HD	04/04/77	217	7	27	1976	6° 62'	- 02	1385462° 30	247	-24° 36'
764	0445313	HD	04/04/77	218	7	27	1976	6° 62'	- 02	1385462° 30	247	-24° 36'
1 DAYS MISSING												
765	045339	HD	03/26/77	220	8	23	1976	6° 62'	• 00	375652° 07	247	-24° 36'
766	045351	HD	03/26/77	221	8	23	1976	6° 62'	• 00	375652° 07	247	-24° 36'
767	045342	HD	04/04/77	222	8	23	1976	6° 62'	• 00	375652° 07	247	-24° 36'
768	045342	HD	04/04/77	223	8	23	1976	6° 62'	• 00	375652° 07	247	-24° 36'
769	045332	HD	04/04/77	224	8	23	1976	6° 62'	• 00	375652° 07	247	-24° 36'

REC	AC TAPE	PROC	DY	MN	DM	YEAR	R	LAT	LONG	E1	P1	BX	
770	045331	HD	04/06/77	225	8	12	1976	5.63	.08	21.86	457555.80	.36	-22.36
	1 DAYS MISSING												
771	045324	HD	04/06/77	227	9	14	1976	6.63	-.02	18.99	251714.64	.17	-19.88
772	045343	HD	04/06/77	228	8	15	1976	6.63	-.00	17.48	162460.84	.32	-22.85
773	045347	HD	04/06/77	249	9	16	1976	6.63	-.00	16.02	214524.85	.27	-20.62
	1 DAYS MISSING												
774	045345	HD	04/07/77	231	8	16	1976	5.63	-.00	13.11	101856.90	.20	-18.96
	1 DAYS MISSING												
775	045317	HD	04/06/77	233	8	20	1976	6.63	-.00	10.22	60831.81	.30	-21.48
776	045312	HD	04/06/77	229	8	21	1976	6.63	-.00	9.78	93043.10	.30	-21.33
777	045344	HD	04/07/77	234	8	23	1976	6.63	-.00	7.34	143452.02	.23	-21.72
778	045334	HD	04/07/77	235	8	24	1976	6.63	-.00	5.96	1432318.70	.27	-21.86
779	045335	HD	04/07/77	236	8	25	1976	6.63	-.00	4.45			
	INCONSISTENT DAYS												
780	045336	HD	04/07/77	237	8	26	1976	5.63	-.00	3.00	366874.39	.23	-21.38
	1 DAYS MISSING												
781	045346	HD	04/07/77	238	8	26	1976	5.63	-.00	1.56	413368.37	.23	-20.43

REC	AC TAPE	P2OC	UY	MN	ON	YEAR	F	LAT	LONG	E1	P1	BX
806	045383	HD	05/04/77	265	9	21 1976	6° 63'	324° 11'	472747.58	.21	-13.98	
807	045386	HD	05/04/77	266	9	22 1976	6° 63'	322° 66'	432946.60	.27	-14.58	
808	045425	HD	04/05/77	2267	9	22 1976	6° 63'	321° 21'	425492.02	.31	-14.25	
809	045414	HD	04/05/77	2268	9	22 1976	6° 63'	319° 76'	425005.99	.27	-14.26	
810	045410	HD	04/05/77	2269	9	22 1976	6° 63'	318° 38'	280344.34	.21	-11.54	
811	045387	HD	04/05/77	278				316° 05'	21 1805158.75			
	1 DAYS MISSING											
812	045315	HD	04/06/77	272	9	29 1976	5° 15'	305° 16'	32226947.90	.27	-12.24	
813	045394	HD	04/06/77	273	9	30 1976	5° 15'	303° 41'	32226947.90	.28	-12.25	
814	045367	HD	04/05/77	222	9	29 1976	5° 15'	300° 07'	32105060.70			
815	045395	HD	04/05/77	274	9	30 1976	5° 15'	300° 14'	2421371.25			
816	045393	HD	04/05/77	275	9	30 1976	5° 15'	300° 25'	11414205.92			
817	045393	HD	04/05/77	276	9	30 1976	5° 15'	300° 32'	280344.32			
	INCONSISTENT DAYS											
818	045406	HD	04/05/77	278	10	5 1976	5° 15'	305° 16'	32226947.90	.27	-12.24	
819	045426	HD	04/04/77	279	10	6 1976	5° 15'	303° 41'	32226947.90	.28	-12.25	
820	045399	HD	05/04/77	280	10	7 1976	5° 15'	300° 07'	32105060.70			
821	045399	HD	05/04/77	281	10	8 1976	5° 15'	300° 14'	2421371.25			
822	045407	HD	04/03/77	282	10	9 1976	5° 15'	300° 25'	11414205.92			
823	045407	HD	04/03/77	283	10	10 1976	5° 15'	300° 32'	280344.32			
824	045407	HD	04/03/77	284	10	11 1976	5° 15'	300° 38'	INCONSISTENT DAYS			
825	045407	HD	04/03/77	285	10	12 1976	5° 15'	300° 45'	32226947.90			
826	045407	HD	04/03/77	286	10	13 1976	5° 15'	300° 52'	11414205.92			
827	045407	HD	04/03/77	287	10	14 1976	5° 15'	300° 59'	280344.32			
828	045407	HD	04/03/77	288	10	15 1976	5° 15'	301° 06'	INCONSISTENT DAYS			
829	045407	HD	04/03/77	289	10	16 1976	5° 15'	301° 13'	32226947.90			
830	045407	HD	04/03/77	290	10	17 1976	5° 15'	301° 20'	11414205.92			
831	045407	HD	04/03/77	291	10	18 1976	5° 15'	301° 27'	280344.32			
832	045407	HD	04/03/77	292	10	19 1976	5° 15'	301° 34'	INCONSISTENT DAYS			
833	045407	HD	04/03/77	293	10	20 1976	5° 15'	301° 41'	32226947.90			
834	045407	HD	04/03/77	294	10	21 1976	5° 15'	301° 48'	11414205.92			
835	045407	HD	04/03/77	295	10	22 1976	5° 15'	301° 55'	280344.32			
836	045407	HD	04/03/77	296	10	23 1976	5° 15'	302° 02'	INCONSISTENT DAYS			
837	045415	HD	05/05/77	297	10	24 1976	5° 15'	302° 09'	32226947.90			
838	045433	HD	05/05/77	298	10	25 1976	5° 15'	302° 16'	11414205.92			
839	045435	HD	05/05/77	299	10	26 1976	5° 15'	302° 23'	280344.32			
	INCONSISTENT DAYS											
840	045430	HD	05/05/77	300	10	27 1976	5° 15'	302° 30'	INCONSISTENT DAYS			
841	045422	HD	05/05/77	301	10	28 1976	5° 15'	302° 37'	32226947.90			
842	045436	HD	05/05/77	302	10	29 1976	5° 15'	303° 04'	11414205.92			
843	045424	HD	05/05/77	303	10	30 1976	5° 15'	303° 11'	280344.32			
844	045426	HD	05/05/77	304	10	31 1976	5° 15'	303° 18'	INCONSISTENT DAYS			

REC	AC TAPE	PROC	DAY	MN	DH	YEAR	P	LAT	LON	E1	P1	BX
845	045423	HD	05/05/77	305	10	31	1976	6.63	327831.56	-5.38		
846	045417	HD	05/05/77	306	11	1	1976	5.63	383972.85	2.02		
	1	DAYS MISSING										
847	045439	HD	05/04/77	308	11	3	1976	6.66	3290191.57	5.97		
	045437	HD	05/05/77	310	11	3	1976	6.67	3342198.57	5.98		
	045435	HD	05/05/77	311	11	3	1976	6.68	332842956.57	5.99		
	045433	HD	05/05/77	312	11	3	1976	6.69	332241112954.57	6.00		
	045431	HD	05/05/77	313	11	3	1976	6.70	3325050.57	6.01		
	045429	HD	05/05/77	314	11	3	1976	6.71	3325050.57	6.02		
	045427	HD	05/05/77	315	11	3	1976	6.72	3325050.57	6.03		
	045425	HD	05/05/77	316	11	3	1976	6.73	3325050.57	6.04		
	045423	HD	05/05/77	317	11	3	1976	6.74	3325050.57	6.05		
	045421	HD	05/05/77	318	11	3	1976	6.75	3325050.57	6.06		
	1	DAYS MISSING										
855	045583	HD	06/01/77	320	11	15	1976	6.76	323970.59	3.60		
	045581	HD	06/01/77	321	11	16	1976	6.77	3240183.59	3.61		
	045579	HD	06/01/77	322	11	17	1976	6.78	3240247.59	3.62		
	045577	HD	06/01/77	323	11	18	1976	6.79	3240302.59	3.63		
	045575	HD	06/01/77	324	11	19	1976	6.80	3240357.59	3.64		
	045573	HD	06/01/77	325	11	20	1976	6.81	3240412.59	3.65		
	045571	HD	06/01/77	326	11	21	1976	6.82	3240477.59	3.66		
	045569	HD	06/01/77	327	11	22	1976	6.83	3241190.59	3.67		
	045567	HD	06/01/77	328	11	23	1976	6.84	3241190.59	3.68		
	045565	HD	06/01/77	329	11	24	1976	6.85	3241190.59	3.69		
	1	DAYS MISSING										
866	045485	HD	05/13/77	329	11	24	1975	5.63	67163.47	-31.22		
	1	DAYS MISSING										
867	045498	HD	05/17/77	330	11	25	1976	6.86	322904203.59	3.60		
	045496	HD	05/17/77	331	11	26	1976	6.87	322904203.59	3.61		
	045494	HD	05/17/77	332	11	27	1976	6.88	322904203.59	3.62		
	045492	HD	05/17/77	333	11	28	1976	6.89	322904203.59	3.63		
	045490	HD	05/17/77	334	11	29	1976	6.90	322904203.59	3.64		
	045488	HD	05/17/77	335	11	30	1976	6.91	322904203.59	3.65		
	045486	HD	05/17/77	336	11	31	1976	6.92	322904203.59	3.66		
	045484	HD	05/17/77	337	11	32	1976	6.93	322904203.59	3.67		
	045482	HD	05/17/77	338	11	33	1976	6.94	322904203.59	3.68		
	045480	HD	05/17/77	339	11	34	1976	6.95	322904203.59	3.69		
	045478	HD	05/17/77	340	11	35	1976	6.96	322904203.59	3.70		
	045476	HD	05/17/77	341	11	36	1976	6.97	322904203.59	3.71		
	045474	HD	05/17/77	342	11	37	1976	6.98	322904203.59	3.72		
	045472	HD	05/17/77	343	11	38	1976	6.99	322904203.59	3.73		
	045470	HD	05/17/77	344	11	39	1976	7.00	322904203.59	3.74		
	045468	HD	05/17/77	345	11	40	1976	7.01	322904203.59	3.75		
	045466	HD	05/17/77	346	11	41	1976	7.02	322904203.59	3.76		
	045464	HD	05/17/77	347	11	42	1976	7.03	322904203.59	3.77		
	045462	HD	05/17/77	348	11	43	1976	7.04	322904203.59	3.78		
	045460	HD	05/17/77	349	11	44	1976	7.05	322904203.59	3.79		
	045458	HD	05/17/77	350	11	45	1976	7.06	322904203.59	3.80		
	045456	HD	05/17/77	351	11	46	1976	7.07	322904203.59	3.81		
	045454	HD	05/17/77	352	11	47	1976	7.08	322904203.59	3.82		
	045452	HD	05/17/77	353	11	48	1976	7.09	322904203.59	3.83		
	045450	HD	05/17/77	354	11	49	1976	7.10	322904203.59	3.84		
	045448	HD	05/17/77	355	11	50	1976	7.11	322904203.59	3.85		
	045446	HD	05/17/77	356	11	51	1976	7.12	322904203.59	3.86		
	045444	HD	05/17/77	357	11	52	1976	7.13	322904203.59	3.87		
	045442	HD	05/17/77	358	11	53	1976	7.14	322904203.59	3.88		
	045440	HD	05/17/77	359	11	54	1976	7.15	322904203.59	3.89		
	045438	HD	05/17/77	360	11	55	1976	7.16	322904203.59	3.90		
	045436	HD	05/17/77	361	11	56	1976	7.17	322904203.59	3.91		
	045434	HD	05/17/77	362	11	57	1976	7.18	322904203.59	3.92		
	045432	HD	05/17/77	363	11	58	1976	7.19	322904203.59	3.93		
	045430	HD	05/17/77	364	11	59	1976	7.20	322904203.59	3.94		
	045428	HD	05/17/77	365	11	60	1976	7.21	322904203.59	3.95		
	045426	HD	05/17/77	366	11	61	1976	7.22	322904203.59	3.96		
	045424	HD	05/17/77	367	11	62	1976	7.23	322904203.59	3.97		
	045422	HD	05/17/77	368	11	63	1976	7.24	322904203.59	3.98		
	045420	HD	05/17/77	369	11	64	1976	7.25	322904203.59	3.99		
	045418	HD	05/17/77	370	11	65	1976	7.26	322904203.59	4.00		
	045416	HD	05/17/77	371	11	66	1976	7.27	322904203.59	4.01		
	045414	HD	05/17/77	372	11	67	1976	7.28	322904203.59	4.02		
	045412	HD	05/17/77	373	11	68	1976	7.29	322904203.59	4.03		
	045410	HD	05/17/77	374	11	69	1976	7.30	322904203.59	4.04		
	045408	HD	05/17/77	375	11	70	1976	7.31	322904203.59	4.05		
	045406	HD	05/17/77	376	11	71	1976	7.32	322904203.59	4.06		
	045404	HD	05/17/77	377	11	72	1976	7.33	322904203.59	4.07		
	045402	HD	05/17/77	378	11	73	1976	7.34	322904203.59	4.08		
	045400	HD	05/17/77	379	11	74	1976	7.35	322904203.59	4.09		
	045398	HD	05/17/77	380	11	75	1976	7.36	322904203.59	4.10		
	045396	HD	05/17/77	381	11	76	1976	7.37	322904203.59	4.11		
	045394	HD	05/17/77	382	11	77	1976	7.38	322904203.59	4.12		
	045392	HD	05/17/77	383	11	78	1976	7.39	322904203.59	4.13		
	045390	HD	05/17/77	384	11	79	1976	7.40	322904203.59	4.14		
	045388	HD	05/17/77	385	11	80	1976	7.41	322904203.59	4.15		
	045386	HD	05/17/77	386	11	81	1976	7.42	322904203.59	4.16		
	045384	HD	05/17/77	387	11	82	1976	7.43	322904203.59	4.17		
	045382	HD	05/17/77	388	11	83	1976	7.44	322904203.59	4.18		
	045380	HD	05/17/77	389	11	84	1976	7.45	322904203.59	4.19		
	045378	HD	05/17/77	390	11	85	1976	7.46	322904203.59	4.20		
	045376	HD	05/17/77	391	11	86	1976	7.47	322904203.59	4.21		
	045374	HD	05/17/77	392	11	87	1976	7.48	322904203.59	4.22		
	045372	HD	05/17/77	393	11	88	1976	7.49	322904203.59	4.23		
	045370	HD	05/17/77	394	11	89	1976	7.50	322904203.59	4.24		
	045368	HD	05/17/77	395	11	90	1976	7.51	322904203.59	4.25		
	045366	HD	05/17/77	396	11	91	1976	7.52	322904203.59	4.26		
	045364	HD	05/17/77	397	11	92	1976	7.53	322904203.59	4.27		
	045362	HD	05/17/77	398	11	93	1976	7.54	322904203.59	4.28		
	045360	HD	05/17/77	399	11	94	1976	7.55	322904203.59	4.29		
	045358	HD	05/17/77	400	11	95	1976	7.56	322904203.59	4.30		
	045356	HD	05/17/77	401	11	96	1976	7.57	322904203.59	4.31		
	045354	HD	05/17/77	402	11	97	1976	7.58	322904203.59	4.32		
	045352	HD	05/17/77	403	11	98	1976	7.59	322904203.59	4.33		
	045350	HD	05/17/77	404	11	99	1976	7.60	322904203.59	4.34		
	045348	HD	05/17/77	405	11	100	1976	7.61	322904203.59	4.35		
	045346	HD	05/17/77	406	11	101	1976	7.62	322904203.59	4.36		
	045344	HD	05/17/77	407	11	102	1976	7.63	322904203.59	4.37		
	045342	HD	05/17/77	408	11	103	1976	7.64	322904203.59	4.38		
	045340	HD	05/17/77	409	11	104	1976	7.65	322904203.59	4.39		
	045338	HD	05/17/77	410	11	105	1976	7.66	322904203.59	4.40		
	045336	HD	05/17/77	411	11	106	1976	7.67	322904203.59	4.41		

INCONSISTENT DAYS

FEC	AC TAPE	P2OC	CY	MN	DM	YEAR	F	LAT	LONG	E1	P1	BX		
1008	045613	HD	06/17/77	115	*	25	1977	6.62	- .00	219.97	323589.67	.25	20.06	
1009	045612	HD	06/15/77	116	*	26	1977	6.62	- .01	219.99	46790.96	.25	14.83	
	2 DAYS MISSING													
1010	045636	HD	06/30/77	119	*	29	1977	6.62	.03	220.04	254026.69	.19	27.45	
	1 DAYS MISSING													
1011	045614	HD	06/15/77	121	*	1	1977	6.62	- .00	220.07	361775.00	.29	9.19	
	1 DAYS MISSING													
1012	045794	HD	09/13/77	123	*	5	1977	6.62	- .01	220.12	517409.26	.22	14.87	
	3 DAYS MISSING													
1013	045777	HD	09/15/77	127	*	7	1977	6.62	- .00	220.03	387087.20	.28	12.76	
1014	045772	HD	09/13/77	128	*	9	1977	6.62	- .01	220.01	35569687.32	.22	11.76	
1015	045797	HD	09/13/77	129	*	13	1977	6.61	- .01	219.97	3769453.32	.15	15.43	
1016	045782	HD	09/13/77	130	*	13	1977	6.61	- .02	219.99	3252924525.33	.18	9.96	
1017	045795	HD	09/12/77	131	*	13	1977	6.62	- .01	219.99	465479.94	.14	2.96	
1018	045787	HD	09/12/77	132	*	13	1977	6.62	- .01	219.93	4303152.16	.10	9.96	
1019	045774	HD	09/12/77	133	*	13	1977	6.62	- .00	219.91	1036614.13	.14	6.95	
1020	045773	HD	09/12/77	134	*	15	1977	6.62	- .00	219.97	12.63	.12	6.43	
1021	045781	HD	09/20/77	135	*	16	1977	6.62	- .00	219.90	3756660.27	.10	8.83	
1022	045796	HD	09/20/77	136	*	17	1977	6.62	- .00	219.89	456173.27	.12	4.73	
1023	045779	HD	09/20/77	137	*	19	1977	6.62	- .00	219.89	497994.97	.10	8.83	
	1 DAYS MISSING													
1024														
1025	045842	HD	10/12/77	140	*	77	1977	6.62	- .06	219.89	583471.76	.21	2.65	
1026	045775	HD	09/15/77	141	*	77	1977	6.62	- .00	219.88	338671.93	.17	11.76	
1027	045778	HD	09/13/77	142	*	77	1977	6.62	- .01	219.89	48161.71	.21	11.76	
1028	045785	HD	09/13/77	143	*	77	1977	6.62	- .00	219.89	3168213.20	.15	4.73	
1029	045783	HD	09/13/77	144	*	77	1977	6.62	- .00	219.89	265921.90	.15	7.90	
1030	045780	HD	09/13/77	145	*	77	1977	6.62	- .00	219.89	311050.61	.15	6.95	
1031	045781	HD	09/20/77	146	*	77	1977	6.62	- .00	219.91	26204.90	.15	7.92	
1032	045793	HD	09/20/77	147	*	77	1977	6.62	- .01	219.94	39802.02	.23	3.72	
1033	045774	HD	09/20/77	148	*	77	1977	6.62	- .00	219.95	264310.56	.18	3.72	
1034	045779	HD	09/20/77	149	*	77	1977	6.62	- .00	219.95	467.01	.22	6.63	
	1 DAYS MISSING													
1035														
1036	029053	HD	12/03/77	152	*	77	1977	6.62	- .07	219.97	37716.72	.16	14.29	
1037	029057	HD	12/03/77	153	*	77	1977	6.62	- .02	220.00	163549.74	.22	11.76	
1038	029050	HD	12/03/77	154	*	77	1977	6.62	- .02	220.02	484774.25	.22	17.43	
1039	045804	HD	09/14/77	155	*	77	1977	6.62	- .01	220.05	454703.93	.15	11.33	
1040	045808	HD	09/14/77	156	*	77	1977	6.62	- .01	220.07	351819.53	.14	11.16	
	1 DAYS MISSING													

REC	AC TAPE	PROC	DY	MN	DM	YEAR	R	LAT	LONG	E1	P1	P2	BX
104-1	045812	HD	09/14/77			1977	6-61			0928916			111-11
104-2	045808	HD	09/14/77			1977	6-62			307439-66			111-11
104-3	045799	HD	09/14/77			1977	-0-01			229234-79			111-11
INCONSISTENT DAYS													
104-4	045798	HD	09/14/77			1977	6-63			05107461057			111-11
104-5	045804	HD	09/14/77			1977	6-64			21493705651			111-11
104-6	045802	HD	09/14/77			1977	6-65			21493705651			111-11
104-7	045809	HD	09/14/77			1977	6-66			21493705651			111-11
104-8	045801	HD	09/14/77			1977	6-67			21493705651			111-11
104-9	045807	HD	09/14/77			1977	6-68			21493705651			111-11
INCONSISTENT DAYS													
105-1	045813	HD	09/14/77			1977	6-69			09210501051			111-11
105-2	045803	HD	09/14/77			1977	6-70			09210501051			111-11
105-3	045800	HD	09/14/77			1977	6-71			09210501051			111-11
105-4	045808	HD	09/14/77			1977	6-72			09210501051			111-11
105-5	045805	HD	09/14/77			1977	6-73			09210501051			111-11
105-6	045802	HD	09/14/77			1977	6-74			09210501051			111-11
105-7	045809	HD	09/14/77			1977	6-75			09210501051			111-11
105-8	045806	HD	09/14/77			1977	6-76			09210501051			111-11
105-9	045803	HD	09/14/77			1977	6-77			09210501051			111-11
INCONSISTENT DAYS													
106-1	045812	HD	09/14/77			1977	6-78			09210501051			111-11
106-2	045808	HD	09/14/77			1977	6-79			09210501051			111-11
106-3	045799	HD	09/14/77			1977	6-80			09210501051			111-11
INCONSISTENT DAYS													
107-1	045813	HD	09/14/77			1977	6-81			09210501051			111-11
107-2	045803	HD	09/14/77			1977	6-82			09210501051			111-11
107-3	045800	HD	09/14/77			1977	6-83			09210501051			111-11
107-4	045808	HD	09/14/77			1977	6-84			09210501051			111-11
107-5	045805	HD	09/14/77			1977	6-85			09210501051			111-11
107-6	045802	HD	09/14/77			1977	6-86			09210501051			111-11
107-7	045809	HD	09/14/77			1977	6-87			09210501051			111-11
107-8	045806	HD	09/14/77			1977	6-88			09210501051			111-11
107-9	045803	HD	09/14/77			1977	6-89			09210501051			111-11
INCONSISTENT DAYS													
108-1	045812	HD	09/14/77			1977	6-90			09210501051			111-11
108-2	045808	HD	09/14/77			1977	6-91			09210501051			111-11
108-3	045799	HD	09/14/77			1977	6-92			09210501051			111-11
INCONSISTENT DAYS													
109-1	045813	HD	09/14/77			1977	6-93			09210501051			111-11
109-2	045803	HD	09/14/77			1977	6-94			09210501051			111-11
109-3	045800	HD	09/14/77			1977	6-95			09210501051			111-11
109-4	045808	HD	09/14/77			1977	6-96			09210501051			111-11
109-5	045805	HD	09/14/77			1977	6-97			09210501051			111-11
109-6	045802	HD	09/14/77			1977	6-98			09210501051			111-11
109-7	045809	HD	09/14/77			1977	6-99			09210501051			111-11
109-8	045806	HD	09/14/77			1977	6-100			09210501051			111-11
109-9	045803	HD	09/14/77			1977	6-101			09210501051			111-11
INCONSISTENT DAYS													
110-1	045812	HD	09/14/77			1977	6-102			09210501051			111-11
110-2	045808	HD	09/14/77			1977	6-103			09210501051			111-11
110-3	045799	HD	09/14/77			1977	6-104			09210501051			111-11
INCONSISTENT DAYS													
111-1	045813	HD	09/14/77			1977	6-105			09210501051			111-11
111-2	045803	HD	09/14/77			1977	6-106			09210501051			111-11
111-3	045800	HD	09/14/77			1977	6-107			09210501051			111-11
111-4	045808	HD	09/14/77			1977	6-108			09210501051			111-11
111-5	045805	HD	09/14/77			1977	6-109			09210501051			111-11
111-6	045802	HD	09/14/77			1977	6-110			09210501051			111-11
111-7	045809	HD	09/14/77			1977	6-111			09210501051			111-11
111-8	045806	HD	09/14/77			1977	6-112			09210501051			111-11
111-9	045803	HD	09/14/77			1977	6-113			09210501051			111-11
INCONSISTENT DAYS													
112-1	045812	HD	09/14/77			1977	6-114			09210501051			111-11
112-2	045808	HD	09/14/77			1977	6-115			09210501051			111-11
112-3	045799	HD	09/14/77			1977	6-116			09210501051			111-11
INCONSISTENT DAYS													
113-1	045813	HD	09/14/77			1977	6-117			09210501051			111-11
113-2	045803	HD	09/14/77			1977	6-118			09210501051			111-11
113-3	045800	HD	09/14/77			1977	6-119			09210501051			111-11
113-4	045808	HD	09/14/77			1977	6-120			09210501051			111-11
113-5	045805	HD	09/14/77			1977	6-121			09210501051			111-11
113-6	045802	HD	09/14/77			1977	6-122			09210501051			111-11
113-7	045809	HD	09/14/77			1977	6-123			09210501051			111-11
113-8	045806	HD	09/14/77			1977	6-124			09210501051			111-11
113-9	045803	HD	09/14/77			1977	6-125			09210501051			111-11
INCONSISTENT DAYS													
114-1	045812	HD	09/14/77			1977	6-126			09210501051			111-11
114-2	045808	HD	09/14/77			1977	6-127			09210501051			111-11
114-3	045799	HD	09/14/77			1977	6-128			09210501051			111-11
INCONSISTENT DAYS													
115-1	045813	HD	09/14/77			1977	6-129			09210501051			111-11
115-2	045803	HD	09/14/77			1977	6-130			09210501051			111-11
115-3	045800	HD	09/14/77			1977	6-131			09210501051			111-11
115-4	045808	HD	09/14/77			1977	6-132			09210501051			111-11
115-5	045805	HD	09/14/77			1977	6-133			09210501051			111-11
115-6	045802	HD	09/14/77			1977	6-134			09210501051			111-11
115-7	045809	HD	09/14/77			1977	6-135			09210501051			111-11
115-8	045806	HD	09/14/77			1977	6-136			09210501051			111-11
115-9	045803	HD	09/14/77			1977	6-137			09210501051			111-11
INCONSISTENT DAYS													
116-1	045812	HD	09/14/77			1977	6-138			09210501051			111-11
116-2	045808	HD	09/14/77			1977	6-139			09210501051			111-11
116-3	045799	HD	09/14/77			1977	6-140			09210501051			111-11
INCONSISTENT DAYS													
117-1	045813	HD	09/14/77			1977	6-141			09210501051			111-11
117-2	045803	HD	09/14/77			1977	6-142			09210501051			111-11
117-3	045800	HD	09/14/77			1977	6-143			09210501051			111-11
117-4	045808	HD	09/14/77			1977	6-144			09210501051			111-11
117-5	045805	HD	09/14/77			1977	6-145			09210501051			111-11
117-6	045802	HD	09/14/77			1977	6-146			09210501051			111-11
117-7	045809	HD	09/14/77			1977	6-147			09210501051			111-11
117-8	045806	HD	09/14/77			1977	6-148			09210501051			111-11
117-9	045803	HD	09/14/77			1977	6-149			09210501051			111-11
INCONSISTENT DAYS													
118-1	045812	HD	09/14/77			1977	6-150			09210501051			111-11
118-2	045808	HD	09/14/77			1977	6-151			09210501051			111-11
118-3	045799	HD	09/14/77			1977	6-152			09210501051			111-11
INCONSISTENT DAYS													
119-1	045813	HD	09/14/77			1977	6-153			09210501051			

REC	AC TAPE	PROC	DY	MN	UM	YEAR	R	LAT	LONG	E1	P1	BX
1082	045880	HD	10/14/77	7	19	1977	6.62	-0.00	220.00	5 06437.11	2 335207.95	
1083	045854	HD	10/12/77	120	19	1977	6.62	-0.00	219.96	4 97029.00	2 354561.95	
1084	045851	HD	10/14/77	21	19	1977	6.62	-0.00	219.95	4 79061.00	2 295656.95	
1085	045855	HD	10/14/77	22	19	1977	6.62	-0.00	219.93	4 79731.00	2 295657.95	
1086	045856	HD	10/07/77	23	19	1977	6.62	-0.00	219.92	4 69294.00	2 295658.95	
1087	045876	HD	10/07/77	24	19	1977	6.62	-0.00	219.91	4 53574.00	2 295659.95	
1088	045861	HD	10/07/77	25	19	1977	6.62	-0.00	219.90	4 64297.00	2 295660.95	
1089	045869	HD	10/08/77	26	19	1977	6.62	-0.00	219.88	2 98137.96	1 75605.95	
1090	045863	HD	10/08/77	27	19	1977	6.62	-0.00	219.87	2 49689.00	1 75605.95	
1091	045866	HD	10/09/77	28	19	1977	6.62	-0.00	219.86	2 39655.00	1 75605.95	
1092	045860	HD	10/09/77	29	19	1977	6.62	-0.00	219.86	5 24555.00	1 75605.95	
1093	045870	HD	10/12/77	30	19	1977	6.62	-0.00	219.86	5 24555.00	1 75605.95	
1094	045877	HD	10/12/77	21	19	1977	6.62	-0.00	219.85	4 51180.61	.17 12.57	
1095	045889	HD	10/03/77	213	3	1	1977	6.62	-0.00	219.85	4 51180.61	.17 12.57
1 DAYS MISSING												
INCONSISTENT DAYS												
1096	045866	HD	10/03/77	214	3	1	1977	6.62	-0.00	219.85	4 6863.00	
1097	045864	HD	10/08/77	215	8	1	1977	6.62	-0.12	219.85	3 6886.00	
1098	045875	HD	10/08/77	216	8	1	1977	6.62	-0.01	219.87	1 94139.95	
1099	045874	HD	10/09/77	217	8	0	1977	6.62	-0.01	219.87	2 11721.17	
1100	045892	HD	10/08/77	218	8	0	1977	6.62	-0.01	219.87	2 493644.00	
1101	045884	HD	10/08/77	219	8	0	1977	6.62	-0.01	219.88	3 8971.00	
1102	029041	HD	12/03/77	220	3	0	1977	6.62	-0.01	219.88	5 17266.37	
INCORRECT DAYS												
1 DAYS MISSING												
1103	029027	HD	12/03/77	222	9	1	1977	6.62	-0.01	219.90	4 00599.34	
1104	029030	HD	12/03/77	223	8	1	1977	6.62	-0.01	219.92	3 99604.23	
1 DAYS MISSING												
1105	045877	HD	10/03/77	225	8	1	1977	6.62	0.00	219.94	5 08318.00	
1106	045903	HD	10/12/77	226	8	1	1977	6.62	0.00	219.95	5 21456.00	
1107	045883	HD	10/08/77	227	8	1	1977	6.62	0.00	219.95	4 66262.00	
1108	029045	HD	12/03/77	228	8	1	1977	6.62	0.01	220.00	4 78432.00	
1109	045882	HD	10/03/77	229	8	1	1977	6.62	0.01	220.00	5 21066.00	
1110	045888	HD	10/08/77	230	8	1	1977	6.62	0.01	220.00	5 88526.00	
1111	029051	HD	12/03/77	231	8	1	1977	6.62	0.01	220.00	5 09351.95	
1112	029062	HD	12/03/77	232	8	1	1977	6.62	0.01	220.00	5 09358.00	
1113	029028	HD	12/03/77	233	8	1	1977	6.62	0.01	220.00	5 09358.00	
1114	029048	HD	12/03/77	234	8	1	1977	6.62	0.01	220.00	5 09358.00	
1 DAYS MISSING												

	BX	8.66	9.16	9.65	10.14	10.73	11.31	11.89	12.47	13.05	13.63	14.21
P1		2.5	2.4	2.0	1.9	1.7	1.6	1.5	1.4	1.3	1.2	1.1
E1		7.8	7.0	6.2	5.4	4.6	3.8	3.0	2.2	1.4	0.6	0.0
LON		9.9	9.8	9.6	9.5	9.5	9.6	9.6	9.6	9.6	9.6	9.6
-AT		0.1	0.1	0.1	0.0	0.0	0.0	0.0	0.0	0.0	0.0	0.0
F		6.2	6.2	6.2	6.2	6.2	6.2	6.2	6.2	6.2	6.2	6.2
YEAR		1977	1977	1977	1977	1977	1977	1977	1977	1977	1977	1977
DAY		236	228	220	314	235	235	235	235	235	235	235
MN		8	8	8	8	8	8	8	8	8	8	8
CY		3.6	3.7	3.8	3.9	3.9	3.9	3.9	3.9	3.9	3.9	3.9
PROG		12/1	12/1	12/1	12/1	12/1	12/1	12/1	12/1	12/1	12/1	12/1
AC TAPE		HD	HD	HD	HD	HD	HD	HD	HD	HD	HD	HD
PEC		1115	1116	1117	1118	1119	1120	1121	1122	1123	1124	1125

V. REPRINTS

**Modulation of Trapped Energetic Electrons at 6.6 R_e
by the Direction of the Interplanetary Magnetic Field**

G. A. Paulikas and J. B. Blake

Reprinted from

**Geophysical
Research
Letters**

Volume 3, Number 5, May 1976

T

MODULATION OF TRAPPED ENERGETIC ELECTRONS AT 6.6 R_e BY THE DIRECTION OF THE INTERPLANETARY MAGNETIC FIELD

G. A. Paulikas and J. B. Blake
Space Sciences Laboratory

The Aerospace Corporation
El Segundo, California

Abstract. Energetic ($E > 1.6$ MeV, > 3.9 MeV) trapped electron fluxes observed at the synchronous altitude during 1974 and 1975 by an experiment aboard ATS-6 exhibit a modulation in intensity which is correlated with the passage of sector structure boundaries of the interplanetary magnetic field past the earth. The electron fluxes reach equilibrium intensities during the time the magnetosphere is in a given IMF sector which are highest in the fall for (+) sectors and highest in the spring for (-) sectors.

Introduction

We have observed a periodicity in the magnetospheric energetic electron fluxes ($E > 1$ MeV) at $6.6 R_e$ associated with the passage of sector boundaries (Wilcox, 1968) of the interplanetary magnetic field. The changes in the electron flux, associated with each boundary passage, are the major intensity excursions of the electron fluxes during conditions of low solar activity. Furthermore, maximum intensity reached by the energetic electrons in the intervals between sector boundary passage is dependent upon the direction of the interplanetary magnetic field.

Changes in the intensity of trapped energetic electrons which could be associated with changes in the conditions existing in the interplanetary medium, and thus ultimately with the properties of magnetic field and plasma structure of the solar atmosphere, have been reported by Williams (1966) and Rothwell (1968). The observations which led these authors to conclude that the outer zone was markedly responsive to the sector structure of the interplanetary medium were obtained in the time interval near solar minimum in the middle 1960's. In 1968 we used ATS-1 data on energetic electrons which were obtained between late 1966 and early 1968 at the synchronous orbit in an attempt to verify the conclusions of Williams and Rothwell. Although the experimental situation in a synchronous orbit is somewhat "cleaner" than observations made aboard low-altitude spacecraft or high-altitude spacecraft in elliptical orbits, we failed to establish that any close correlation existed between changes in the electron fluxes observed at $6.6 R_e$, and changes in the direction of the interplanetary field. To be sure, sector boundary passages did give rise to major excursions in the flux levels of energetic

Copyright 1976 by the American Geophysical Union.

electrons; however equally large excursions also occurred when there were no IMF boundaries in the vicinity of the earth. These conclusions, now more than five years old, were once again checked in the course of the present study using the sector boundary catalog prepared by Svaalgaard (1975).

We were thus surprised to find that omnidirectional electron fluxes (hourly averages), as determined from data obtained by The Aerospace Corporation experiment aboard ATS-6 in 1974 and 1975, exhibit a very pronounced periodicity which is very clearly associated with the passage of interplanetary magnetic-field sector boundaries. ATS-6 was stationed at $6.6 R_e$ and at $94^\circ W$ during the time period under consideration; the experiment which yielded the data presented here is fully described in Paulikas et al. (1975). Figure 1 illustrates the observations made at noon local time. Similar plots have been constructed for other local times and these plots exhibit identical periodicities. A limited set of data from the synchronous spacecraft ATS-1, located at $150^\circ W$, and ATS-5, located at $105^\circ W$, also are available to us for portions of the time period under discussion. (ATS-5 data were graciously provided by C. E. McIlwain). Such comparisons as we have made indicate that ATS-1, ATS-5 and ATS-6 all observe the modulation; clearly the entire outer magnetosphere is involved. Evidently, strong, periodic modulation of the outer-zone trapped-particle intensities by the interaction between the magnetosphere and the interplanetary medium is a function of the general level of solar activity and emerges as the dominant process affecting the outer zone during conditions of solar minimum. During periods of high solar activity, the periodic modulation is masked by the more-or-less irregular occurrence of magnetic storms which destroy the coherence that the energetic electron fluxes would otherwise be expected to develop in response to interplanetary conditions.

Discussion

The outer-zone energetic electrons observed by ATS-6 are one of the end products of the interaction of the solar wind with the earth's magnetosphere. The magnetospheric substorm is the basic process which energizes magnetospheric plasma and transports these energetic particles into the stable-trapping region of the magnetosphere (McPherron et al., 1975). In the

absence of magnetic storms, the temporal evolution of the energetic electron population is a measure of the relative strength of the source (i.e., substorms) as compared to particle sinks. Our observations can be considered as representing an averaged, smoothed output of the solar wind-magnetosphere engine, with the equilibrium level of energetic electron fluxes indicative of the rate of occurrence of substorms, and hence the rate of "quiescent" energy transfer into the magnetosphere (Russell, 1974). In contrast, the changes in the electron fluxes at the time of boundary passage are associated with major disruption of the energetic electron population by magnetic storms.

We interpret our results using the phenomenological studies of Arnould (1974), Burton et al., (1975), Burch (1973), and Russell and McPherron (1973). The thrust of the findings of these authors, as summarized in the review of Russell (1974), is that the energy flow from the solar wind into magnetosphere mimics in some ways the behavior of a half-wave rectifier familiar in electronic applications. The input of energy into the magnetosphere proceeds only if the magnetosphere sees a southward component of the interplanetary magnetic field; a northward IMF component apparently inhibits the transfer of energy into the magnetosphere. Thus, to first approximation, the dynamics of the magnetosphere are a function of the orientation of the magnetosphere in solar-equatorial coordinates (the natural coordinates of the flow of the solar wind plasma). The geometrical arguments and coordinate transformations required to determine whether the magnetosphere sees a net northward or net southward component of the interplanetary magnetic field are somewhat complex and the reader should refer to the paper of Russell and McPherron (1973) for a complete and critical discussion of the problem. For our present purposes, we can summarize briefly: the interaction between solar wind and magnetosphere is expected to be strongest when the magnetosphere is immersed in a southward pointing interplanetary field. This occurs during northern hemisphere spring, when the earth is in a (-) sector of the interplanetary field, and in the fall, when the earth is in a (+) sector of the interplanetary field.

The data obtained during the fall of 1974 and presented in Figure 1 are consistent with this picture. The energetic electron fluxes appear to build up to higher levels during (+) sectors (i.e., generally southward IMF) than during (-) sectors. Note also that (-) to (+) sector transitions cause much deeper depressions in the electron flux than (+) to (-) transitions. Examination of the behavior of D_{st} for this period shows that a magnetic storm is associated with each (-) to (+) transition.

A limited set of data obtained in early 1975 (Fig. 2) verifies the expectation that in spring (-) sectors are more effective generators of energetic electron fluxes. The IMF sector structure during the time period covered by Fig. 2 is broken by days of mixed polarity; nevertheless, the data of Fig. 2 are, if anything, an even more striking demonstration that the level of energetic electron flux at 6.6

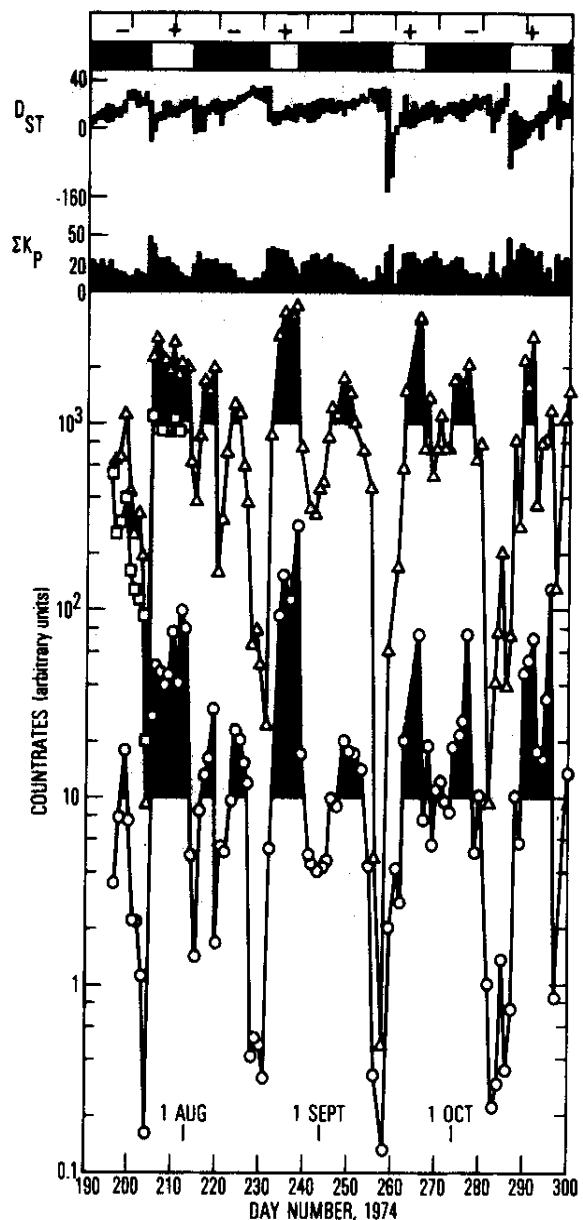


Figure 1. Hourly averages of energetic electron count rates observed in the late summer and fall of 1974 by ATS-6 and ATS-1 are plotted as a function of Day Number, 1974. Also plotted (at the top of the figure) are the polarity of the interplanetary magnetic field as inferred by Svalgaard (1975), the daily sum of K_p and the range of D_{st} for each day. Local time for all particle data is local noon; the sector boundary transitions are assumed to occur at 0000 UT for the days indicated. Circles and triangles are ATS-6 observations of > 3.9 and > 1.6 MeV electrons respectively, squares are ATS-1 observations of > 1.9 MeV electrons. For emphasis we have shaded those portions of the curves where $E > 1.6$ MeV count rates exceed 10^3 /sec and $E > 3.9$ MeV count rates exceed 10^2 /sec.

R_e is a strong function of the direction of the interplanetary field.

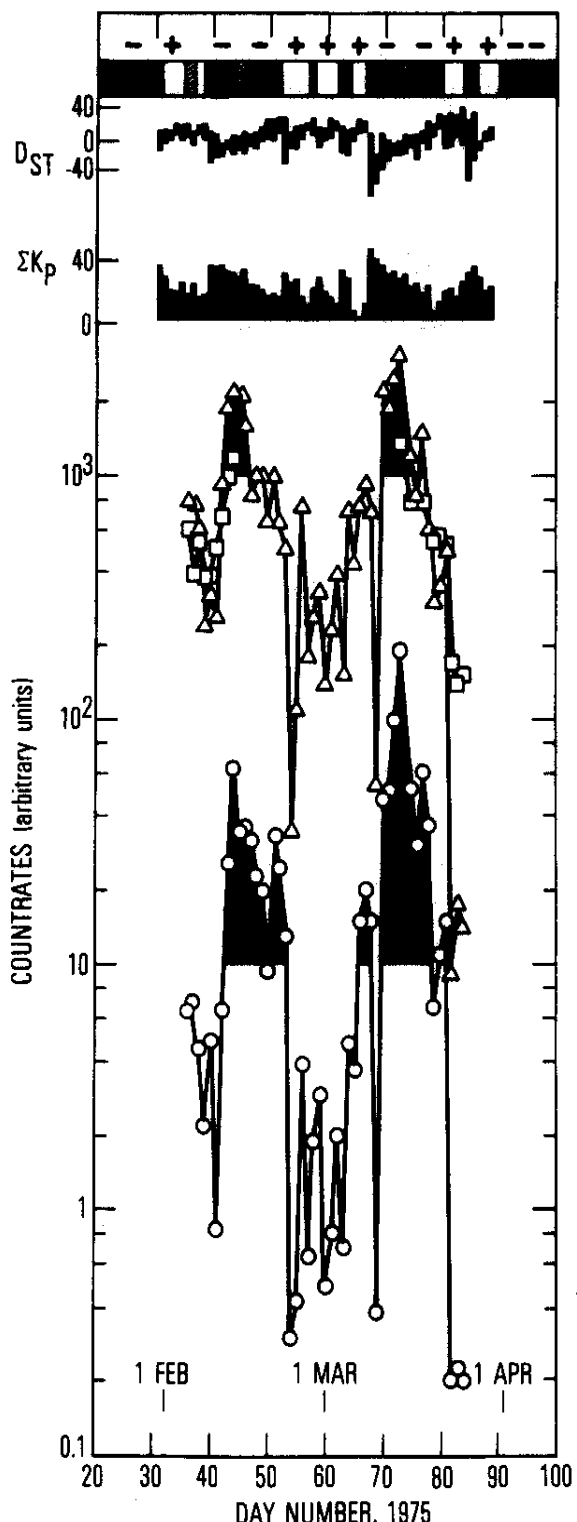


Figure 2. Hourly averages of energetic electron count rates observed in the spring of 1975 by ATS-6 and ATS-1. All other comments from the caption of Fig. 1 apply. The IMF sector structure during this period exhibited some days of mixed polarity, these days are indicated by cross-hatching.

At this stage of the data analysis we cannot unequivocally separate temporal changes in the electron flux from changes in the geometry of the trapping region. The work of Owens and Frank (1968) very clearly shows that the region around the earth containing energetic particles expands and contracts. ATS-6 observations, by themselves, cannot provide information regarding the extent of the trapping region. If we focus our attention on the properties of the region near ATS-6 we find, using data from the UCLA magnetometer on ATS-6 (graciously made available by R. L. McPherron), that during the time periods of Figs. 1 and 2 there do not appear to be any significant changes in the local field geometry at ATS-6 which are a function of the gross direction of the interplanetary field inferred by Svalgaard (1975).

It must be recalled that, because of drift shells splitting, a measurement of the omnidirectional flux by our experiment at one local time at the synchronous orbit represents the sum of the flux which exists over a range of L values at other local times. Our data have global rather than local properties. In addition, it is well known that large drift loss cones can develop in the angular distribution at synchronous altitude because of the proximity of the synchronous orbit to the trapping boundary. Such changes in the angular distribution would be interpreted by our experiment as flux changes. There are suggestions in the data, for example, in comparisons of relative flux changes at ATS-1, ATS-5 and ATS-6 as a function of IMF direction, that there may indeed be changes in the average pitch-angle distribution of energetic electrons (and therefore changes in the geometry of the trapping region) which are a function of the interplanetary field direction.

Correlations between the state of the magnetosphere and interplanetary conditions appear to be most successful when the magnetospheric parameters used in such studies represent some global characteristic of the magnetosphere. The auroral electrojet index A_e (Arnoldy, 1971), properties of polar magnetic fields (Burch, 1973), the size of the polar cap (Akasofu, 1975) and the D_{st} index (Burton, et al., 1975) are examples of such global quantities. We can now add the energetic electron fluxes at the synchronous orbit to the list of indicators of the coupling strength between the interplanetary medium and the magnetosphere.

The changes in the energetic electron flux at $6.6 R_E$ should be reflected in corresponding changes in the intensity of the energetic electrons precipitating into the atmosphere. Hence, one might expect to see aeronomic effects in and below the D-region at high latitudes (the depth in the atmosphere reached by precipitating relativistic electrons is ≈ 50 km.) The magnitude of such aeronomic effects should be a function of the direction of the interplanetary magnetic field.

Acknowledgements

The efforts of many people made our experiment on ATS-6 a success. We are particularly grateful

to Sam Imamoto, Gloria Roberts and Frances Twillie of The Aerospace Corporation, Frank McNally and Bill King of Westinghouse, and Bob Wales and Paul McKowan of NASA-Goddard. This work was supported in part by the U. S. Air Force Space and Missile Systems Organization under Contract F04701-75-C-0076 and in part by the National Aeronautics and Space Administration Contract NASW-2879.

References

- Akasofu, S. I., "The Roles of the North-South Component of the Interplanetary Magnetic Field on Large Scale Auroral Dynamics Observed by the DMSP Satellite," Planet. Space Sci., 23, 1349, 1975.
- Arnoldy, R. L., "Signature in the Interplanetary Medium for Substorms," J. Geophys. Res., 76, 5189, 1971.
- Burch, J. L., "Effects of Interplanetary Magnetic Sector Structure on Auroral Zone and Polar Cap Magnetic Activity," J. Geophys. Res., 78, 1047, 1973.
- Burton, R. K., R. L. McPherron and C. T. Russell, "The Terrestrial Magnetosphere: A Half-wave Rectifier of the Interplanetary Electric Field," Science, 189, 717, 1975.
- McPherron, R. L., C. T. Russell and M. P. Aubry, "Satellite Studies of Magnetospheric Substorms on August 15, 1968: 9. Phenomenological Model for Substorms," J. Geophys. Res., 78, 3131, 1973.
- Owens, H. D., and L. A. Frank, "Electron Omnidirectional Intensity Contours in the Earth's Outer Radiation Zone at the Magnetic Equator," J. Geophys. Res., 73, 199, 1968.
- Paulikas, G. A., J. B. Blake, and S. S. Imamoto, "ATS-6 Energetic Particle Radiation Measurements at Synchronous Altitude," IEEE Trans. Aerospace and Electronic Systems, AES-11, 1138, 1975.
- Rothwell, P., quoted in J. M. Wilcox, "The Interplanetary Magnetic Field, Solar Origin and Terrestrial Effects," Space Sci. Revs., 8, 258, 1968.
- Russell, C. T., "The Solar Wind and Magnetospheric Dynamics," Correlated Interplanetary and Magnetospheric Observations, edited by D. E. Page, D. Reidel Publishing Company, Dordrecht-Holland, 1974.
- Russell, C. T., and R. L. McPherron, "Semiannual Variation of Geomagnetic Activity," J. Geophys. Res., 78, 92, 1973.
- Svalgaard, L., "An Atlas of Interplanetary Sector Structure 1957-1974," Stanford University Institute for Plasma Research Report 629, June 1975.
- Williams, D. J., "A 27-Day Periodicity in Outer Zone Trapped Electron Intensities," J. Geophys. Res., 71, 1851, 1966.
- Wilcox, J. J., "The Interplanetary Magnetic Field Solar Origin and Terrestrial Effects," Space Sci. Revs., 8, 258, 1968.

(Received March 8, 1976;
accepted April 1, 1976.)

Energetic Electrons at the Synchronous Altitude 1974-1977

G. A. Paulikas, J. B. Blake, and H. H. Hilton
Space Sciences Laboratory

The Ivan A. Getting Laboratories
The Aerospace Corporation
El Segundo, California 90245

August 1977

**This work was supported, in part, by SAMSO under Contract F04701-76-C-0077 and
in part by NASA under Contracts NASW-2762, NASW-2879 and NAS5-23788.**

CONTENTS

	<u>Page</u>
Abstract	-i-
I. Introduction	1
II. Overview of the Observations	3
III. Average Fluxes and $P(F > F_x)$ Distributions	5
IV. Diurnal Variations	6
V. Effects of the Interplanetary Medium on Energetic Electrons	8
VI. Future Work	9
VII Acknowledgements	9
References	10
Figure Captions	12
Appendix A: A Description of Instrument Response	34
Appendix Figure Captions.	37

Abstract

A description of the energetic (140 kev to > 3.9 Mev) electron environment observed at the synchronous altitude during the 1974-1977 time interval is presented. These results were obtained by an experiment carried on the geostationary ATS-6 spacecraft. Observations were made at several longitudes. Electron fluxes exhibit a complex temporal behavior ranging in time scale from a diurnal variation to a semi-annual variation. Average fluxes are computed and compared with earlier studies and models.

-i-

Energetic Electrons at the Synchronous Altitude 1974-1977

I. Introduction

The synchronous orbit, because of its obvious utility for terrestrial applications, is undoubtedly the single most heavily populated orbit in space. Many spacecraft, spread over longitude, are in this orbit today, and the plans of various nations (Ref. 1, Ref. 2) emphasize an even heavier utilization of it for future communications, earth observations, meteorology, and data relay spacecraft. It is clear that the investment in such space systems is likely to run into the billions of dollars.

The premium on a precise, quantitative understanding of the space environment and the impact of the environment on space systems is enormous. Even savings of fractions of a percent, derived as a result of better information regarding the energetic radiation (for example, extending the life of a spacecraft and thus decreasing the replenishment rate) translate directly into savings which run into the tens of millions of dollars.

The purpose of this report is to summarize, in a format useful to the designers and operators of synchronous orbiting of space systems, the observations of energetic electrons at the synchronous altitude made by The Aerospace Corporation particle spectrometer flown on the ATS-6 spacecraft. Preliminary results have been reported in a series of internal reports (Refs. 3-8). In this report we shall concentrate on defining the average properties of the electron population as it existed in the 1974-1977 time interval at the synchronous orbit. Thus this report can be viewed as a sequel to earlier work (Refs. 9-12) which treated the properties of the particle population at the synchronous orbit during earlier epochs. It seems useful to begin by describing some of the salient features of the ATS-6 observing program which we conducted and to point out how the present data and results may be similar to, or differ from, earlier work because of differences in epoch, instrumentation, spacecraft orientation and the location of the spacecraft in longitude.

The observations described here were made between mid-1974 and early 1977. This time interval straddled to solar minimum (as defined by sunspot number) (Fig. 1). In contrast, earlier observation of energetic radiation at the synchronous orbit made by

instruments aboard ATS-1 and ATS-5 were made during times near the peak of solar activity: late 1966 to early 1968 in the case of ATS-1 and mid 1969 to early 1972 in the case of ATS-5. As is well known, the magnetosphere is relatively more quiescent during periods of low solar activity as contrasted to the time period near solar maximum. As we shall see below, periodic manifestations of solar-wind magnetosphere interactions emerge prominently in the ATS-6 data; in contrast, impulsive solar events which occur at frequent intervals during solar maximum and tend to mask the more regular features of magnetospheric dynamics are infrequently observed in the present data set. The ATS-6 data is thus unique because it represents the first observations of the particle populations of the synchronous orbit made during the interval near solar minimum.

The instrumentation used to obtain our data has been described elsewhere (Ref. 13); a brief summary of the relevant features is given in Appendix A. Briefly, we measured the directional fluxes of electrons in the 140-600 kev interval and the omnidirectional fluxes above thresholds of 700 kev, 1.55 Mev and 3.9 Mev. Energetic proton data were also obtained (during solar proton events; these data are not discussed here).

The ATS-6 was earth oriented so that the axes of the detectors were pointed radially outward along the earth-satellite line. Thus the (directional) 140-600 kev channel (E1) measured only one segment of the angular distribution, the precise segment depending on the (rather variable) orientation of the local magnetic field with respect to the detector axis. The omnidirectional fluxes (E2, E3, E4) obtained from the ATS-6 data were obtained from countrates registered by particles which could reach the detectors through a 2π steradian acceptance angle looking out along the earth-satellite line. In contrast, on ATS-1, for example, the rapid spin of the spacecraft coupled with a relatively slow count accumulation time served to form a true average of the in situ radiation.

During the period covered by our data, the ATS-6 spacecraft was moved several times to different longitudes. Because the geographic equator does not coincide everywhere with the geomagnetic equator, a spacecraft at the synchronous orbit may be at significantly different magnetic latitudes, depending on the longitude at which the spacecraft is stationed. ATS-6 observations began while the spacecraft was on the

equator at 94°W , where the magnetic latitude is about 11° . Subsequently the spacecraft was moved to 35°E and finally to 140°W . At both of these locations the magnetic equator is nearly coincident with the geographic equator.

The displacement of the spacecraft as little as 11° off the magnetic equator has a significant effect on the observations. We find that the geomagnetic field may quite often, particularly near local midnight, assume a configuration with a strong radial component, i.e. the magnetic field at $6.6 R_e$ appears, at these times, to assume a configuration expected to be found near the magnetotail. Such tail-like configurations are characterized by the absence of very energetic electrons. The fluxes observed at 94°W , i.e. somewhat off the magnetic equator, exhibit a significantly more dynamic behavior on the timescale of a day than seen at the magnetic equator where the geomagnetic field exhibits a more regular behavior, however, the long-term average fluxes do not reflect a very significant longitudinal difference. Spacecraft longitude is taken as a parameter in the data analysis, although, as we shall see below, temporal variations in the average particle fluxes are considerably larger than effects due to change in longitude.

For the purposes of this report, we have formed hourly averages, centered on the half hour, of all the electron data presently available to us. These hourly averages are the basic material from which further analysis proceeds. Daily averages, running 27 day averages, probability distributions are all formed from hourly averages.

II. Overview of the Observations

Figures 2 through 5 give an overview of the observations of energetic electrons from mid 1974 through early 1977. Plotted here are daily averages of the electron fluxes, together with data on the sector structure of the interplanetary magnetic field as a function of time. The location in longitude of ATS-6 and the periods of spacecraft movement are indicated on the figures and separately summarized in Table I.

The dynamic nature of the energetic electron fluxes, particularly at the higher energies, is immediately apparent. The dominant periodicity (in addition to the diurnal variations (see Refs. 11 and 15) which is not visible on a plot of daily averages) is the

TABLE I
ATS-6 Geographic and Geomagnetic Locations

Time Interval	Geographic Longitude	Magnetic Latitude*
Day 165, 1974-140, 1975	94°W	11°
Day 140, 1975-180, 1975	In transit	—
Day 180, 1975-214, 1976	35°E	5°
Day 214, 1976-330, 1976	In transit	—
Day 330, 1976-present	140°W	0°

* Derived from UCLA ATS-6 Magnetometer Data
(Courtesy R. L. McPherron)

strong modulation of the energetic electron fluxes on a timescale corresponding to the solar rotation period as well on a timescale consistent with either a two- or four-sector structure of the interplanetary field. (The effects of the interplanetary sector structure on the energetic particle population has been discussed previously in Ref. 11.).

It will be immediately appreciated by the reader that long term averages of these data, used for the purposes of accurate estimates of the radiation environment, must be approached with caution because of the large variation in the fluxes occurring on several timescales.

If we now form 27-day running averages of the data presented above, we obtain Figure 6 through 9. In these figures we again see the strong effects of solar rotation-to-rotation variability of the electron fluxes. This effect is particularly noticeable in the data for the more energetic electrons and stands out particularly well in late 1976 - early 1977. Also visible is a semi-annual variation in the energetic electron fluxes, with a maxima found near the equinoxes and minima near the solstices. To be sure, the moves of the spacecraft complicate the determination of the amplitude of this variation but it appears that the semi-annual variation is comparable to, if not greater than, the longitudinal effect. The semi-annual variation in the electron flux is presumably but a reflection of the well known semi-annual variation in geomagnetic activity (Ref. 17).

III. Average Fluxes and $P(F > F_x)$ Distributions

Using the data base discussed above, we have computed the probability distributions $P(F)$ and $P(F > F_x)$ in a manner analogous to that first described by in Ref. 18. $P(F > F_x)$ is the probability of observing a flux greater than F_x for some particular energy threshold, while $P(F)$ is the differential probability distribution. These curves have been computed for the several time intervals of interest and are presented as Figs. 10 through 15. Also computed, and indicated on the figures are u , the mean of $\log_{10}F$, J , the \log_{10} of the mean flux and s , the standard deviation about u . Note, from the $P(F)$ curves that the distribution is not necessarily gaussian in $\log_{10}F$, in contrast to assumptions made in analyses of earlier data sets.

Table II summarizes the data presented in Figs. 10-15, while Fig. 16 presents spectra of the average flux for the various longitudes and time intervals covered by our data, together with the spectrum predicted by the AE-4 model (Ref. 9, 10). The points noted below can serve as a summary of our findings.

1. At energies greater than about 1.5 Mev, the ATS-6 data indicate the presence of a somewhat harder electron spectrum than the AE-4 model would predict. At energies below \approx 1.5 Mev, our data indicate, in general, fewer electrons than AE-4. These conclusions are, however, tempered by the fact that the electron fluxes are highly variable and one can find significant time intervals (for example the late 1966 - early 1967 interval illustrated in Figs. 14 and 15) where the spectral shape at the higher energies approached that which one might expect from AE-4.
2. Longitudinal effects (caused by differences in magnetic latitude) in the mean flux are relatively minor. This conclusion must be tempered by the fact that no systematic analysis of simultaneous observations made at several longitudes has yet been carried out. There is some limited evidence (based on ATS-1/ATS-6 comparisons, Refs. 3, 12) that longitudinal flux differences ($150^{\circ}\text{W}/94^{\circ}\text{W}$) may be as large as a factor of two.
3. Although the mean fluxes observed may not be similar, the probability distributions $P(F > F_x)$ differ show systematic differences because there are far more flux dropouts off the equator. The differences are significant only near the $P(F > F_x) \approx 1$ axis.

IV. Diurnal Variations

It is of interest to compare the diurnal variations observed at the several longitudes and at the several particle energies. The mean flux for the three available longitudes is presented in Fig. 17, 18, 19 as a function of local time. As had been found previously (Ref. 11), the diurnal variation is larger at the higher electron energies. There does not seem to be any significant systematic change of the diurnal variation with longitude.

TABLE II
COMPARISON OF ATS-6 DATA AND AE-4 MODEL
MEAN FLUX (cm⁻² sec⁻¹)

	ATS-6			AE-4
	94°W, $\lambda_M \approx 11^\circ$	35°E, $\lambda_M \approx 0^\circ$	140°W, $\lambda_M \approx 0^\circ$	
Energy	Day 166, 74-Day 140, 75	Day 180, 75-Day 214, 76	Day 137, 76-Day 210, 76	Day 330, 76-Day 120, 77
> 140 keV	5.35×10^6	5.29×10^6	4.84×10^6	4.16×10^6
> 700 keV	5.01×10^5	5.50×10^5	4.17×10^5	2.45×10^5
> 1.55 Mev	1.32×10^2	1.35×10^5	7.76×10^4	5.37×10^4
> 3.9 Mev	6.46×10^2	6.8×10^2	1.25×10^2	77.6

* Day 90, 76 - 214, 76 only

V. Effects of the Interplanetary Medium on Energetic Electrons

We had earlier discovered (Ref. 14) that the flux level of the energetic electrons at the synchronous orbit - and therefore presumably the flux of energetic electrons in the entire outer magnetosphere - was modulated by the passage of the sector boundaries of the interplanetary magnetic field (IMF) past the earth. Briefly, we found that the flux levels were higher during northern hemisphere fall when the earth was immersed in a positive sector than during the passage of a negative sector of the interplanetary magnetic field. Conversely, in the spring, negative sectors served to generate higher energetic electron fluxes. This finding was found to be in agreement with the picture of solar wind-magnetosphere interaction proposed by Russell and McPherron (Ref. 17).

The findings described above were based on a very limited set of data. In the past year we have attempted to confirm and extend our conclusions using the more than 2½ years of data presently available. The relevant points can be seen by examining Figures 2-5, where we have plotted the daily averages of the energetic electron fluxes, together with the sector structure of the interplanetary field (see the caption of Figure 2 for explanation of IMF data presentation). It can be seen from these figures that the sector structure of the interplanetary field provides the dominant modulation of electron fluxes. Our conclusion that higher fluxes result in the fall from + sectors than from - sectors (and that the converse holds true in the spring) can be verified by inspection of these figures. We are now in the process of trying to assess more quantitatively the relationship between the vector of the interplanetary field and the velocity of the solar wind and the generation of energetic particles in the magnetosphere.

This study, if successful, may lead to techniques for the quantitative prediction of the energetic electron fluxes at the synchronous altitude, using as input solar wind and IMF data. It appears that using data on the local (i.e. near earth) solar wind, radiation fluxes could be predicted several days in advance because of an apparent time lag between changes in interplanetary conditions and the generation by magnetospheric processes of energetic electron fluxes. Should our knowledge of solar physics, i.e. our understanding of the structure and properties of coronal holes and the

solar wind advance sufficiently, then solar data, coupled with an appropriate understanding of interplanetary transport processes, might enable radiation predictions to be made of the order of a week ahead of time.

We mention this potential benefit, because it is clear that in the future, applications spacecraft of many varieties are likely to proliferate in the synchronous orbit (see Refs. 1 and 2, for example), and modest advances in radiation prediction - particularly for manned spaceflight applications, may yield extremely beneficial results.

VI. Future Work

We plan to update and revise this report as additional ATS-6 data are reduced and analyzed. At the time of writing (August 1977) the experiment continues to function well. With luck (and NASA's continued interest) ATS-6 will cover the rising portion of the solar activity cycle and provide unique data in this respect.

In addition, we plan to analyze ATS-1 data, which were acquired simultaneously with ATS-6 during portions of 1974, 1975 and 1976. The comparison between data from spacecraft fixed in longitude (ATS-1) and the ATS-6 which sampled a range of longitude should provide definitive information of the variation of the properties of the electron radiation with longitude at the synchronous orbit.

VII. Acknowledgments

The ATS-6 experiment which yielded the results described in this report was developed with the able assistance of Sam Imamoto and Gloria Roberts. The data reduction efforts were handled by Doretha (Ross) Mayfield. This work was carried out as part of the program of Mission Oriented Investigations and Experimentation supported at The Aerospace Corporation by the USAF Space and Missile System Organization under Contract No. F04701-76-C-0077. Portions of the data reduction efforts were supported by NASA under Contracts NASW-2762, NASW-2879 and NAS5-23788.

References

1. D. P. Hearth, ed., Outlook for Space, NASA Report SP-386, January, 1976.
2. L. Bekey and H. Mayer, 1980-2000: Raising Our Sights for Advanced Space Systems, Aeronautics and Astronautics, 14, 34, 1976.
3. G. A. Paulikas and J. B. Blake, Electron Radiation in the Synchronous Orbit, ATM-76 (6260-20)-1, The Aerospace Corp., October, 1975.
4. G. A. Paulikas, Electron Radiation in the Synchronous Orbit (Cont'd.), ATM-76(6260-20)-3, The Aerospace Corp., August, 1976.
5. G. A. Paulikas and J. B. Blake, Electron Environment at Synchronous Altitude (Cont'd.), ATM-77(2260-20)-1, The Aerospace Corp., October, 1976.
6. G. A. Paulikas and M. Schulz, Upper Limits to the Energetic Electron Flux at the Synchronous Orbit, ATM-76(6260-20)-2, The Aerospace Corp., April, 1976.
7. G. A. Paulikas and J. B. Blake, Energetic Electron Environment at Synchronous Altitude, ATM-77(2260-20)-2, The Aerospace Corp., April, 1977.
8. G. A. Paulikas and H. H. Hilton, Radiation Environment at Synchronous as observed 1974-1977, ATM-77(2872)-9, The Aerospace Corp., June, 1977.
9. G. W. Singley and J. I. Vette, The AE-4 Model of the Outer Radiation Zone Electron Environment, NASA-NSSDC 72-06, August, 1972.
10. G. W. Singley and J. I. Vette, A Model Environment for Outer Zone Electrons, NASA-NSSDC 72-13, December, 1972.
11. G. A. Paulikas and J. B. Blake, The Particle Environment at the Synchronous Altitudes, in Models of the Trapped Radiation Environment, Vol. VII: Long Term Variations, NASA SP-3024 (1971).

12. A. L. Vampola, J. B. Blake and G. A. Paulikas, A New Study of the Outer Zone Electron Environment: A Hazard to CMOS, Paper 77-40 presented at the 15th AIAA Aerospace Sciences Meeting, Los Angeles, January 1977; to be published in Journal of Spacecraft and Rockets, October, 1977.
13. G. A. Paulikas, J. B. Blake, S. S. Imamoto, ATS-6 Energetic Particle Radiation Measurement at Synchronous Altitude, IEEE Trans. on Aerospace and Elect. Systems, AES-11, 1138, 1976.
14. G. A. Paulikas and J. B. Blake, Modulation of Trapped Energetic Electrons at $6.6 R_e$ by the Direction of the Interplanetary Magnetic Field, Geophys. Res. Lett., 3, 277, 1976.
15. G. A. Paulikas, J. B. Blake, S. C. Freden and S. S. Imamoto, Observations of Energetic Electrons at Synchronous Altitude, I. General Features and Diurnal Variations, J. Geophys. Res. 73, 4915, 1968.
16. L. Svalgaard, An Atlas of Interplanetary Sector Structure 1957-1974, SUIPR Report No. 629, Institute for Plasma Research, Stanford University, June 1975.
17. C. T. Russell and R. L. McPherron, Semiannual Variation of Geomagnetic Activity, J. Geophys. Res., 78, 92, 1973.
18. J. L. Vette and A. B. Lucero, Models of the Trapped Radiation Environment, Volume III: Electrons at the Synchronous Altitude, NASA SP-3024, 1967.

Figure Captions

- Figure 1.** Relationship between the intervals of data acquisition on energetic electrons at synchronous altitudes by experiments on board ATS spacecraft and the 11-year solar activity cycle as defined by the Zurich sunspot number
- Figure 2.** Daily average fluxes for 1974 for the four channels of ATS-6 electron data. The trace at the bottom of each panel gives the sector structure of the interplanetary magnetic field as determined by Svalgaard (Ref. 16). Positive sector days are indicated by the upper line, negative sector days by the lower line. Days when polarity is mixed are indicated by a point falling between the two lines.
- Figure 3.** Same as Figure 1, except for 1975. The data for the > 3.9 Mev channel are suspect after Day 140, 1975 and have been deleted.
- Figure 4.** Same as Figure 1, except for 1976. The data for the > 3.9 Mev channel are suspect between Day 1 and Day 90 and have been deleted.
- Figure 5.** Same as Figure 1, except for 1977. Isolated days of data are indicated by unconnected points.
- Figure 6.** Running 27 day average electron fluxes for the four channels of ATS-6 energetic electron data obtained in 1974. Interplanetary magnetic field sector structure is indicated on each panel of data (see Fig. 2 caption for explanation).
- Figure 7.** Same as Figure 7, for 1975. $E > 3.9$ Mev data after Day 140 is suspect and have been deleted.
- Figure 8.** Same as Figure 7, for 1976. $E > 3.9$ Mev data between Day 1 and Day 90 are suspect and have been deleted.
- Figure 9.** Same as Figure 7, for 1977.

- Figure 10.** Normalized differential probability $P(F)$ of observing a flux F_x for the four ATS-6 electron channels during the interval Day 165, 1974 to Day 140, 1975 when ATS-6 was located at 94°W . This figure was constructed by sorting the observations into bins 0.1 wide in $\log_{10} F_x$. Data for all local times are included. The electron energies are E1: 140-600 kev, E2 > 700 kev, E3 > 1.55 Mev and E4 > 3.9 Mev. The units of F_x are $\text{cm}^{-2} \text{sec}^{-1}$ for all channels except E1 where the units are $\text{cm}^{-2} \text{sec}^{-1} \text{sr}^{-1}$ instead. The notation "ALL" on the figure indicates that all polarities of the interplanetary magnetic field are included in this analysis. The column U gives the mean of the logarithms of the (hourly average) fluxes during this interval, the column J gives the logarithm of the mean flux and S is the logarithm of the standard deviation from U.
- Figure 11.** The data of Figure 10 are presented as integral probabilities $P(F > F_x)$ of observing a flux greater than F_x during the Day 165, 1974 to Day 140, 1975 time interval. All other comments apply.
- Figure 12.** Same as Figure 10, except the time interval is Day 180, 1975 to Day 214, 1976 where ATS-6 was located at 35°E . The E4 curve contains data from the interval 90, 76 to 214, 76.
- Figure 13.** The data of Figure 12 are presented as integral probabilities of observing a flux greater than F_x during the Day 180, 1975 to Day 214, 1976 time interval. All other comments apply.
- Figure 14.** Same as Figure 10, except the time interval is Day 330, 1976 to Day 120, 1977 where ATS-6 was located at 140°W . The prominent peak in E4 near an apparent flux of $\approx 10 \text{ cm}^{-2} \text{sec}^{-1}$ is due to the galactic cosmic ray background (see Appendix A) because the energetic electron flux was very low during this time period -see Figures 4, 5, and 8, 9.
- Figure 15.** The data of Figure 14 are presented as integral probabilities of observing a flux greater than F_x during the Day 330, 1976 to Day 120, 1977 time interval. All other comments apply. Note that for a flux of $\approx 15 \text{ cm}^{-2} \text{sec}^{-1}$ in the E4 channel all "electrons" are really galactic cosmic rays or their products.

Figure 16. Electron energy spectra constructed using the average fluxes for each time interval indicated. The fluxes measured in the 140-600 keV directional channel have been multiplied by 4π to obtain a measure of the omnidirectional flux in this energy interval. The $E_e > 3.9$ Mev point associated with the Day 180, 1975 to Day 214, 1976 curve was obtained using data from the Day 92, 1976 to Day 210, 1976 interval.

Figure 17. Diurnal variation of the average electron flux observed during the time interval Day 165, 1974 - Day 140, 1975 when ATS-6 was located at 94°W .

Figure 18. Same as Figure 17, except that the time interval is Day 180, 1975 to Day 214, 1976 when ATS-6 was located at 35°E . The E4 channel is not shown.

Figure 19. Same as Figure 17, except that the time interval is Day 330, 1976 to Day 120, 1977. ATS-6 was at 140°W at this time.

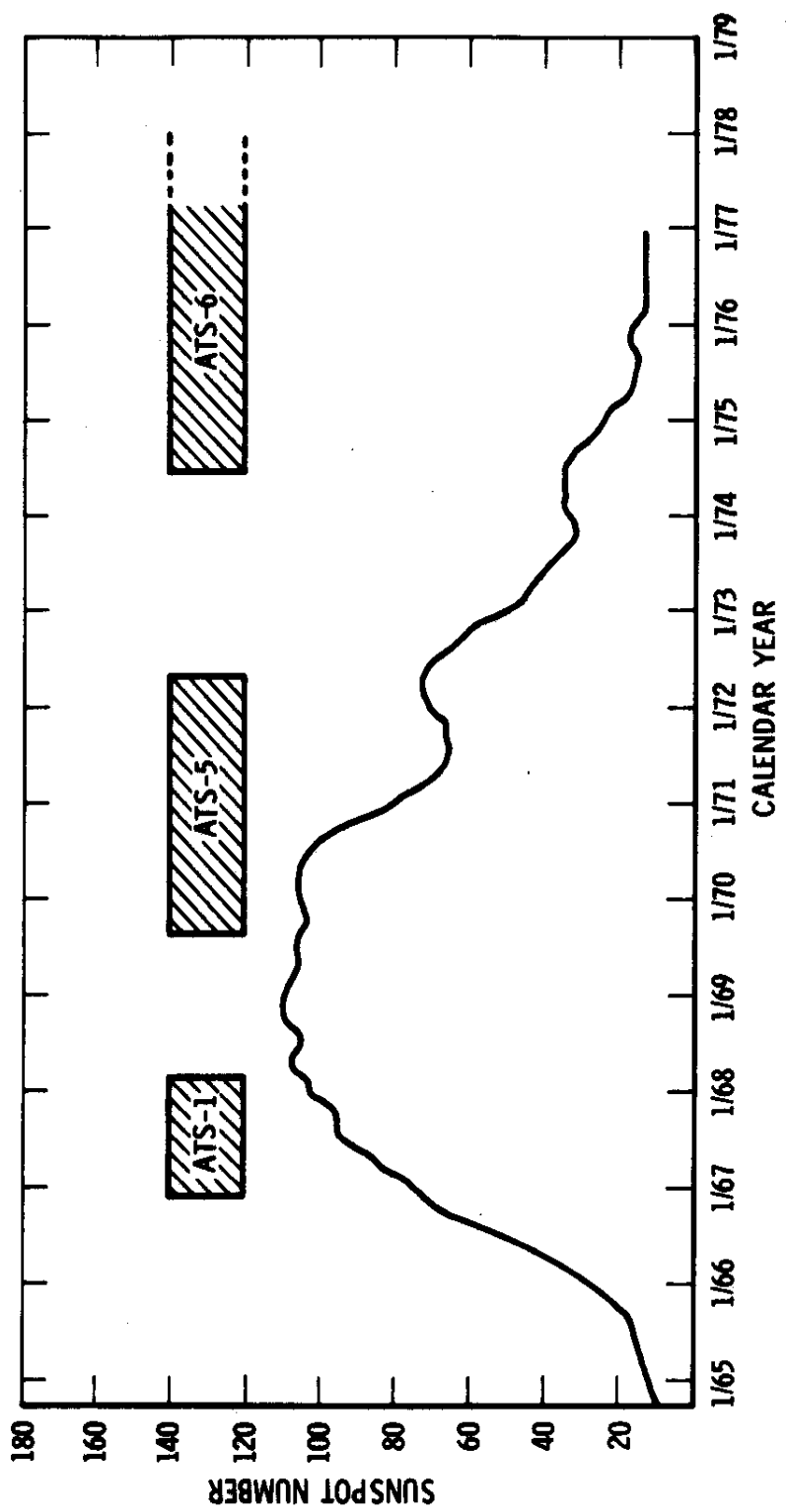


Fig.
1

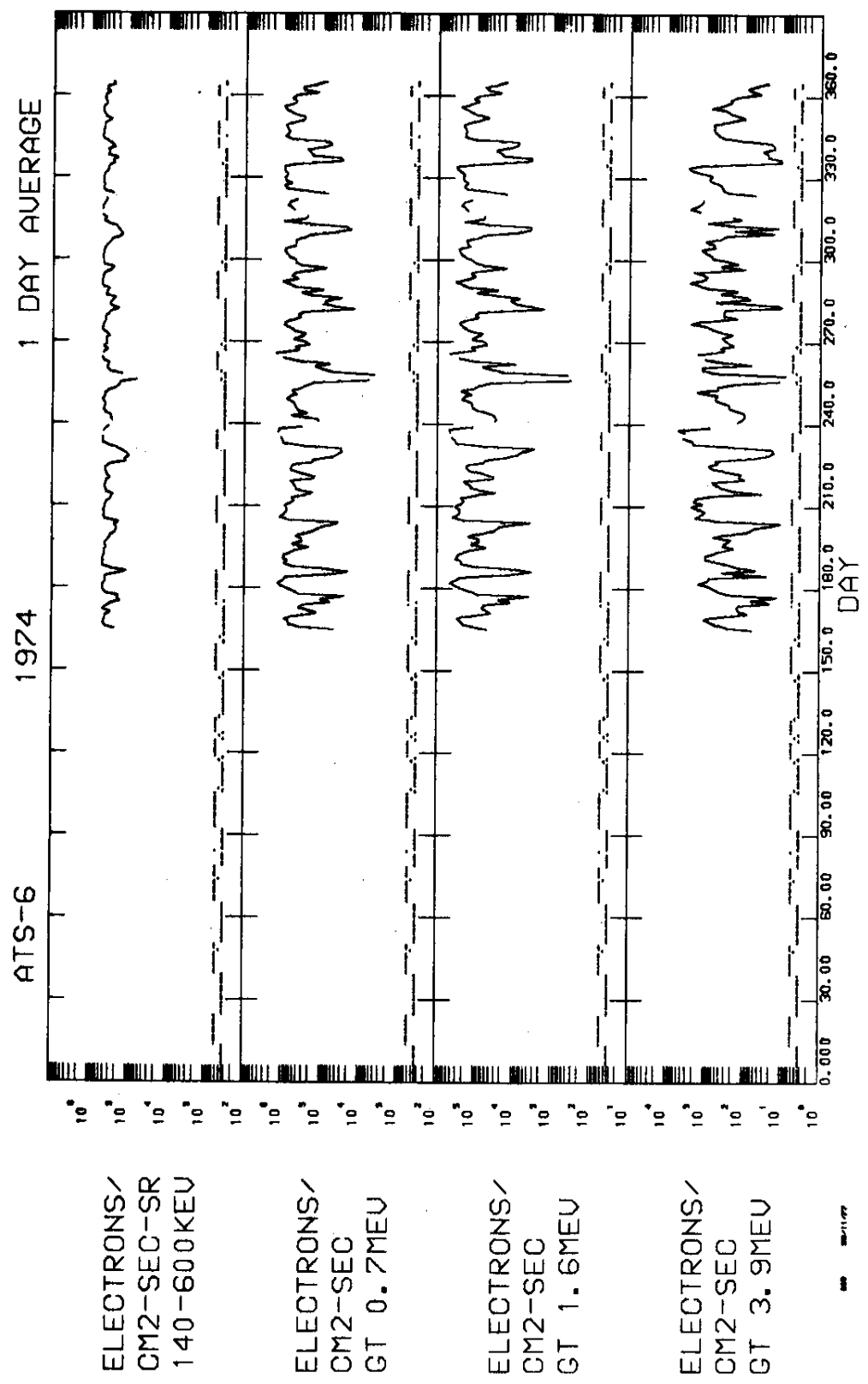


Fig.
2

7

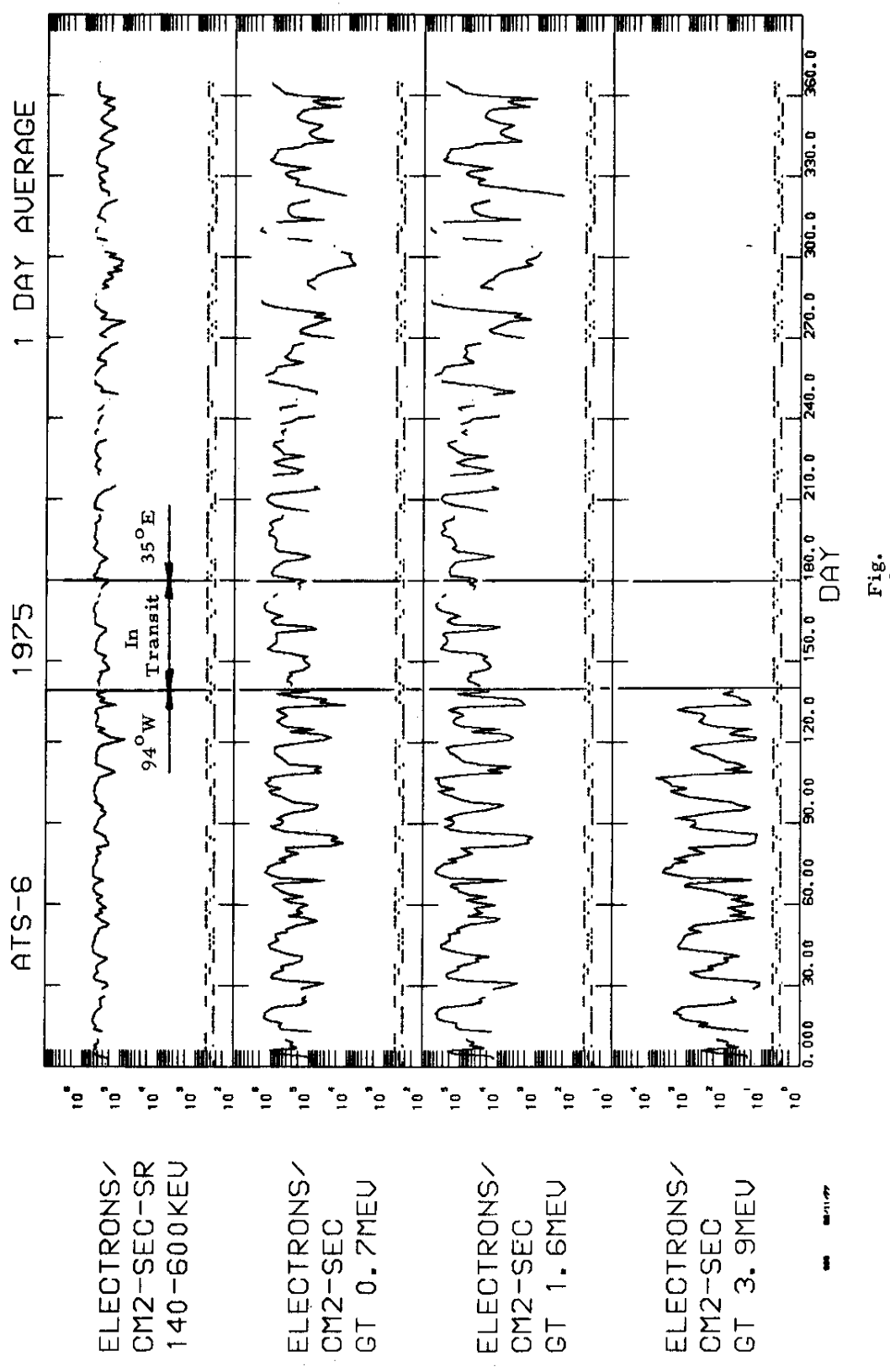


Fig.
3

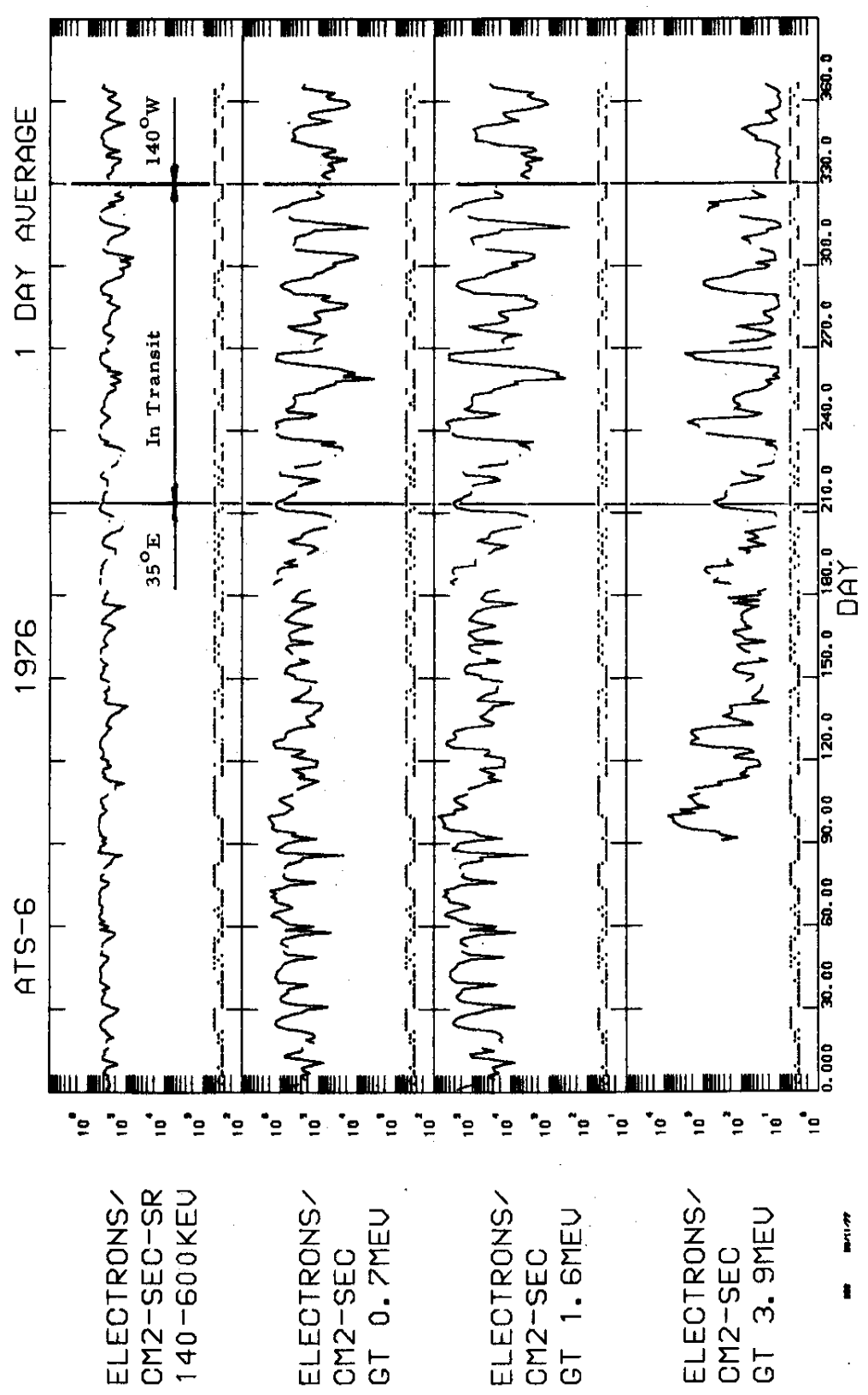


Fig.
4

7

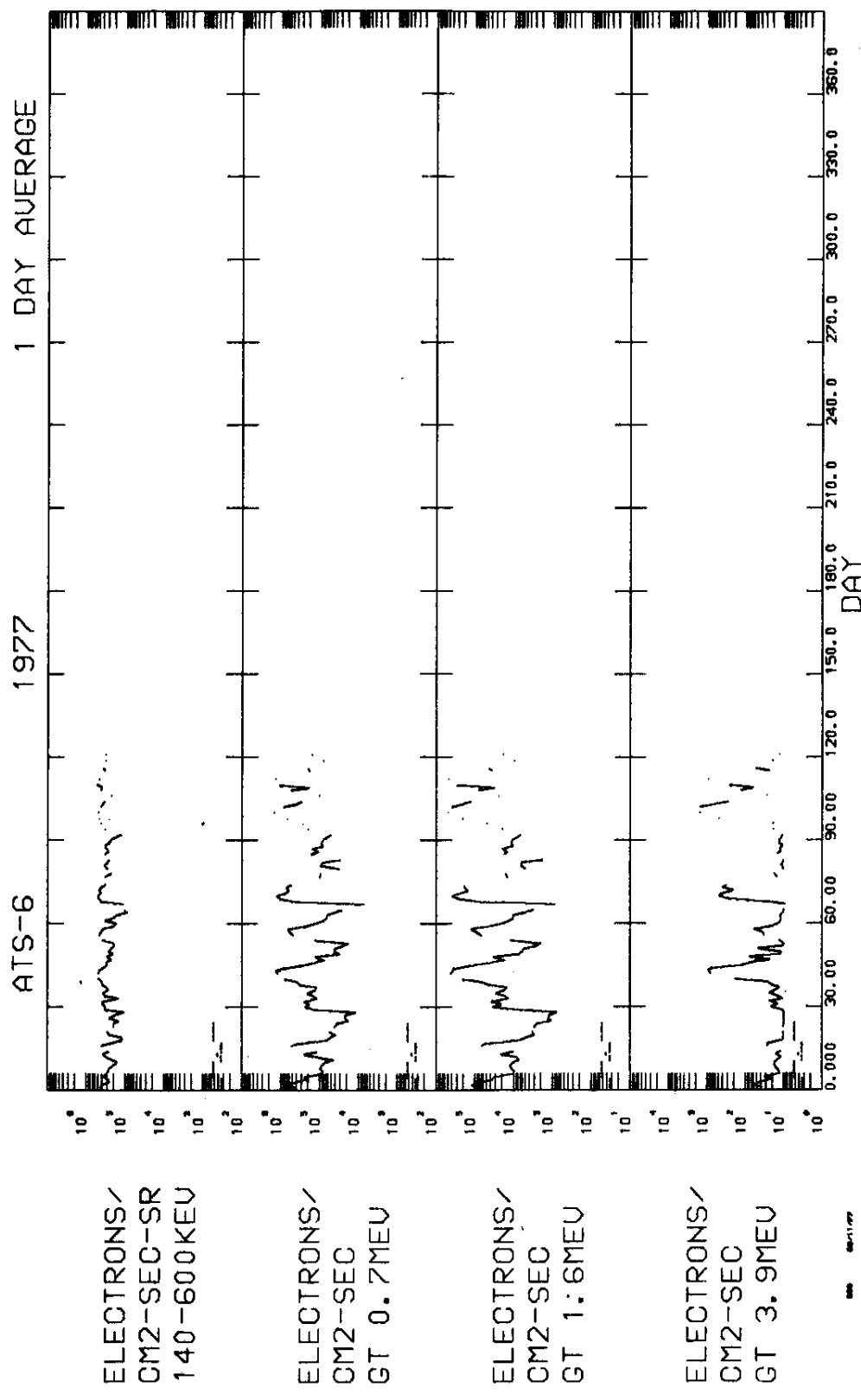


Fig.
5

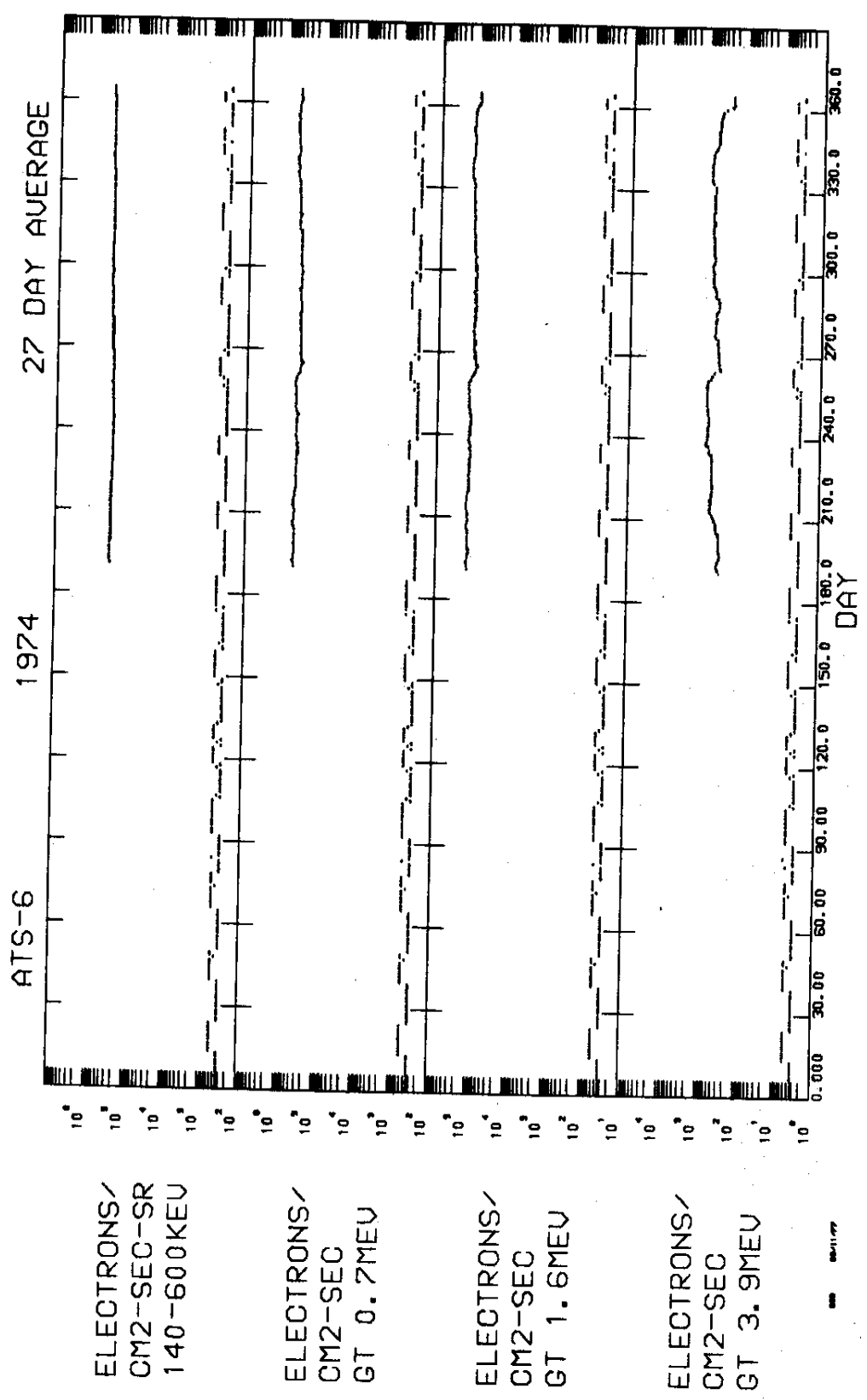


Fig.
6

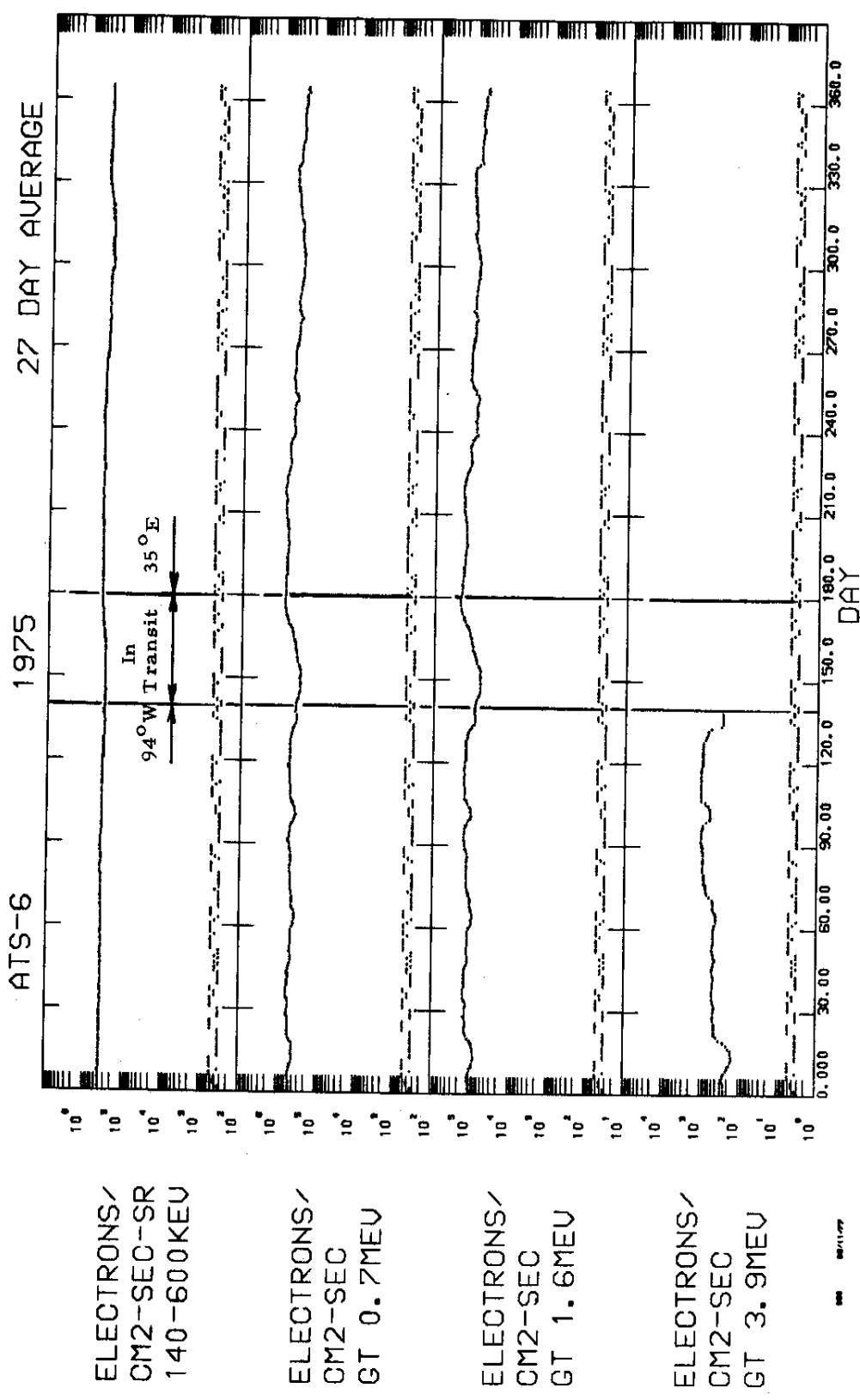


Fig.
7

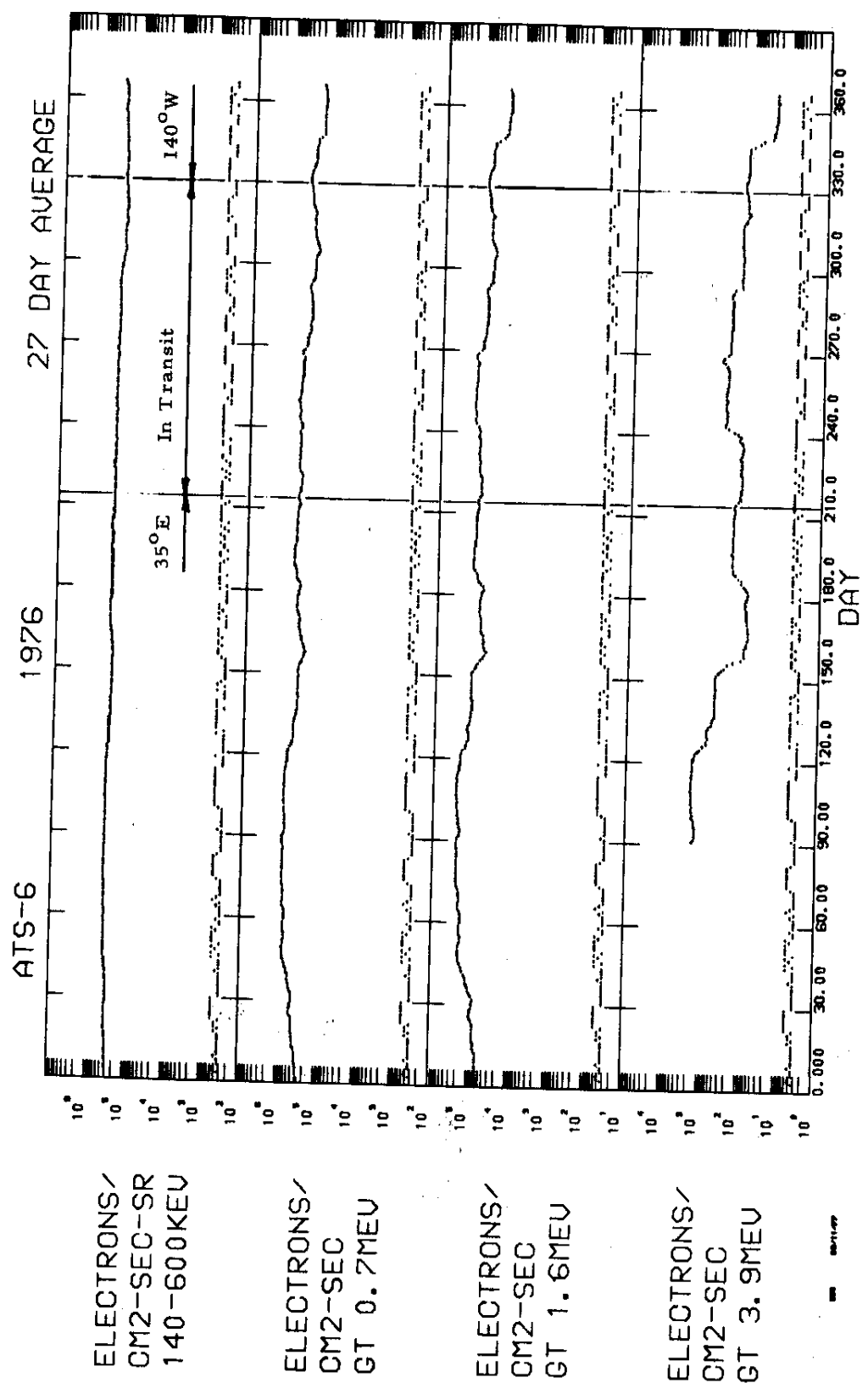


Fig.
8

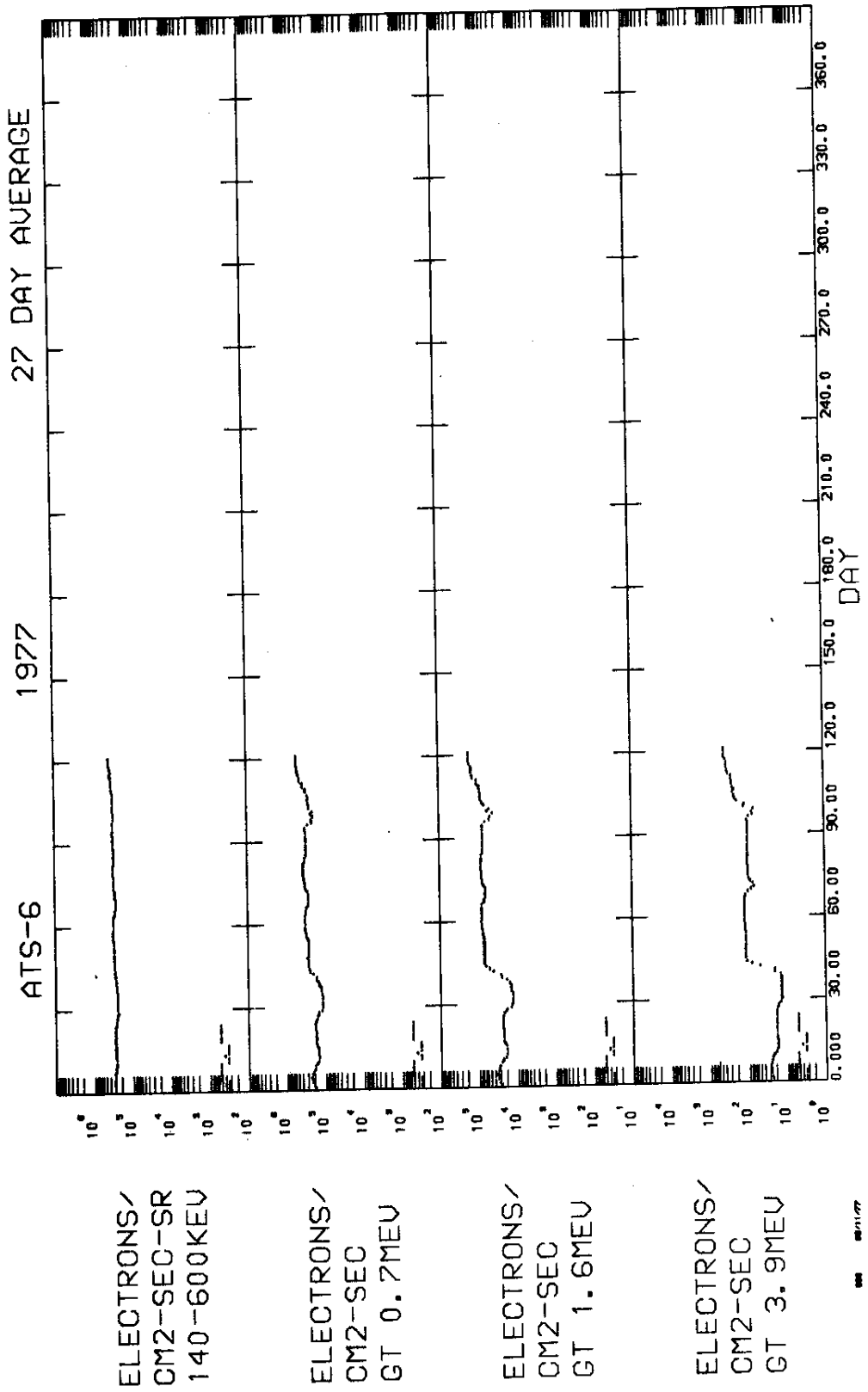


Fig.
9

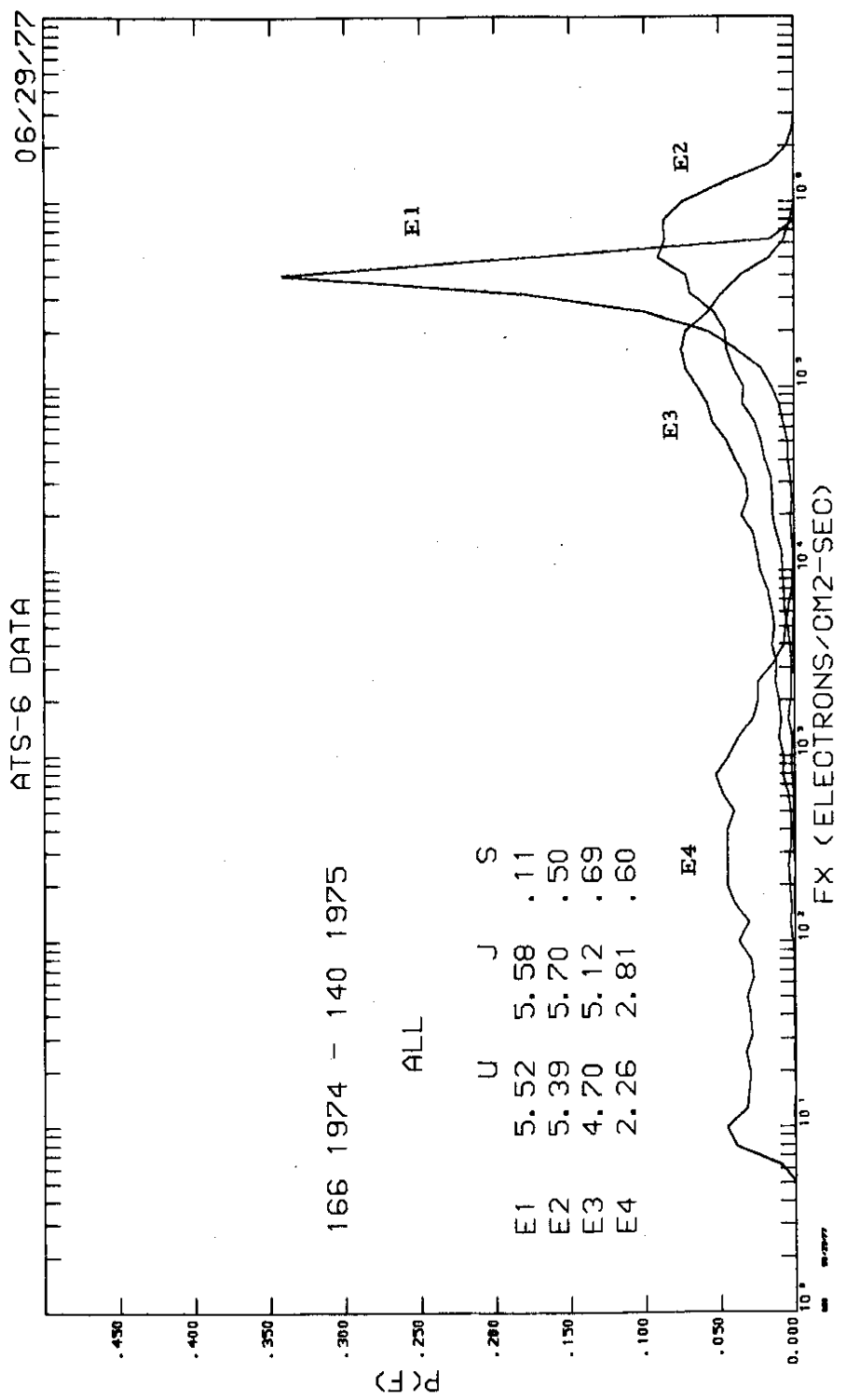


Fig.
10

8

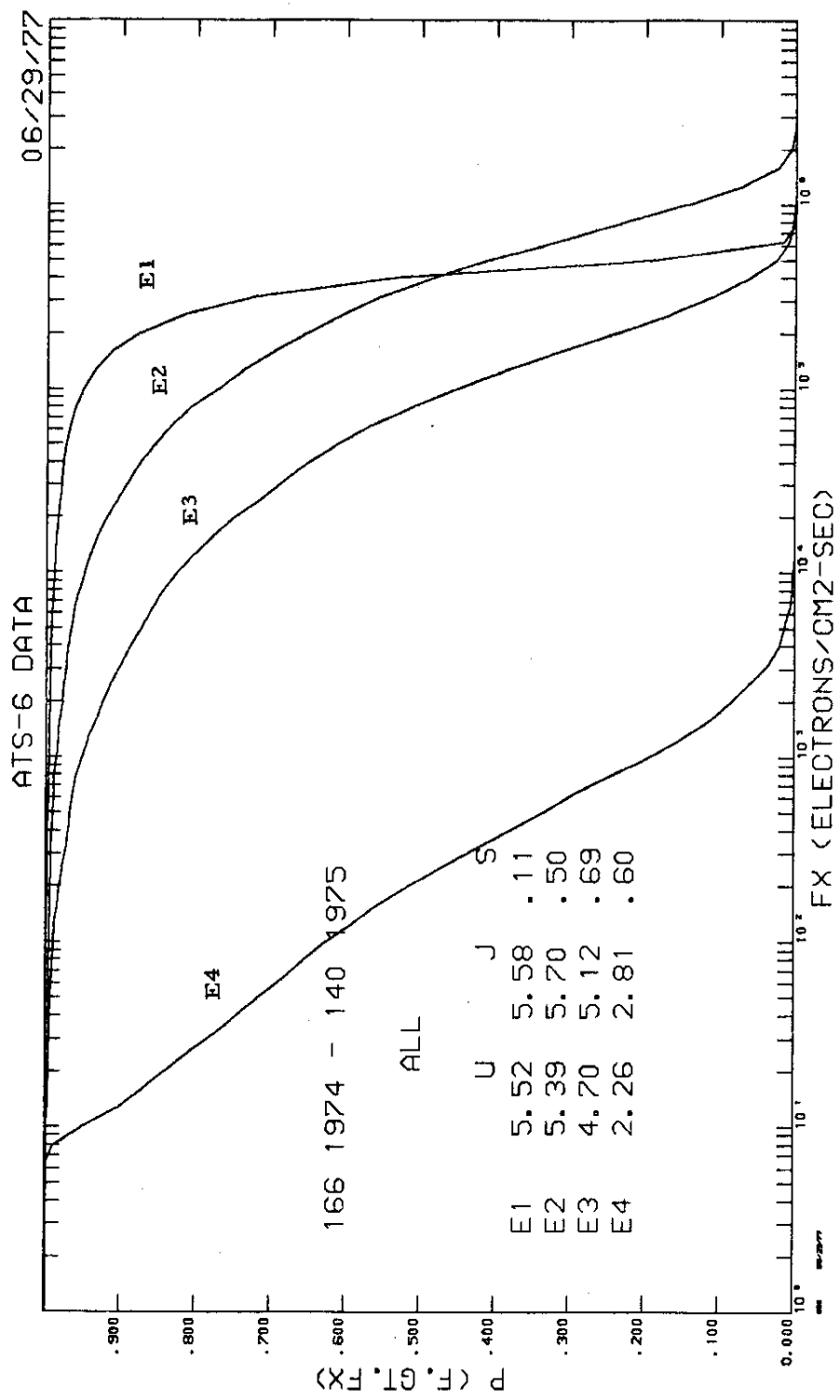


Fig.
11

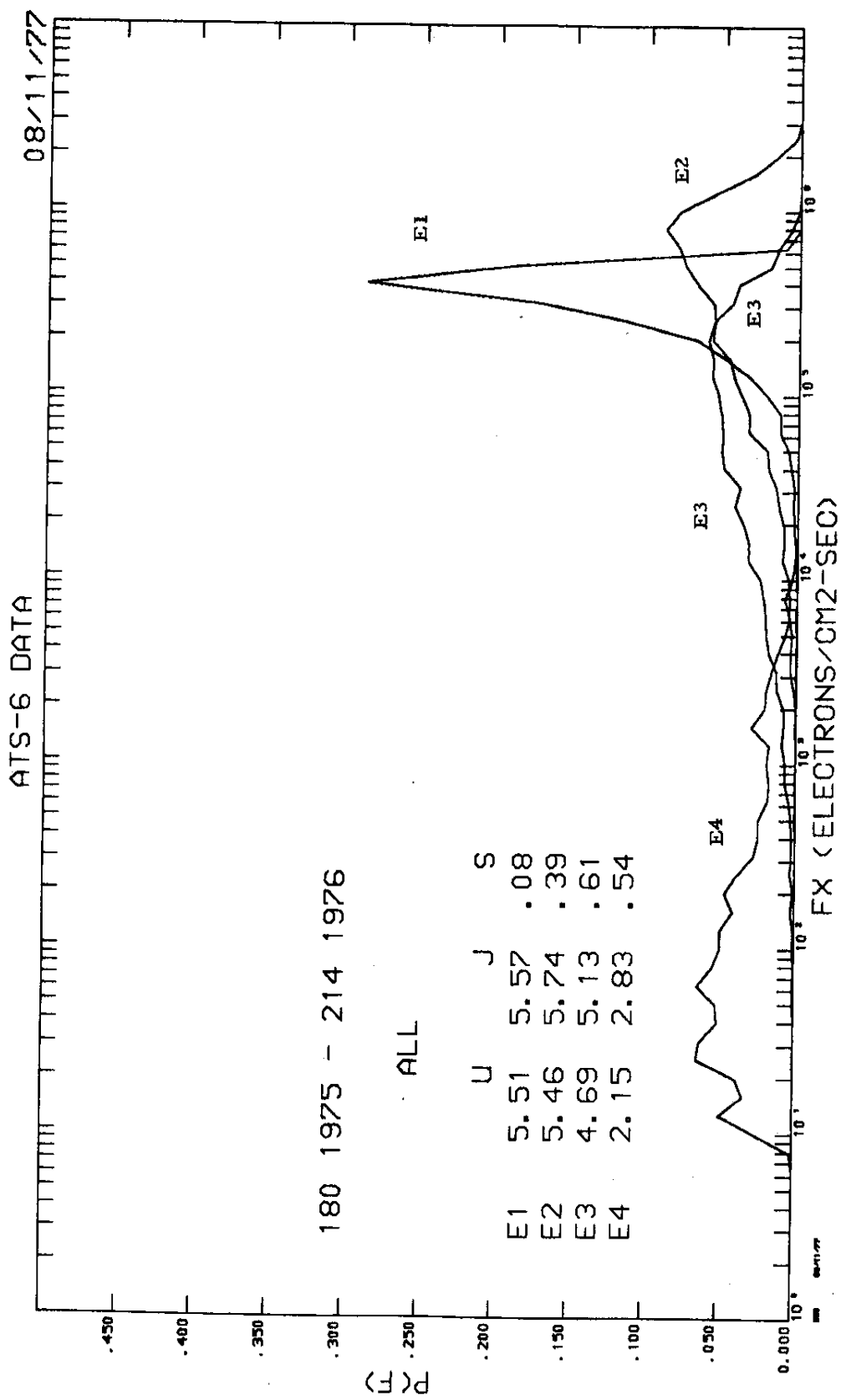


Fig.
12

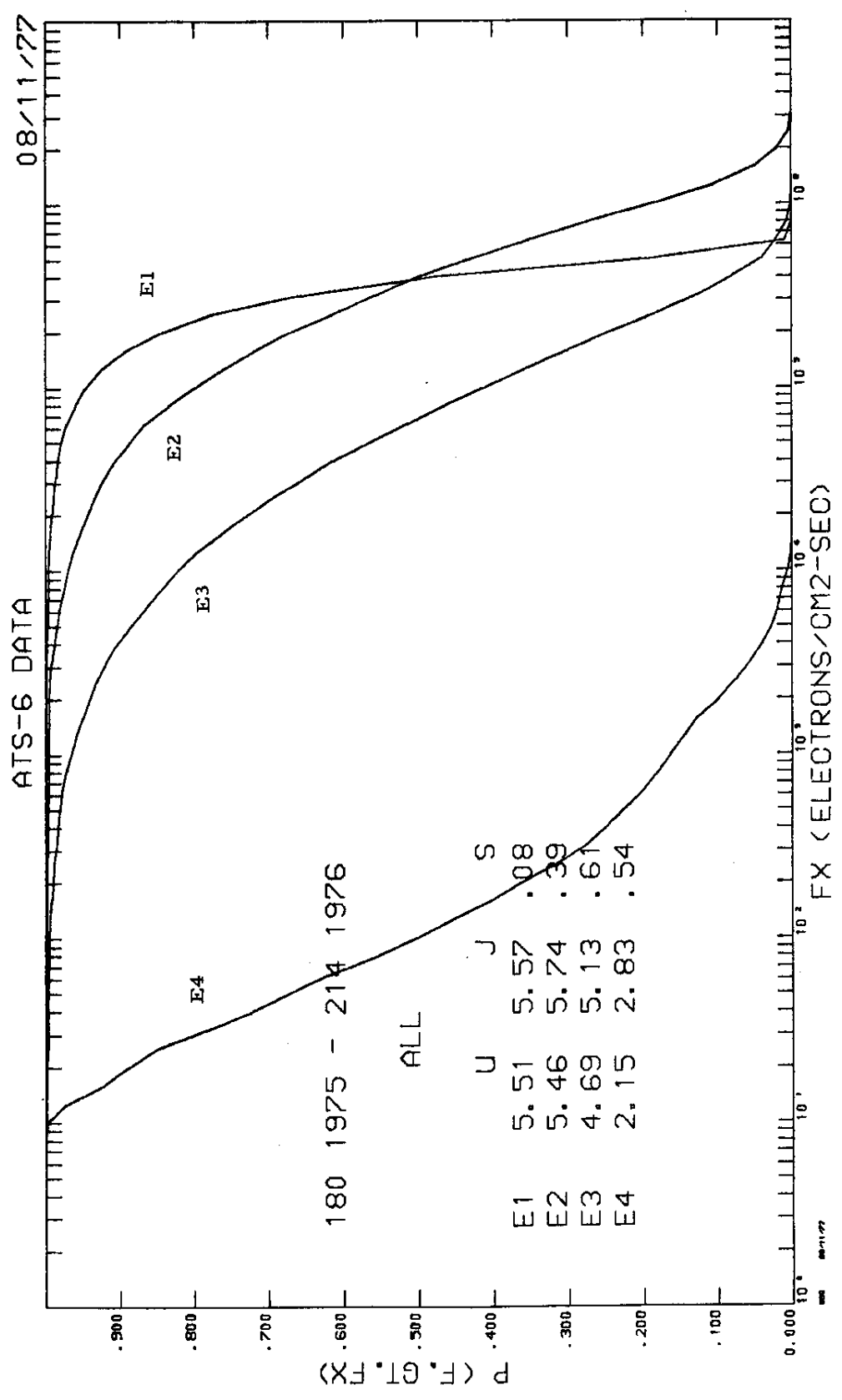


Fig.
13

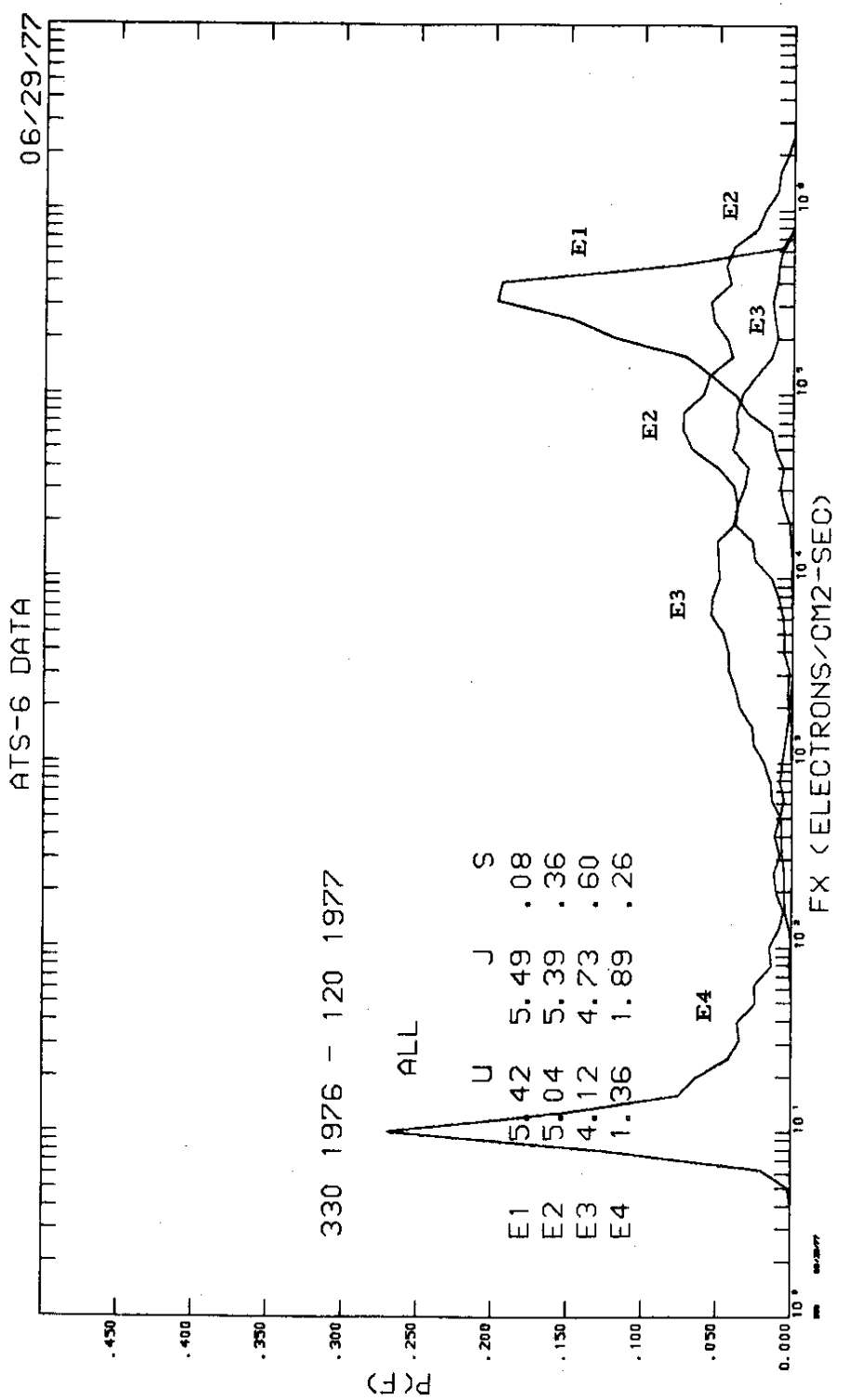
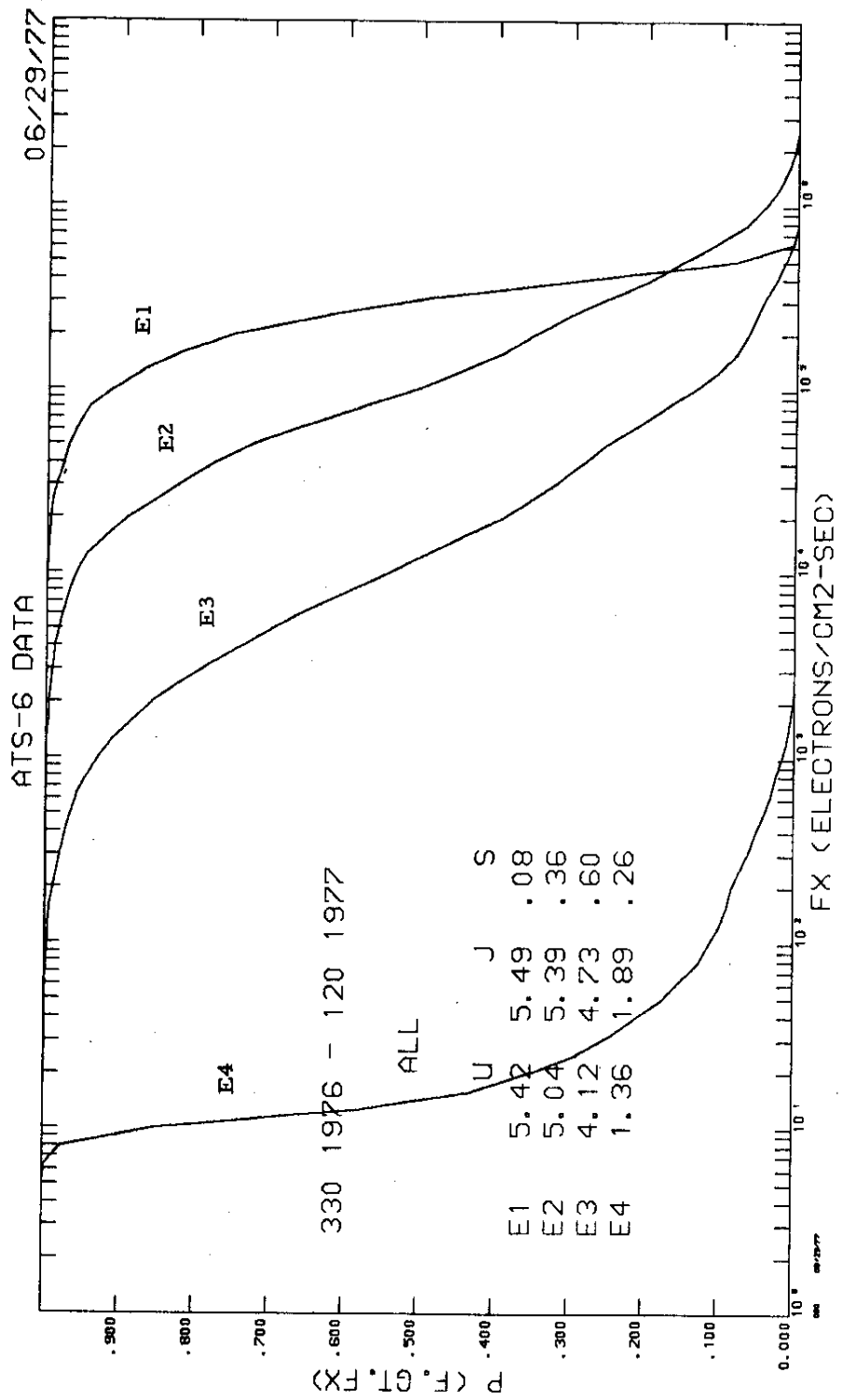


Fig.
14.



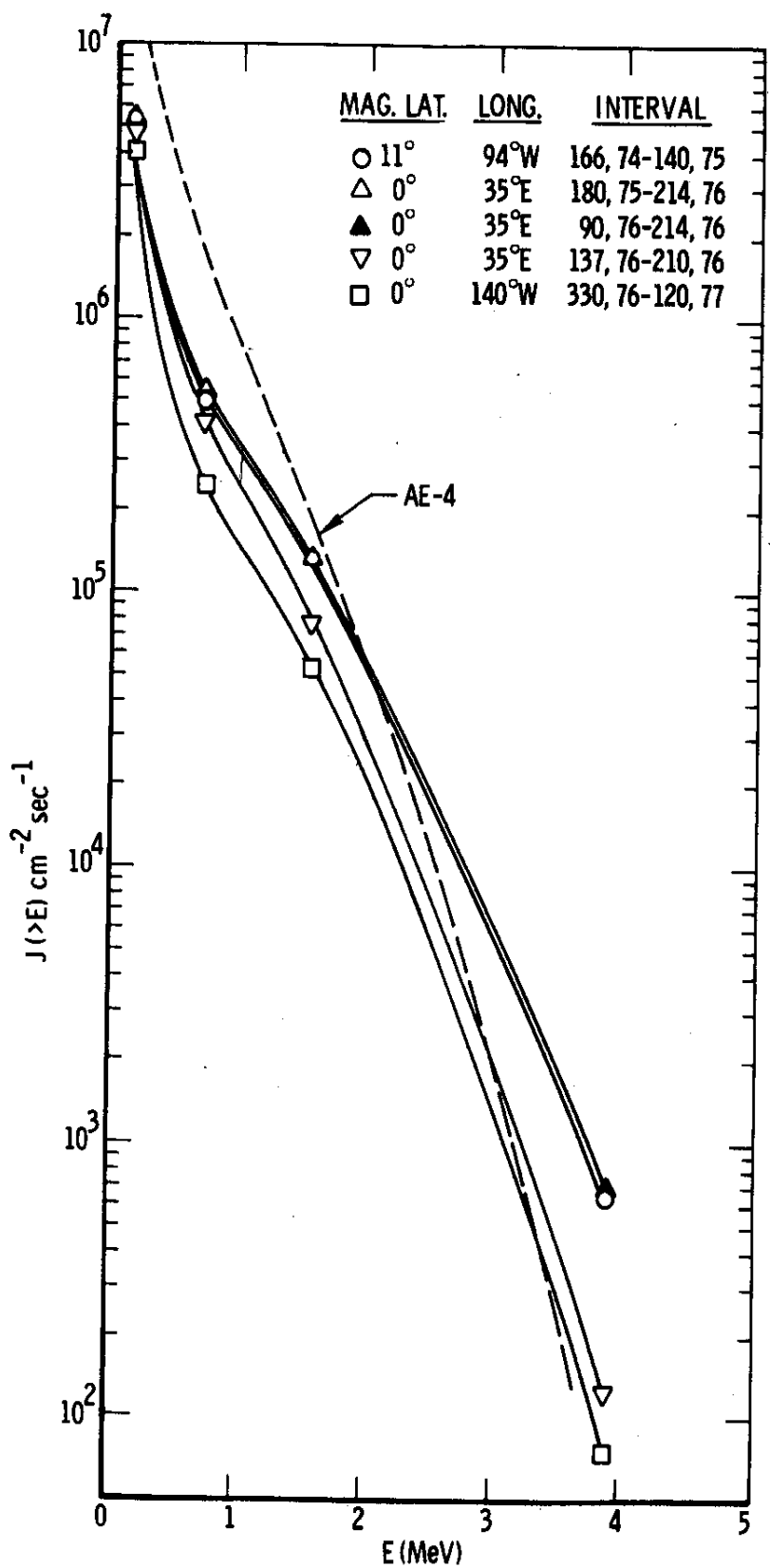


Fig.
16

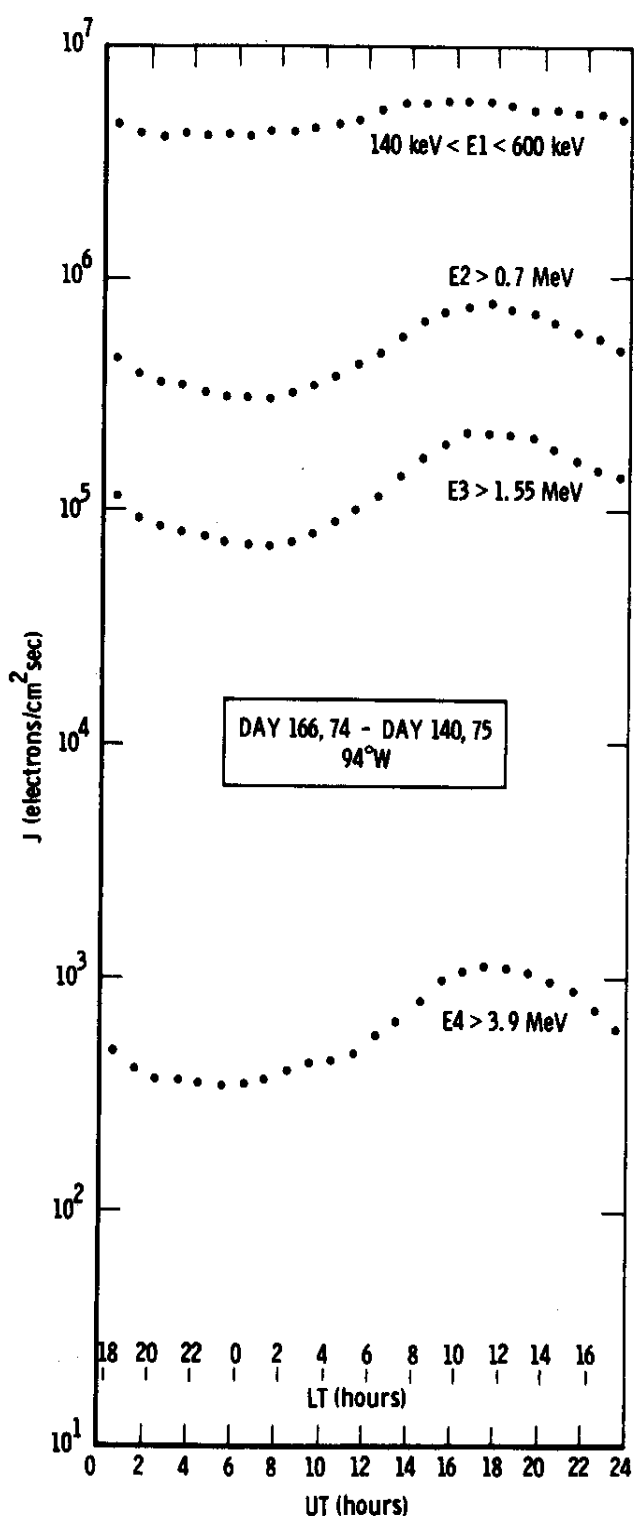


Fig.
17

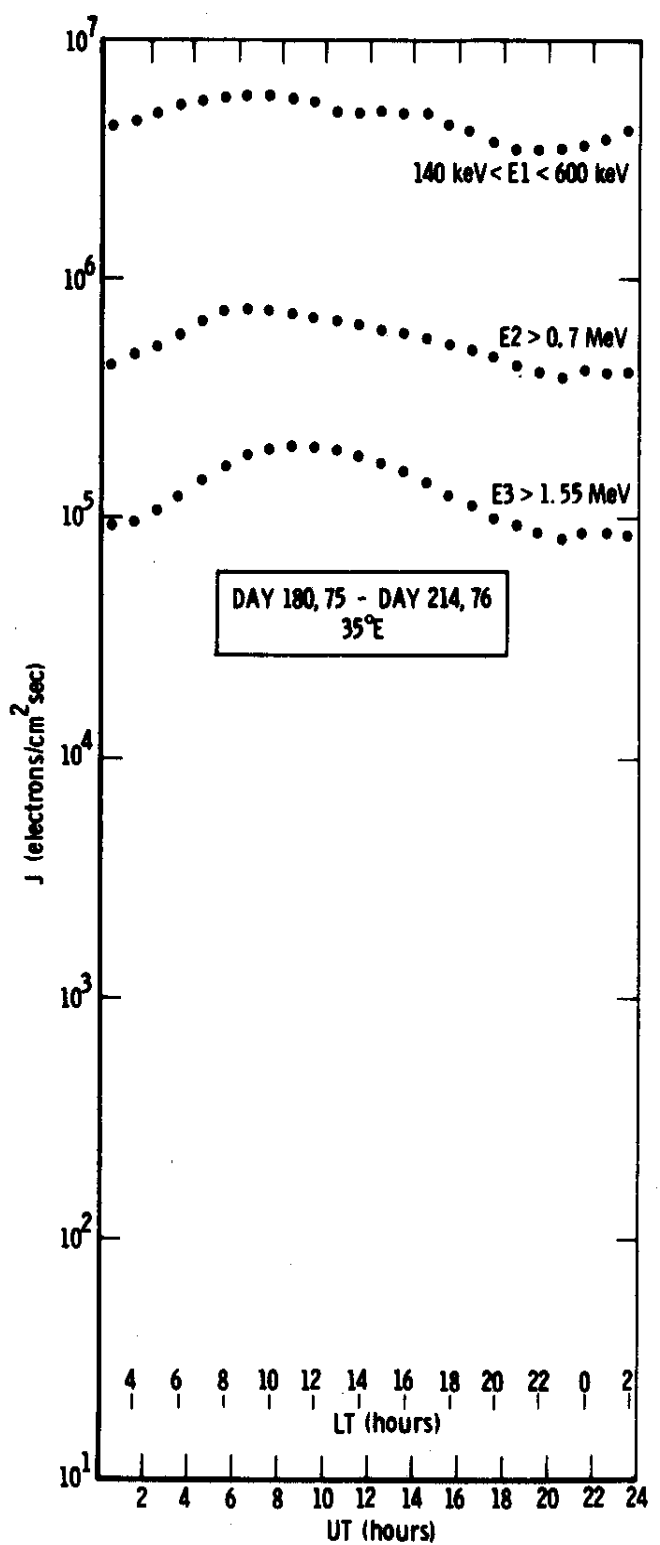


Fig.
18

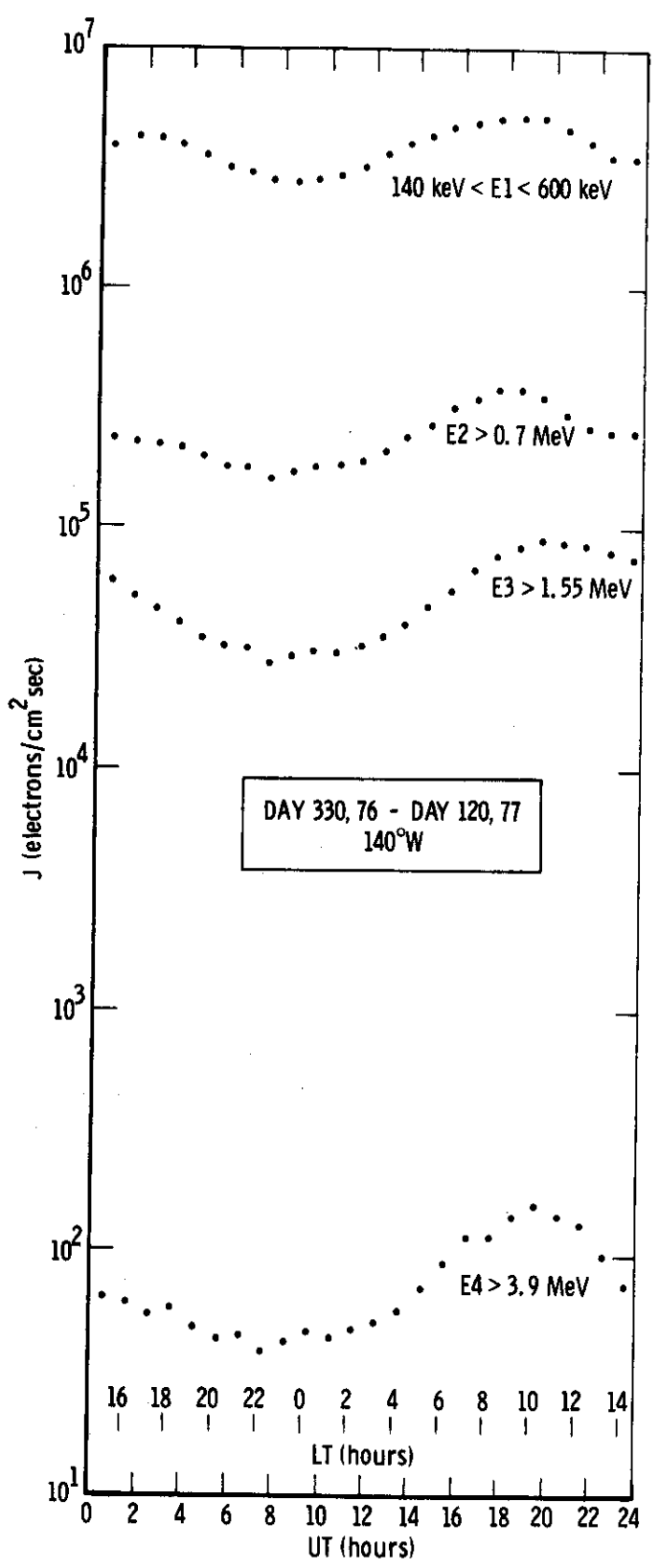


Fig.
19

Appendix A: A Description of Instrument Response

A full description of the ATS-6 Aerospace Corporation experiment has been presented in Ref. 13. Here we summarize, for ready reference, those salient features of the instrument response which may be of interest or assistance in interpretation of the results presented in earlier portions of this report.

Instrument Description

Figure A-1 shows a schematic block diagram of the detector/electronic system. The electron channels, E1, E2, E3, E4 are derived from Sensors 1-4 respectively. Figure A-2 shows the experiment.

Electron Detection

The responses of the electron channels are illustrated in Figures A-3 and A-4 respectively. These data, integrated over the angular acceptance angles of each detector give the average detector geometric factor as a function of energy. It has proven convenient to integrate these energy dependent geometric factors over various (assumed) shapes of the incident electron spectrum and finding a threshold (or set of thresholds for the E1 channel) which minimizes the variation of the geometric factor with spectral shape. The results are presented in Table A-1. The ϵ -G factors given in this table were used to convert from counts to flux above the indicated thresholds (or, for E1, in the indicated energy interval).

Proton Contamination

Proton channels which measure trapped and solar proton fluxes are also associated with each detector. In principle, the proton data can be used to correct for any proton contamination of the electron data. In practice, we found that during the 1974-1977 interval, solar proton activity was very low and no systematic correction was required; instead, days of data where some solar proton contamination (primarily of the E3, E4 channels) was suspected were rejected from the analysis. The sporadic fluxes of low energy (several Mev) trapped protons which we occasionally observed did not have any effect on the electron channels. Galactic cosmic rays and the products generated by their interaction with the spacecraft gave

rise to a significant background in the E4 channel. This background has a diurnal signature characteristic of cosmic rays (i.e. a maximum near local midnight and a minimum near local noon). During time periods when the trapped electron flux was low, for example the late 1976 - early 1977 time period, this background can be clearly visible in the E4 data (see Fig. 5) as an apparent flux of $\approx 10 \text{ cm}^{-2} \text{ sec}^{-1}$. The true flux is more likely $\approx 5 \text{ cm}^{-2} \text{ sec}^{-1}$ because the geometric factor of the E4 channel for these very energetic, minimum ionizing particles is a factor of two larger than quoted in Table A-1. This background has not been subtracted from our results; although of galactic origin, the radiation masquerading as "energetic electrons" is always present at the synchronous orbit, is practically indistinguishable from energetic electrons, and may be of some practical consequence as an ever-present background.

Bremsstrahlung Effects

During our calibrations, the bremsstrahlung efficiencies of the E2, E3, E4 channels were measured. Upper limits for the efficiencies were determined; those upper limits fall well below 10^{-4} relative to the direct detection of electrons. In all cases, we find that the galactic cosmic ray background exceeds that which might be generated by bremsstrahlung.

Accuracy of Results

The dominant source of error in this experiment arises because of the uncertainty, estimated to be $\approx 20\%$, in the geometric factors. All other experimental sources of error are minimal. While, under some circumstances, counting statistics may contribute additional uncertainty, in this paper we are dealing with long term flux averages which effectively eliminate counting statistics as an error source. It is important to reiterate that our measurements deal with a high variable phenomenon characterized by significant deviations from the mean. Comparisons of our results with those of others need to take this into account and also recognize that important long term effects (related to the 11 year solar cycle) in the structure of the radiation belts exist.

TABLE A-1
Omnidirectional Geometric Factors

Channel	Passband or Threshold (Mev)	ϵG
E1	0.140-0.600	$0.115 \text{ cm}^2 \text{sr}$
E2	0.700	0.00349 cm^2
E3	1.55	0.0176 cm^2
E4	3.90	0.0688 cm^2

Appendix Figure Captions

Figure A-1 Schematic block diagram of detector/electronic system.

Figure A-2. Overall view of the energetic particle spectrometer on ATS-6. Directional detectors (E1 channel) are housed inside the cylindrical collimator structure in the foreground.

Figure A-3. Efficiency of detection of electrons in the E1 channel. This channel has a nominal energy sensitivity of 140-600 keV. Sensitivity of this channel below the nominal electronic threshold is associated with the finite noise of the detector.

Figure A-4. Effective area of the E2, E3 and E4 electron channels as a function of electron energy. This effective area, when integrated over the angular response of the detector, yields the omnidirectional geometric factor. Bremsstrahlung efficiencies fall well below lower limits of this figure.

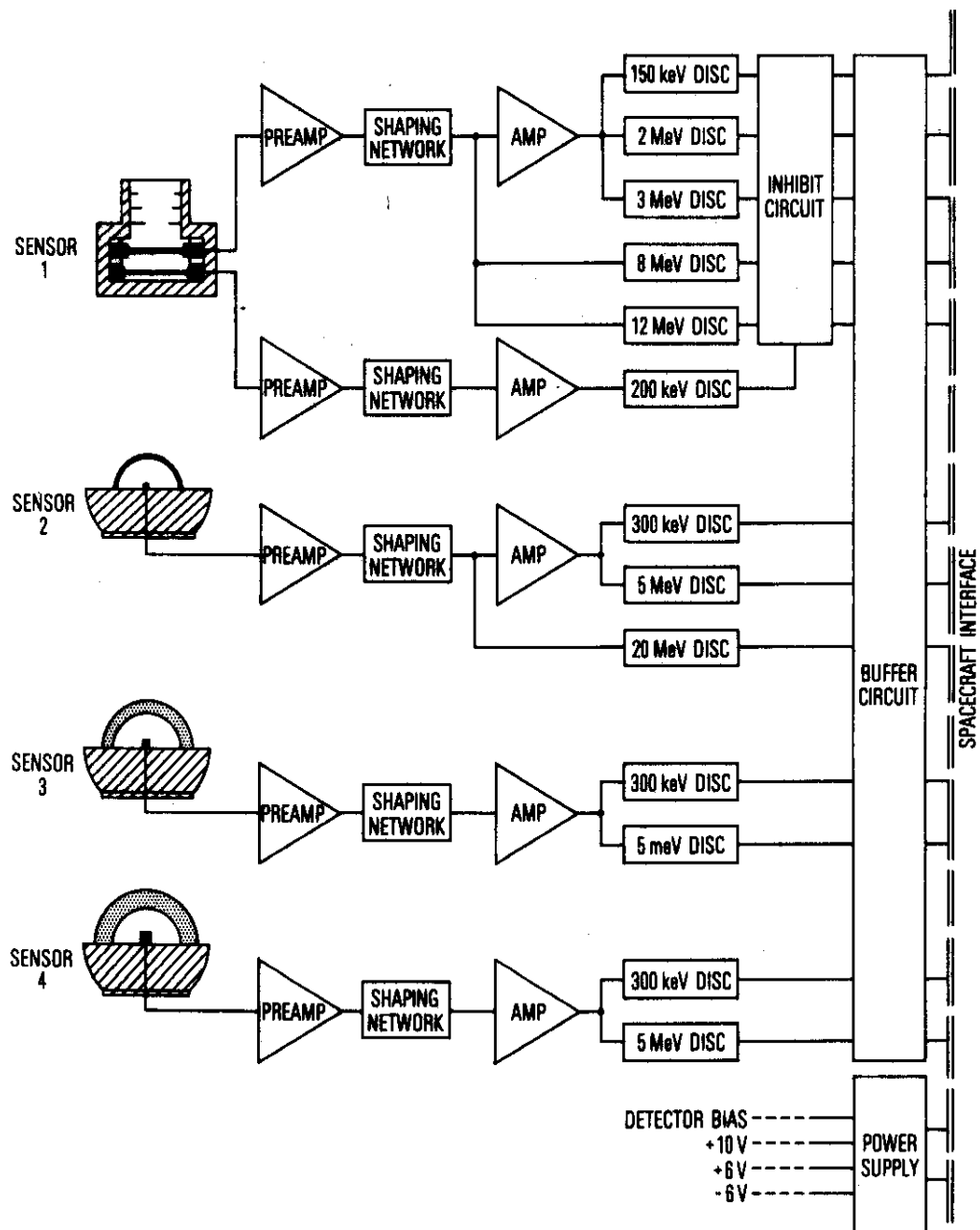
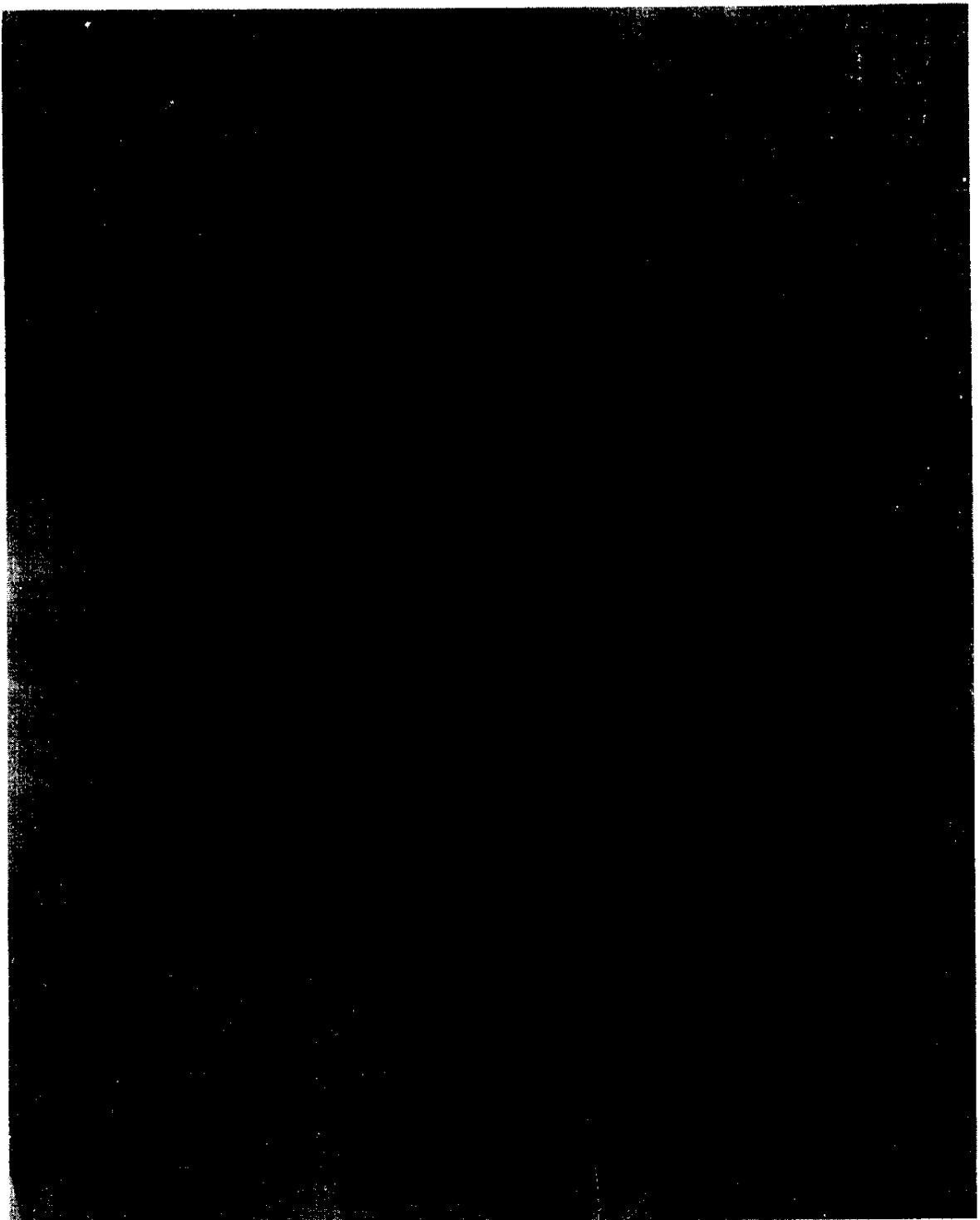


Fig.
A-1



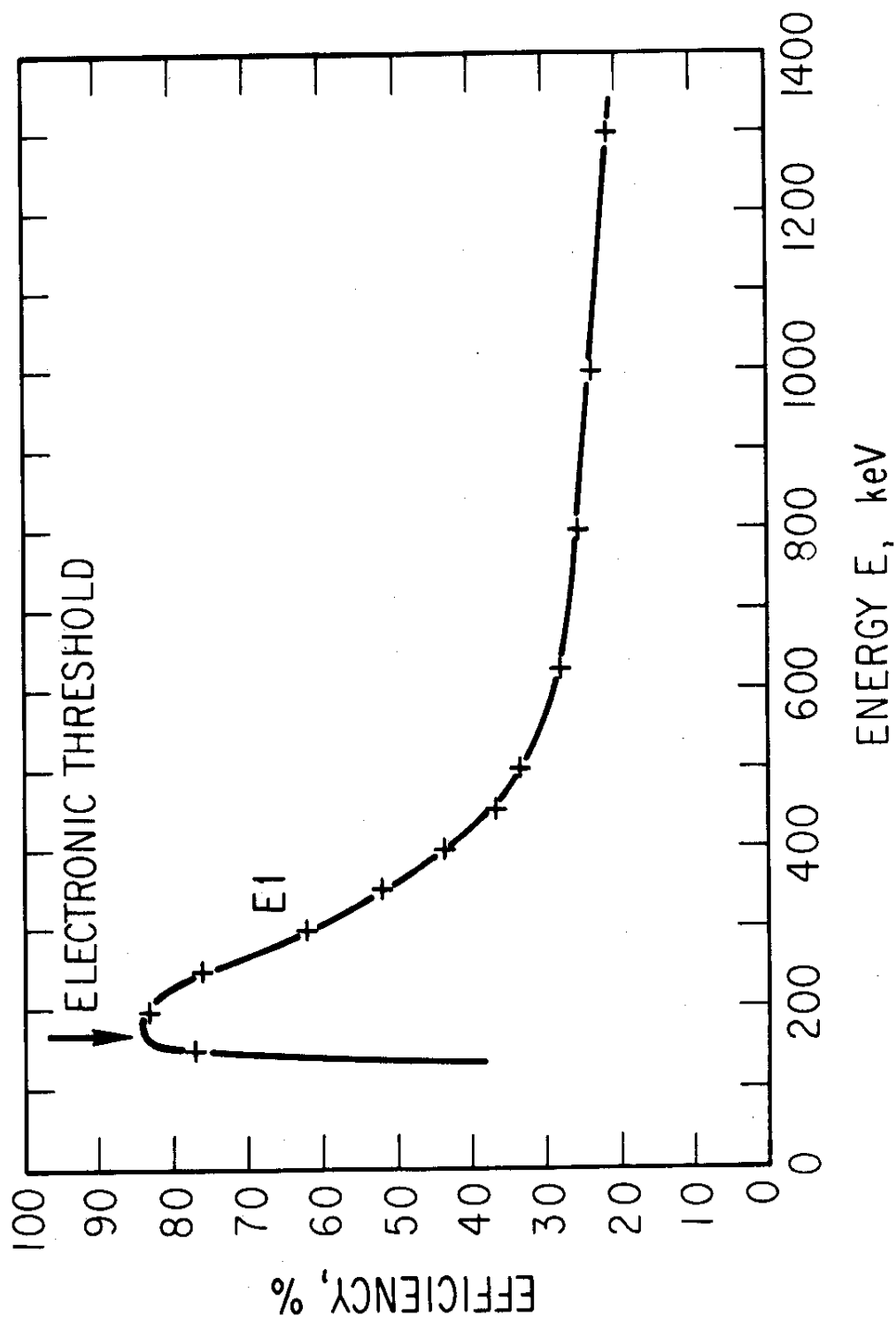


Fig.
A-3

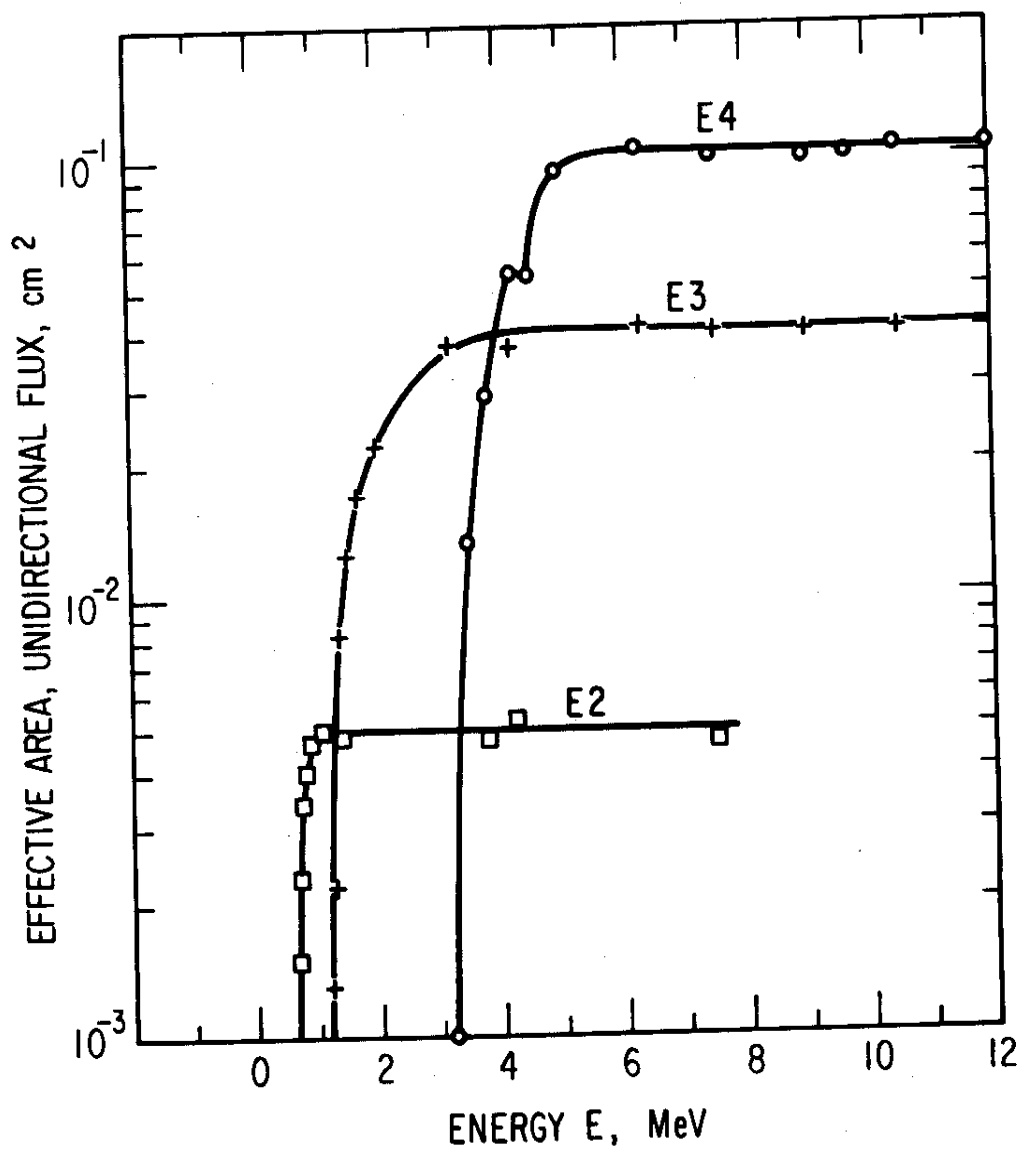


Fig.
A-4

DISTRIBUTION

Internal

J. B. Blake
G. W. King
E. B. Mayfield
R. X. Meyer
F. A. Morse

G. A. Paulikas
R. D. Rawcliffe
H. R. Rugge
H. H. Hilton
J. Frawley

External

NASA Goddard Space Flight Center
Greenbelt, MD 20771
Attn: L. Dubach, Code 601
J. P. Corrigan, Code 410
C. D. Wende, Code 410

NASA STIF
P.O. Box 8757
Baltimore/Washington Int. Airport
Baltimore, MD 21240

Octal Dump

DUMP OF TAPE X-406

INPUT TAPE X-406 ON MS2
DATA INPUT 09 FL=1=1

D-30956
ATS-6
6/11/74 - 12:34:14

FILE	RECORD	1 LENGTH	4960 BYTES	42550000000	00000000245/	000000000000	000000000000	300000000000
((1	555510045533	4250353365042	231330566312	403317304076	37246106162	60573722222
(48)	50160000000	0000000036661	172264730455	662473666063	377777777777	777777776057	777777777777
(96)	777777776057	377777777777	777760573777	605737777777	377777776057	777777777777	777777776057
(144)	777777777777	605737777777	777760573777	605737777777	377777776057	777777777777	777777776057
(192)	377777777777	777760573777	777777777777	777777777777	605737777777	777777777777	777777777777
(240)	605737777777	777777777777	777777777777	777760573777	605737777777	777777777777	777777777777
(288)	777717426124	12621560270	174262075666	625376251742	644025454433	473217427670	557426357014
(336)	22653114142	74534620201	53121742751	632504554766	174271125252	550174431742	656056124203
(384)	23613370214	745262060643	640124256057	377777777777	777760573777	777777777777	605737777777
(432)	377777777777	777760573777	777777777777	605737777777	777777777777	777777777777	777777777777
(480)	605737777777	777777777777	377777777777	777760573777	777777777777	605737777777	777777777777
(528)	777760573777	777777777777	605737777777	777777777777	377777777777	777777776057	377777777777
(576)	777777776057	377777777777	777760573777	777777777777	605737777777	777777776057	777777777777
(624)	255074623270	17416223012	51527216057	605737777777	605737777777	777777777777	777777777777
(672)	377777777777	777760573777	777777777777	777777777777	777777777777	777777777777	777777777777
(720)	605737777777	777777777777	377777777777	777760573777	777777777777	777777777777	777777777777
(768)	777717374770	336163273072	174040715642	135137131740	501455122475	736517407106	147446021002
(816)	327502571741	535757673536	72051741475	446073000303	1740573732072	024562621737	73175202614
(864)	434271165523	173755400340	61524476057	377777777777	777760573777	605737777777	777777777777
(912)	377777777777	777760573777	777777777777	605737777777	605737777777	777777777777	777777777777
(960)	605737777777	777777777777	377777777777	777760573777	777777777777	777777777777	777777777777
(1008)	777717256674	435336256200	172650317551	414011661726	645532330432	424117275252	506374256461
(1056)	433540101727	660005352470	316217275550	544176744603	172741154123	600236431726	446204722342
(1104)	755476241211	17256142362	007113216057	377777777777	777760573777	605737777777	777777777777
(1152)	377777777777	777760573777	777777777777	605737777777	605737777777	777777777777	777777777777
(1200)	605737777777	777777777777	377777777777	777760573777	777777777777	777777777777	777777777777
(1248)	777717166216	263053477107	171645452747	414405111716	402700560134	027017164540	000000000000
(1296)	357310341716	554355730261	215017166366	411366411366	171671111111	111111116057	377777777777
(1344)	00000000000	171656166161	161616166057	377777777777	777760573777	605737777777	777777777777
(1392)	377777777777	777760573777	777777777777	605737777777	605737777777	777777777777	777777777777
(1440)	605737777777	777777777777	377777777777	777760573777	777777777777	605737777777	777777777777
(1488)	777717164540	00000000000	171565444444	444444441715	402700560134	027017164540	000000000000
(1536)	303673211716	405162740516	274017156743	434343434343	171543504772	230632401715	61321142172
(1584)	564272135056	171561616161	616161616057	377777777777	777760573777	605737777777	777777777777
(1632)	377777777777	777760573777	777777777777	605737777777	605737777777	777777777777	777777777777
(1680)	605737777777	777777777777	377777777777	777760573777	777777777777	605737777777	777777777777
(1728)	777717137111	111111111111	171352666666	622544531126	225417143555	555555555555	171640155553
(1776)	405117021713	720314253647	607217144474	434343434343	171543504772	230632401715	61321142172
(1824)	506747460000	000000000000	171452605734	120754746057	377777777777	777760573777	605737777777
(1872)	377777777777	777760573777	777777777777	605737777777	605737777777	777777777777	777777777777
(1920)	605737777777	777777777777	377777777777	777760573777	777777777777	605737777777	777777777777
(1968)	777700000000	000000000000	000000000000	436775550356	617317137111	111111111111	171452747744
(2016)	560674746000	000000000000	000000000000	712624313303	171711111111	111111111111	405117145350
(2064)	071326335204	171677263154	171452605734	120754746057	377777777777	777760573777	777777777777
(2112)	377777777777	777760573777	777777777777	605737777777	605737777777	777777777777	777777777777
(2160)	605737777777	777777777777	377777777777	777760573777	777777777777	605737777777	777777777777
(2208)	777700000000	000000000000	000000000000	775042535606	746717167715	310413173411	171722504253
(2256)	000000000000	000000000000	000000000000	000000000000	000000000000	000000000000	000000000000
(2304)	000000000000	000000000000	000000000000	000000000000	000000000000	000000000000	000000000000
(2352)	377777777777	777760573777	777777777777	777760573777	777777777777	605737777777	777777777777
(2400)	605737777777	777777777777	377777777777	777760573777	777777777777	605737777777	777777777777
(2448)	777717167473	171674625402	030446711715	251472537555	501312142441	312617002442	17167514255
(2496)	37550121716	763561265172	12461716737	171474733105	003453001716	54740132573	7607017165674
(2544)	252671145165	171474413126	170024426057	377777777777	777760573777	777777776057	777777777777
(2592)	377777777777	777760573777	777777777777	605737777777	605737777777	777777777777	777777777777
(2640)	605737777777	777777777777	377777777777	777760573777	777777777777	605737777777	777777777777
(2688)	777760573777	777777777777	777777777777	777760573777	777777777777	605737777777	777777777777
(2736)	777777777777	777777777777	777777777777	777777777777	777777777777	605737777777	777777777777
(2020315171717	2020315171717	2020315171717	2020315171717	2020315171717	2020315171717	2020315171717	2020315171717

Jane

6/11/74 - 12:34:14

FILE	1	RECORD	196	LENGTH	4960 BYTES	12
(0)	333737404344	555510045533	435034365042	415500000000	000000000555
(48)	400410000000	000000002666	172265005315	152015676066	001666245022
(96)	77777776052	37777777777	777760573777	77777777777	736417304115
(144)	77777777777	60573777777	77777777777	60573777777	326031065022
(192)	610541712640	47141742625	770327014563	572117407117	77777777777
(240)	174174276264	32701321741	174247013707	155307022752	174165542550
(288)	262317424611	006600553137	174251233754	154320417174	740003611742
(336)	363373271742	425065143024	231217424076	174247272661	475032631742
(384)	313324044660	174177316701	125646161740	466276214010	504073152600
(432)	635562413753	640317407464	006472176345	173776767160	517161236004
(480)	173452714304	024011311734	173542305726	20557011737	517065557030
(4896)	77777777777	777760573777	77777777777	60573777777	3321
(4944)	77777777777	60573777777	77777777777	60573777777	431317523273
(528)	240117373737	213024365133	174044541046	412127415352	53732523532
(576)	227204321740	61634315156366	173051110430	174055637501	735501631740
(624)	670533550257	173745435513	541472521735	101517354342	324571741100
(672)	504414647536	562317365461	652513122712	173545200270	653753111734
(720)	173452714304	024011311734	61751346654	307015423421	173542305726
(768)	506561224200	6375121664017	400246436733	002517375301	145541655506
(816)	5766667647017	560017365464	453574064747	560241051735	605516363577

(864)	147193052047	173456451152	764004721724	526376544562	663217254336	513076537607	172471224034	276467761725
(912)	571146714431	546017245403	10702111144	172364124661	002731121723	54137335103	767317235516	050753412117
(960)	172356612343	571514531723	57230276033	656117236334	571576475775	172364075733	626021031723	633564374572
(1008)	747317244035	774545714635	172450765747	035030251725	61543243113	624317264303	352563237473	172554703561
(1056)	445710051725	440365152262	166617247457	344233451723	172456706642	241161421725	635210621517	105017236332
(1104)	766772207702	522500523	52250051715	720314253647	3375405150	171562271751	536654741715	
(1152)	472602062270	517517165463	146314631463	171640371401	231256101715	707070707070	70707157070	707070707070
(1200)	171552525252	525252521716	416161616161	616117156200	0000000000	171557124601	342023517125	613172544252
(1248)	205617157564	272135056427	171560000000	716232676076	322217165666	145364357666	17164011111	
(1296)	11111111715	660335317442	460317157100	776670122064	171571212460	534151301715	71111111111	11117154707
(1344)	070707070707	171641616161	616161611714	717262307172	623017154701	437160307634	17146611046	635065651714
(1392)	171360247136	301031134247	301031134247	171540571100	123634361714	616161616161	616117146161	616161616161
(1440)	171461616161	616161611715	470707070707	070717156544	444444444444	171540632420	722407451715	4613724040470
(1488)	644217147203	142536476072	171467130215	173454101714	624407406266	470017154402	234650270402	171452605271
(1536)	120754471715	475073755431	275017156170	677001107655	171547277221	357310341715	655417355063	426217155616
(1584)	161616161616	171461616161	616161611711	722407451316	335417137610	545716225100	171356550453	552112731712
(1632)	620000000000	000000000000	000000000000	171360173376	55256141714	437434343433	434317127070	707070707070
(1680)	171352525252	525252521713	707070707070	797017127100	776670122064	171353505642	72135561713	24412235264
(1728)	263117137162	326760763222	17137033574	661640121712	715205610044	715217117172	623071726230	1713525252
(1776)	525252521713	531126225445	311217135266	666666666666	1717171212460	534151301714	436264763315	016717135252
(1824)	5252525252	171352525252	525252520000	000000000000	000000000000	000000000000	000000000000	000000000000
(1872)	000000000000	000000000000	000000000000	000000000000	000000000000	000000000000	000000000000	000000000000
(1920)	000000000000	000000000000	000000000000	000000000000	000000000000	000000000000	000000000000	000000000000
(1968)	000000000000	000000000000	000000000000	000000000000	000000000000	000000000000	000000000000	000000000000
(2016)	172036140000	000000000000	000000000000	000000000000	000000000000	000000000000	000000000000	000000000000
(2064)	000000000000	000000000000	000000000000	000000000000	000000000000	000000000000	000000000000	000000000000
(2352)	672457556407	744000000000	000000000000	000000000000	000000000000	000000000000	000000000000	000000000000
(2400)	000000000000	000000000000	000000000000	000000000000	000000000000	000000000000	000000000000	000000000000
(2448)	000000000000	000000000000	000000000000	000000000000	000000000000	000000000000	000000000000	000000000000
(2496)	423630160000	000000000000	000000000000	000000000000	000000000000	000000000000	000000000000	000000000000
(2544)	312617002442	171674413126	170024401717	523545050655	325417174146	676616706256	172043774562	2164264651720
(2592)	4213164547211	31261715276	545605302041	171762775635	220411321717	602500403640	5344171270533	114476562300
(2640)	171661454040	347137213054	171662436435	453200531716	561550104034	771217147514	72553755013	172267433772
(2688)	361217177037	150370341627	171752054601	537421717747	520502514700	517217205170	4760134142315	171772356271
(2736)	5611420251717	643656050753	411617176051	610303517271	171776323644	557360321720	476225773734	667517204241
(2784)	225136737242	171745761607	166506640000	000000000000	000017117565	371642004744	171356743152	317633661713
(2832)	643530103113	424717136402	051503412320	000000000000	000000000000	707070707070	707071313525	525252525252
(2880)	000000000000	000000000000	000000000000	000000000000	000000000000	000000000000	000000000000	000000000000
(2928)	175217137213	505642721350	171340122251	636166261712	715205610044	715217137141	630346071416	171352525252
(2976)	525252521711	714163034607	141617127121	246053415130	171171212460	534151301713	526057711207	544717127070
(3024)	707070707070	171352525252	047735010235	050160513405	37351147465	605127077412	220744706051	
(3072)	340072155761	010060520207	106732107661	605203715264	113177716422	603160521063	552112531301	
(3120)	605213562434	143246306052	144535460763	507660521022	456726215520	605203610064	434717176052	054323621055
(3168)	434560522016	36052352762	605203252762	336113162602	035671653072	6303605020206	105535572362	60503644662
(3216)	143052546051	371723657107	131760513711	447371452466	605136336022	637767236051	354774573434	407060513463
(3264)	230112403124	605134372177	411640641721	755032772130	422217234343	247525645366	172450334643	163533641723
(3312)	771560043621	146117225030	556633513440	172272760204	641601261720	714515266101	117517204307	416466346514
(3360)	172144067741	253177261720	447534163231	15071205122	711553653041	171774054640	737024651720	604736050133
(3408)	451317214647	257644373551	172247663353	1723412571722	4571635627	0373621721721	630320216650	172170227227
(3456)	473671301720	630277171720	115660572137	547570522204	171564760140	174271711721	457226046351	30117215672
(3504)	061150032713	172150550672	271031631726	514221427222	421317256135	00327752153	17257273721	717325161725
(3552)	614507150474	507117254152	227315543112	172462244404	636452001725	444350027433	024717255350	607343527130
(3600)	172567040555	3563347561726	407163123171	509717264546	647404107463	172651735726	651257641726	544472334503
(3648)	573517266177	614766571726	172665572607	277701231726	745453166737	325417267637	354636240177	17267620443
(3696)	310165351726	756270010370	275517267437	071326722336	172671461543	631236243157	222717266063	
(3744)	572541474701	172653276310	213007511726	562070251761	017517265373	56032377676	172663356250	426353201726
(3792)	533257260037	152217264076	010021226656	172640407442	541647741726	407206462124	013517264315	550676535546
(3840)	172645775430	201431401726	516106436427	662017265662	352656733730	17265432142	042500571726	652376023376
(3888)	615517267262	225656216644	172633660172	074675701726	75536310771	455617247270	42560571726	172744754522
(3936)	171522317727	427663332554	561717267437	41050365656057	777777777777	330617267415	330617267415	777777777777
(3984)	170670321074	777777777777	777777777777	777777777777	777777777777	605737777777	777777777777	605737777777

(4032) 3777777777777777 777760573777 7777777777777777 605737777777
 (4080) 605737777777 777777776057 377777777777 77760573777 777777777777
 (4128) 777760573777 777777777777 605737777777 777777776057 377777777777
 (4176) 777777776057 377777777777 77760573777 777777777777 605737777777
 (4224) 777777776057 655737777777 777777776057 377777777777 605737777777
 (4272) 377777777777 77760573777 777777777777 605737777777 77760573777
 (4320) 605737777777 777777776057 377777777777 77760573777 377777777777
 (4368) 777760573777 777777777777 605737777777 777777776057 377777777777
 (4416) 777777776057 377777777777 777760573777 777777777777 605737777777
 (4464) 777777776057 605737777777 777777776057 377777777777 777777777777
 (4512) 377777777777 77760573777 777777777777 605737777777 777777777777
 (4560) 605737777777 777777776057 377777777777 77760573777 377777777777
 (4608) 777760573777 777777777777 605737777777 777777776057 377777777777
 (4656) 777777776057 377777777777 777760573777 777777777777 605737777777
 (4704) 777777777777 605737777777 777777776057 377777777777 777777777777
 (4752) 377777777777 77760573777 777777777777 605737777777 777777777777
 (4800) 605737777777 777777776057 377777777777 77760573777 377777777777
 (4848) 777760573777 777777777777 605737777777 777777776057 377777777777
 (4896) 777777776057 377777777777 77760573777 777777777777 605737777777
 (4944) 777777777777 605737777777 777777777777 777777777777 77760573777

FILE	INPUT RECS.	DATA RECORDS INPUT	MAX. SIZE	READ ERROR SUMMARY	INPUT #RECS.	RETRIES TOTAL#
1	196	197	3720	PERM ZERO B SHORT UNDEF.	0 51 0	51 73

EOJ DUMP STOPPED AFTER FILE 1 # OF PERMANENT READ ERRORS 0

START TIME 02/15/78 09:22:48

STOP TIME 02/15/78 09:23:21

INPUT TAPE X-4.11 ON MT3

1121-1217

FILE	1	RECORD	1	LENGTH	4960BYTES
()	3537454235	555513245532	425500000000	000000000001
(48)	000000000000	000000000000	000000000000	000000000000
(96)	77777777607	377777777777	777760776557	65131046131
(144)	777777777777	605737777777	777777777777	65131046131
(192)	655365271046	154117426320	713674457170	17426376420
(240)	174273413372	702172071743	421361546613	507217427547
(288)	200117434312	230011600131	174274572025	331302751743
(336)	5472271742	763627300000	521247525476	174227151147
(384)	173261553376	174251066540	3275017171742	622417251133
(432)	446265441534	551117424146	573106744002	174240064642
(480)	174154175501	463142231741	777672324201	255117424300
(528)	467217425561	751447461755	174265202475	45144661742
(576)	613167071743	627300673167	773517435314	262747502102
(624)	401017755135	174362030122	333326411737	631417232477
(672)	514052561455	322617374451	71205152213	173740412567
(720)	173654760000	224740551737	635117374607	37644137417
(768)	456717376032	257751605076	173772473165	575333341740
(816)	205506614060	635507540271	465617407072	6656074551
(864)	234502203664	174141255463	304011461723	755623265774
(912)	7221334274	227417247254	552164106724	172467764147
(960)	172454555002	563554531724	7302115117053	100317247516
(1008)	722117254274	394643171346	172556361134	45734361725
(1056)	152735631726	451717670493	182617264311	454053261452
(1104)	11424174531	172451731313	3742261712365	700000000000
(1152)	456547621230	156517164772	143661032547	171660514067
(1200)	171572243745	131633541716	441414141414	141417164402
(1248)	777717165773	217732177321	171656655207	375001141715
(1296)	54672071716	500565154355	730217164462	013612231005
(1344)	477223536324	171547162635	534731171715	437227172472
(1392)	531126225465	311217154421	775533106644	171562533405
(1440)	171565267006	664141751715	553075566037	236217156253
(1488)	003317152641	655467720726	171551241032	341747751715
(1536)	372117371715	571246011340	235717155746	162643342077
(1584)	4372651535	171547172221	357310347164	440605556000
(1632)	623465027040	223417137245	145734636360	171371623267
(1680)	171372031625	364760721714	4557006023244	163717127203
(1728)	345217117266	337503533157	300000000000	300000000000
(1776)	345372341712	717262307172	623017135334	0562653340562
(1824)	776670122604	171171212460	53419151300000	000000000000
(1872)	40132441161	551200000000	900000000000	17174565203
(1920)	000000000000	000000000000	000000000000	553404240000
(1968)	000017174054	343233704232	000000000000	000000000000
(2016)	10051000000000	000000000000	000000000000	000000000000
(2064)	315417235614	600000000000	600000000000	414532675467
(2112)	000000000000	000000000000	000000000000	172550000000
(2160)	000000000000	000000000000	000000000000	000000000000
(2208)	000000000000	000000000000	000000000000	000000000000
(2256)	401656210000	000000000000	300000000000	000000000000
(2304)	000000000000	000000000000	000000000000	000000000000
(2352)	75474132573	767117147613	40134345154	171656242526
(2400)	171756573571	525057361716	603136104666	012017157560
(2448)	501317165740	124572522305	171657745542	757247541716
(2496)	110642531717	465371070751	364417175657	357152505736
(2544)	013521132300	171757452135	211323101715	634514113754
(2592)	612416265414	346217176142	404573122435	1716771764376
(2640)	172443300000	212443300000	534517213725	755455213322
(2688)	767117204400	660167136173	171762734703	400021117171
(2736)	75536161716	77435642737	801417171710	275775343216

FILE	1	RECORD	341 LENGTH	496 BYTES
(2784)	67337623447	17165141336	047743311712
(2832)	535056427213	505617144427	213505642721
(288)	17127224745	131633541712	75062632447
(2923)	623317127325	45732457326	171274170360
(2975)	343434541712	172407451316	335417137266
(3024)	172407451316	17117137266	33543333157
(3072)	5626373125	23417245606	502467425043
(3120)	172364421366	512411271723	631644106207
(3168)	522417234721	212107321724	172363136215
(3216)	34735621724	427542262300	32212724453
(3264)	16277671133	172446455763	363154320000
(3312)	300300000000	000000000000	000000000000
(3360)	169000000000	100000000000	100000000000
(3418)	169000000000	000000000000	000000000000
(3456)	300000000000	000000000000	000000000000
(3504)	000000000000	000000000000	000000000000
(3552)	640057704252	360317245550	731634514563
(3600)	172455634395	37544311724	60330214032
(3648)	716117247714	512444577660	172541751506
(3696)	136154641725	47175567146	613673541725
(3744)	355662543234	172477527460	644705051725
(3792)	426347245037	443612516472	46232515070
(3840)	172460604545	273344021724	666404202504
(3888)	622217254106	621474677077	172544226416
(3936)	132525511725	452136745603	511417254601
(3984)	04347421161	172545110647	1041544666057
(4032)	377777777777	562573737777	605737777777
(4080)	605137777777	777777777657	377777777777
(4128)	777760573777	777777777777	605737777777
(4176)	777777776557	377777777777	777760573777
(4224)	777777777777	657377777777	777777776557
(4272)	377777777777	77760573777	777777776557
(4320)	605737777777	777777776557	377777777777
(4368)	777760573777	777777777777	605737777777
(4416)	7777777657	377777777777	777605737777
(4464)	777777777777	657377777777	777777777777
(4512)	377777777777	77760573777	777777777777
(4560)	605737777777	777777777777	605737777777
(4608)	777760573777	777777777777	777777777777
(4656)	7777777657	377777777777	777760573777
(4704)	777777777777	605737777777	777777777777
(4752)	377777777777	777657377777	657377777777
(4800)	605737777777	777777777777	777605737777
(4848)	777760573777	777777777777	777760573777
(4896)	777777776557	377777777777	777777777777
(4944)	777777777777	657377777777	777777777777

FILE	1	RECORD	341 LENGTH	496 BYTES
(0)	333544364144	555510045533	355034345042
(48)	333533000000	000000000000	000000000000
(95)	777777776557	377777777777	777777776557
(144)	777777777777	605737777777	777777777777
(192)	433377725164	450065573777	777777777777
(240)	172407343353	6204731717	605737777777
(288)	401017424653	336106771322	174160740671
(336)	125644651741	524596734527	761617415024
(384)	233547272165	174361274535	275337631736
(432)	510121141445	360362573777	64337344112
(480)	173357217376	473374011735	606734011735
(528)	572717364375	2024060235	173646456264
(576)	2424235231736	635534315743	242417366451
(624)	734212526130	173743124067	321015661732
(672)	531356306613	360060573777	777777777777
(720)	173135303673	67716531731	632033616231
(768)	37617324201	752436347431	754430501732
(816)	17234371732	661516665654	455417327130

(864)	25	314123673	173341163304	134550331722	67153502006	574217234176	330372532474	172345173241	52244531723
(912)	464533473304	75660573777	777777777777	605737777777	777777771723	455160735364	0000317226771	533565535241	
(963)	17234343224	131363441723	443432533677	17117234666	14732202161	172273343773	622712171722	7712443875	
(1058)	55217234266	5253355576152	172271743347	370671421723	427633030474	556617234531	431756167457	172346425201	
(1154)	621157461723	464346325442	36717234330	152522315242	172274741037	630310701722	057617227340	1057617227340	
(1154)	52147124264	172271425713	25447557377	436775537356	617317166413	505642721350	17161712460	53415130716	
(1152)	605140672637	105160573777	777777777777	605737777777	777777771716	726660365422	652717174353	442663676454	
(1200)	171660514067	263710511716	716232676076	32221717545	751024523632	17160334323	16500151717	431051606726	
(1248)	371317174375	077777777777	171662162630	534771071716	733531744246	033517166766	614536435766	171673353174	
(1296)	424603331716	562463704553	255217166554	173556334262	171656573536	727565731715	723450723450	723471715673	
(1344)	53627555735	171552666606	66666661721	73266515523	324617164045	042600450426	171601111111	111111111714	
(1392)	52747444551	173265573777	777777777777	605377777777	777777771715	706512110574	401317145467	016265160675	
(1440)	17164561343	27056311716	4027070560134	0270717156544	444444444444	171645601340	270560171715	75772176437	
(1488)	507717154441	714441714441	171651202675	325414501715	621626305347	710717164212	042410502120	171556533336	
(1536)	727565731716	417333333333	333317156544	444444444444	171552747744	405117021715	573721173721	173717154735	
(1584)	4367755356	171462530000	000000000000	000000000000	000000000000	000000000000	000000000000	000000000000	
(1632)	652525252525	252565573777	777777777777	605737777777	777777771714	53556407751	474117137364	323176151202	
(1680)	17117146303	460714161714	531744246033	531717127121	246053415130	171353031202	675325411713	712124605341	
(1728)	513517137234	57234557234	171453112622	544531121713	530312026753	2541171744407	406266470033	171371314256	
(1776)	374434541713	52747444551	170217145266	666666666666	171352747744	405117021713	541064756260	432317117131	
(1824)	425637443454	000000000000	000000000000	000000000000	000000000000	000000000000	000000000000	000000000000	
(1872)	000000000000	000000000000	000000000000	000000000000	000000000000	000000000000	000000000000	000000000000	
(1923)	000000000000	000000000000	000000000000	000000000000	000000000000	000000000000	000000000000	000000000000	
(1968)	757617174517	763274457261	17167726607	96252331716	77266070625	273300000000	000000000000	000000000000	
(2016)	00000000001720	575632036245	15561716750	42535667476	171677504253	560674761717	404267413732	544017167761	
(2064)	530527067576	17167373471	03225154000	000000000000	000000000000	000000000000	000000000000	000000000000	
(2112)	000000000000	000000000000	000000000000	000000000000	000000000000	000000000000	000000000000	000000000000	
(2160)	000000000000	000000000000	000000000000	000000000000	000000000000	000000000000	000000000000	000000000000	
(208)	000000000000	000000000000	000000000000	000000000000	000000000000	000000000000	000000000000	000000000000	
(2256)	000000000000	000000000000	000000000000	000000000000	000000000000	000000000000	000000000000	000000000000	
(2334)	000000000000	000000000000	000000000000	000000000000	000000000000	000000000000	000000000000	000000000000	
(2352)	56003367510	532260573777	605737777777	777777777777	562023455666	7676171767714	114226376412		
(2430)	171573364635	412320051714	753646354123	10510526310	17051526310	503645301715	751427535755		
(2448)	501317147624	476743407724	171474735105	503453001716	751472553755	501200000000	171474645407		
(2496)	055537221717	555442641625	401617147452	013521132300	171755715402	076216071716	757133301433	755517176452	
(2544)	013521132277	171755544264	162540161713	674645611524	366312147016	660722625371	171746314153	271321541716	
(2592)	764332372677	025160573777	777777777777	605737777777	777777771717	457065176763	554317167204	441176153560	
(2641)	1717464769	47271130562	17151547424	666462645034	171751547424	7177041717	64152110726		
(2688)	745017174335	643626107503	1716151627324	957060421716	42720264212	2005170421716	102654143462	171570166607	
(2736)	726253671717	64264162540	202517175476	363320046364	17176314153	771321541715	523545050655	325517166042	
(2784)	641625462030	171651547424	71772705000	000000000000	000017127213	505642721350	171352747744	405117020000	
(2832)	000000000000	000000000000	000000000000	000000000000	000217135534	600217135534	403466053211		
(2880)	171353256411	645066361713	1715205610044	715205610044	425637443454	171271314256	374434541711	714163034607	
(2928)	141617117213	505642271350	17125114256	374345400000	002000000000	000000000000	000000000000	000000000000	
(2970)	645663561713	525252525252	525217127121	246053415130	171171314256	374434540000	900000000000	00017135311	
(3024)	262254453112	171271111111	1111111111724	600760540460	032417245604	406731344577	172461656152	065072251724	
(3072)	656106513233	763360573777	777777777777	605737777777	777777771724	5357400000764	760117244470	636130673251	
(3120)	172371057323	5575117213	47674223724	31161723511	4514423604	172350431355	242567041723	47370723053	
(3168)	767717234762	7633262001756	172354452017	621131661724	43674345201	33601724426	205266137775	172442323607	
(3216)	377165541724	430142264731	320117244200	054676551010	172444015515	460457271724	462665557231	122017244736	
(3264)	751741774152	172451542067	331377460000	000000000000	000000000000	000000000000	000000000000	000000000000	
(3312)	000000000000	000000000000	000000000000	000000000000	000000000000	000000000000	000000000000	000000000000	
(3368)	000000000000	000000000000	000000000000	000000000000	000000000000	000000000000	000000000000	000000000000	
(3406)	000000000000	000000000000	000000000000	000000000000	000000000000	000000000000	000000000000	000000000000	
(3456)	000000000000	000000000000	000000000000	000000000000	000000000000	000000000000	000000000000	000000000000	
(3504)	000000000000	000000000000	000000000000	000000000000	000000000000	000000000000	000000000000	000000000000	
(3552)	536674236510	632005573777	777777777777	605737777777	777777771724	716732514304	412117247162	107761037303	
(3600)	172476335361	4431571725	423673323372	307117247345	506151434672	172471542151	040470617224	732554573461	
(3648)	141617247546	625576171	476614001713	4344712456173	104617245276	172515655322	172553031745		
(3696)	711016721725	44645676662	323517246741	61473204541	1724365224724	6751051367	152517245604		
(3744)	712331165407	172462355173	736424611725	43022423762	345417254141	020126247555	172541532523	345707041725	
(3792)	425615461747	77561573777	777777777777	605737777777	777777771725	442173137127	134217254222	347565761255	
(3842)	172542284746	6600523261725	437222666402	273217247702	351212756425	172475117270	405751261724	7647732575	
(3888)	26231245027	372116263665	172543146753	545132633125	470446001714	101617254670	617226341704	172556254352	
(3936)	37142461725	57652732314	545717254053	3334172471615	17254623474	621237061725	416420316206	311317247473	
(3984)	7655077773	17254	545717254053	3334172471615	17254623474	621237061725	416420316206	311317247473	

